UNIVERSITY OF NOVA GORICA
GRADUATE SCHOOL
STUDY PROGRAMME: ENVIRONMENTAL SCIENCES

OXIDATION AND DEGRADATION OF ORGANOPHOSPHORUS COMPOUNDS

Mojca BAVCON KRALJ

Dissertation

Mentor: Doc. dr. Polonca Trebše

Nova Gorica, 2007

ZAHVALA

Kot mlado študentko kemije me je pozimi leta 1998 sprejel prof.dr. Mladen Franko in mi navdušeno predstavljal dejavnosti Laboratorija za raziskave v okolju. Poleti istega leta sem prvo počitniško prakso opravljala pod mentorstvom doc. dr. Polonce Trebše. Od takrat sem vpletena v delo Politehnike Nova Gorica, danes ponosne Univerze v Novi Gorici.

Draga mentorica, doc. dr. Polonca Trebše, hvala za skupno prehojeno pot devetih let in za zaupanje, ki si mi ga izkazala. Hvala za vse izkušnje in preizkušnje, ki sva jih skupaj in vsaka zase prestali. Prof. dr. Mladen Franko, hvala za prvi navdih in vso podporo pri delu z laserji.

Članom komisije hvala. Prof. dr. Janez Štupar, hvala za življenjsko veselje, analitsko natančnost in dobroto. Prof. dr. Darko Dolenc, hvala za znanje iz organske analize in jasno osebno mnenje o stvareh. Prof. dr. Mohamed Sarakha, hvala za ideje o fotoreaktorjih in vse praktične nasvete v fotokemiji.

Hvala vsem, ki me obdajate z veseljem in mi lepšate delovne dni. Dragi sodelavci, mladi raziskovalci, pričujoče delo je nastalo pod mojimi rokami z vašim blagoslovom. Številni muhasti inštrumenti so ponovno brenkali v pravem ritmu z vašo pomočjo. Številni sivi dnevi so postali svetli z vašim smehom. Smo mladi, včasih neizkušeni, zaletavi, iskrivih idej, nevarnih zamisli, predvsem pa radi delamo skupaj, vsak dan.
Hvala,

Azameli, za oporo in najino skupno vero v Eno; Alešu za »ne skrbi«; Branki za pozitivno energijo; Evgenu za nasvete; Renati za poslušanje; Vanesi za upanje; Gosii za pogum; Ani za iznajdljivost; Romini in Kseniji za smeh; Dunji za tehtnost; Kristini za razumevanje; Jani za ljubezen do narave. Urh, hvala ti za prijateljstvo, za skupno reševanje težav, kemijskih, instrumentalnih in človeških.

Hvala za odlične starše. Mama, hvala za vso skrb. Tata, hvala za varno zaščito. Obema hvala za ljubezen. Hvala sestrama, Tjaša, ker me dviguješ iz hladne realnosti in me ovijaš v mehko nedorečenost. Erika, ker praviš, da se stvari zgodijo, ker se morajo in me s tvojimi razlagami pomirjaš. Stric Jurij, hvala, da si z nami in nam pomagaš.

Dragi Štefan in najino sonce Fabijan, ljubim vaju. Pomagata mi spoznavati, kdo sem in kam grem. Morda nekoč vendarle spoznam zakaj, …
… zato je v tebi Bog … hvala Ti za vse.

AKNOWLEDGMENTS

In the winter of 1998, Prof. Dr. Mladen Franko met me as a young student of chemistry. He filled me with enthusiasm in explaining the activities of School of Environmental sciences. Thus, in the summer of the same year, I started practice in the laboratory under the mentorship of Dr. Polonca Trebše. Since then I have been interlaced in the activities of Polytechnic Nova Gorica, today very proud University of Nova Gorica.

Dear mentor, Doc. Dr. Polonca Trebše, thank You for the road we have been walking through these nine years and for the confidence You have placed in me. Thank You for the experience and all the trials we underwent together or individually. Prof. Dr. Mladen Franko, thank You for the inspiration and all the support with lasers.

Members of committee, thank You. Prof. Dr. Janez Štupar, thank You for the life enthusiasm, analytical precision and kindness. Prof. Dr. Darko Dolenc, thank You for spreading knowledge of organic analysis and a clear personal opinion. Prof. Dr. Mohamed Sarakha, thank You for ideas related to photoreactors and all practical advice on photochemistry.

Thank You All, to surround me with happiness and to make my days pleasant. Dear colleagues, young researchers, this work was created by my hands, with your blessing. With your help several capricious instruments began to thrum in the right rhythm. With your laugh several gray days became bright. We are young, sometimes inexperienced, quick in decision-making, full of striking ideas and daring intentions, but what we love the most is working together, day after day.

Thank You,

Azamela, for all the support and our faith in the One; Aleš for »don't worry«; Branka for positive energy; Evgen for advice; Renata for listening to me; Vanesa for hope; Gosia for courage; Ana for inventiveness; Romina and Ksenija for laughter; Dunja for substantial arguments; Kristina for understanding me; Jana for loving the Nature. Urh, thank You for friendship, for solving many difficulties together - chemical, instrumental and human.

Thanks to You, excellent parents. Thank You, Mum, for all the care you have providing. Thank You, Dad, for the protection you have been giving me. Thank You, both, for your Love. Thank You sisters. Tjaša, because you rise me from the cold reality and cover me with gentle unknowing. Erika, because you always say that things simply happen, because they have to, and you calm me down with explanations. Uncle Jurij, thank You, for being with us and for helping us.

Dear Štefan and our sunshine Fabijan, I love You. You are helping me to perceive, who I am and where I go. Perhaps, one day I will realize why…
… because it is in You, God… Thank You for everything.

POVZETEK

Organofosforne spojine uporabljajo v kmetijstvu za zaščito zelenjave in sadja pred škodljivci že več kot štirideset let. V zadnjem času pa opažamo čedalje večjo uporabo tudi ostalih biocidnih pripravkov, največ na osnovi neonikotinoidov. V evropski uniji ostajata dva prestavnika organofosfornih spojin (klorpirifos in klorpirifos-metil) v uporabi do leta 2016, medtem ko njihova splošna uporaba v ostalih državah (ZDA, Kitajska) ne upada.

Velika poraba in vnos organofosfornih spojin v naše okolje, zahtevata spremljanje njihovih pretvorb. V našo raziskavo smo zato vključili štiri modelne organofosforne spojine, ki jih običajno najdemo kot aktivne snovi v komercialnih pripravkih: azinfos-metil, diazinon, klorpirifos in malation. Sledili smo dvema glavnima ciljema raziskave:

- razviti oksidacijski predpostopek. Namen predpostopka je v zagotavljanju hitrega, zanesljivega in občutljivega odziva bioanalitske tehnike (na osnovi acetilholin esteraze (AChE), ki je tarčni encim za določevanje organofosfornih spojin) v realnih vzorcih hrane oz. sokov;
- študirati (foto)razgradnjo organofosfornih spojin. Naš cilj je bil doseči učinkovito razgradnjo z identifikacijo nastalih produktov in vrednotenjem strupenosti obsevanih vzorcev za encim AChE.

Za študij kemijske oksidacije smo uporabili vrsto znanih oksidantov: *N*-bromsukcinimid (NBS), natrijev hipoklorit, *m*-kloroperoksibenzojsko kislino, kalijev peroksimonosulfat, cerijev amonijev nitrat, jodovico ter vodikov peroksid. Učinkovito oksidacijo v času krajšem od petih minut smo dosegli z uporabo NBS-a. Delno smo lahko oksidirali še diazinon v diazokson z uporabo natrijevega hipoklorita. Vsi ostali oksidanti pa so se v danih pogojih izkazali kot neučinkoviti. Z izbiro NBS-a v kislih pogojih in natrijevega hipoklorita v alkalnih se lahko učinkovito izognemo stranskim reakcijam hidrolize. Nastale okso-produkte smo določili z uporabo imobilizirane acetilholin esteraze v pretočnem sistemu za injekcijsko analizo in spektrometrije na osnovi termičnih leč (AChE-TLS). To nam je omogočilo določevanje tio-OP v ppb koncentracijskem območju. S pomočjo hitre (5 min) oksidacije lahko analizo posameznega vzorca s pomočjo AChE-TLS bioanalitske tehnike opravimo v 15 minutah. S tem je omogočen lažji in temeljitejši nadzor in odkrivanje vzorcev onesnaženih s holinesteraznimi inhibitorji, vključno z žveplovimi analogi.

Prve eksperimente raziskave fotorazgradnje organofosfornih spojin (azinfos-metil, klorpirifos, malation in malaokson) smo izvedli z uporabo 125 W ksenonove žarnice. Izginevanje izhodnih spojin smo spremljali s plinsko kromatografijo na masno detekcijo (GC-MS), identifikacija nastalih produktov pa je omogočila vpogled v potek razpada (brez mehanistične študije). Strupenost obsevanih vzorcev smo spremljali s pomočjo AChE-TLS bioanalitske tehnike. V razgradnji organofosfatnih spojin sta pomembni predvsem dve glavni reakciji: oksidacija, kjer nastajajo več kot 100-krat bolj strupeni oksoni in cepitev naobčutljivejših vezi (P─S(O) in (O)S─C vezi), ki vodi v nastanek prav tako zelo strupenih trimetilnih estrov. Znižanje encimske aktivnosti v primeru obsevanih vodnih vzorcev kaže na inducirano strupenost med procesom fotorazgradnje.

V nadaljevanju smo se usmerili v (foto)razgradnjo enega fosfatnega pesticida – malationa, njegovega tehničnega pripravka Radotiona in njunih dveh razgradnih produktov (malaokson in izomalation). Na tej skupini spojin smo testirali tri fotorazgradne sisteme: gama sevanje (s ^{60}Co izvorom), fotolizo (emisijski maksimum 254 nm) in fotokatalizo (katalizator TiO_2, svetlobni snop z maksimumom pri 355 nm). Hidroksilni radikali, kot posledica gama sevanja in katalizatorja, v začetku najprej oksidirajo malation v njegov okso produkt - malaokson. Nadaljevanje radikalske reakcije pa vodi v cepitev vezi in nastanek trimetil fosfatnih estrov ([OOS(S)], [OOS(O)], [OSS(O)]). Zadnje smo opazili tudi v obsevanih vzorcih malaoksona in izomalationa. Nastajanje trimetil fosfatnih estrov in malaoksona v primeru radiolize in fotokatalize malationa se dobro ujema z znižanjem aktivnosti AChE. Prav tako pa se odsotnost le-teh ujema z neizraženo strupenostjo vzorcev v procesu fotolize. Pri procesu fotokatalize in fotolize pa smo poleg identifikacije nastalih produktov spremljali še stopnjo mineralizacije. Medtem ko je nastanek sulfata pri obeh procesih primerljiv, je mineralizacija do fosfata pri fotolizi neuspešna. Nastanek fosfata pa pogosto spremljamo kot pomembno spremenljivko v t.i.varnem odstranjevanju organofosfornih spojin.

Študij fotokatalize smo dodatno dopolnili s študijo ozonizacije klorpirifosa. Ugotovili smo, da se izhodna spojina v celoti (v 15 minutah v primeru ozonizacije) ali delno (fotokataliza) pretvarja v

klorpirifos-okson. Nastanek le-tega pa se popolnoma ujema z znižanjem aktivnosti encima. Težava ostaja v tem, da je več kot 100-krat bolj strupen novo nastali okson med procesom ozonacije stabilen in se počasi razgrajuje (tudi po dveh urah ozonacije, le 20% klorpirifos-oksona razpade).

Prikazani rezultati kažejo na pomen sledenja strupenosti razgradnih produktov med procesom razgradnje organofosfornih insekticidov. Bioanalitske tehnike na osnovi AChE zagotavljajo primerno vrednotenje morebitne inducirane strupenosti v obsevanih vzorcih s pesticidi onesnažene vode pred ponovnim vnosom v okolje.

SUMMARY

Organophosphorus compounds have been widely used as insecticides in agricultural practice for more than 4 decades. Nowadays, also other biocides, mostly from the group of neonicotinoides, are gaining in application. Two representatives of OP compounds (chlorpyrifos and chlorpyrifos-methyl), however, will be used for the next ten years in European countries, while the use of OP compounds in general, is not diminished in non-European countries (i.e. China, USA).

Since OP compounds are continuously used and dissipated in our environment, four representatives of OP compounds found as active ingredients: azinphos-methyl, chlorpyrifos, diazinon and malathion was chosen as model compounds in our study. Two major goals were followed:

- development of an oxidation step; in order to achieve a fast, reliable and sensitive detection of OP compounds spread on foodstuffs employing a bioassay based on acetyl cholinesterase (AChE);
- study photodegradation of OP compounds; in order to achieve efficient degradation of the starting compound, with the identification of the formed compounds and with the evaluation of toxicity of irradiated samples on the target enzyme AChE.

The oxidation efficiency of *N*-bromosuccinimide (NBS), hypochloride and other oxidants such as *m*-CPBA, Oxone, CAN, iodine water, hydrogen peroxide in aqueous solution and juice samples spiked was studied in oxidation experiments. The complete conversion into oxons was noticed within five minutes in case of NBS, a partial conversion in case of sodium hypochlorite, and no oxo-products were observed using other oxidants. Since the NBS is efficient in acidic conditions and hypochlorite in alkaline media, the hydrolysis during the oxidation process can be significantly avoided using appropriate pHs. The formed oxo-analogs were verified using GC-MS analysis and detected using AChE-bioassay with thermal lens spectrometry (TLS) detection, which enabled determination of parent thio-compounds at ppb levels. With a rapid (5 min) oxidizing pre-step the AChE-bioassay can serve as a fast pre-screening test (15 min) to identify samples that contain AChE inhibitors, including the thio-OPs.

The first photodegradation experiment using a 125 W xenon parabolic lamp was done on the following organophosphorus compounds: azinphos-methyl, chlorpyrifos, malathion and malaoxon. Gas chromatography-mass spectrometry (GC-MS) was used to monitor the disapperance of starting compounds and formation of degradation products as a function of time (no mechanism of formation was studied). AChE-thermal lens spectrometric bioassay was employed to assess the toxicity of photoproducts. During the photo-process several products were identified suggesting the pathway of OP degradation. Two main reactions were involved in OP degradation. Oxidation, resulting in up to 100-times more powerful oxons and bond cleavage (P─S(O) and (O)S─C bonds were found to be the most susceptible), leading to formation of toxic trimethyl phosphate esters. In fact, all irradiated samples containing OP compounds decreased AChE activity.

Further two experiments were mainly focused on (photo)degradation of the starting material (malathion and commercial product Radotion) and its commonly presented transformation products (malaoxon and isomalathio). Three types of irradiation setups were employed for this purpose: gamma irradiation (^{60}Co source), photolysis (band maximum 254 nm) and photocatalysis (TiO_2 as photocatalyst and broad band maximum 355 nm). The hydroxyl radicals presented in gamma irradiation and photocatalysis resulted in the formation of malaoxon as the first formed compound in the degradation of malathion. Further radical attack cleavaged the molecule and several trimethyl phosphates ([OOS(S)], [OOS(O)], [OSS(O)]) were found in irradiated solutions of malathion, malaoxon and isomalathion. Photolysis lacked of formation of trimethyl phosphates ([OOS(S)], [OOS(O)], [OSS(O)]) and oxons in case of degradation of all three compounds. The reduced activity of AChE was correlated well with the formation of malaoxon and trimethyl phosphates in radiolysis and photocatalysis of malathion. In photolysis experiments, on the other hand, the lack of formation of trimethyl phosphates and malaoxon resulted in no decrease in AChE activity. Photocatalysis and photolysis were evaluated also in terms of the degree of mineralisation. The formation of sulphate was similar in both processes, but the photolysis was inefficient in phosphate formation. The mineralisation into phosphate ion is crucial in safe removal of OP compounds.

Chlorpyrifos was, in addition to TiO_2 photocatalysis, supposed also to ozonation treatment. During both processes, the formation of chlorpyrifos-oxon correlated negatively with the decreased activity of the AChE. It was noticed, that chlorpyrifos the conversion into chlorpyrifos-oxon was rapid (15 min), but the formed chlorpyrifos-oxon was found resistant toward further ozonation process. Even with higher concentrations of ozone only around 20% of the primary compound (after 2 h of ozonation) was degraded.

The presented results demonstrate the importance of toxicity monitoring during the degradation of OPs in processes of waste water remediation, before releasing them into the environment.

LIST OF CONTENTS

LIST OF TABLES

LIST OF FIGURES

1 INTRODUCTION

The extensive use of pesticides, in order to enlarge the production in agriculture, has lead to a growing accumulation of pollutants in the environment over the last decades. Organophosphorus (OP) pesticides are among the most widely spread pollutants used for insect control. They have replaced organochlorine compounds, since they are easily degraded and they are not accumulated in the environment for a long time. The natural degradation pathway of OPs includes mainly homogeneous and heterogeneous hydrolysis (Chambers and Levi, Eds., 1992), which is enhanced by the presence of dissolved metals, humic substances and other compounds present in soil (Noblet et al., 1996; Dannenberg and Pehkonen, 1998; Pehkonen and Zhang, 2002). Light is the second powerful inducent of OP environmental degradation pathway. The photolysis of OP can occur by direct photolysis, since they exhibit absorption max in UV region (240 – 310 nm), but it is largely enhanced by the presence of other species like oxygen or humic substances acting as natural sensitizers (indirect photolysis) (Pehkonen and Zhang, 2002).

Advanced oxidation processes including photodegradation reactions and ozonization are one of the most promising techniques for pollutants removal. However, a lack in mechanism and byproduct studies is perceived (Chiron et al. 2000). Most of the conventional methods (HPLC, GC, LC/MS and GC/MS) for determination of organophosphates and their metabolites are labor intensive, time consuming, and require expensive instrumentation. Thus bioanalytical methods such as biosensors are recently gaining attention. They are rapid, simple and inexpensive, when coupled with conventional detectors (UV/Vis spectrometer, electrodes). Biosensors available for detection of organophosphate pesticides are mainly based on enzymatic methods (Table 1), exhibiting a cholinesterase (ChE) inhibition. A photothermal detection based on thermal lens spectrometry (TLS) was developed (Franko, 2001; Pogačnik and Franko, 1999, 2001a, 2001b, 2003) in order to improve the sensitivity of biosensors.

One of our first studiy in the field of OPs (diazinon, malathion) environmental transformation conducted in different matrices (water, soil and chicory) and conditions (photolysis, hydrolysis) has risen an interest, since the formation of more toxic compound (malaoxon) was proven in all samples (Bavcon et al., 2003). This observation lead us to profound our knowledge in transformation products resulting from different processes (oxidation, photodegradation). By applying UV-Vis bioanalytical FIA method and laser flash photolysis, the photodegradation of coumaphos and azinphos-methyl was investigated in combination with HPLC analysis. The transformation of coumaphos, which lead to the formation of a more toxic oxo organophosphate, confirmed the need for toxicity testing of photodegraded samples containing organophosphorous compounds (Franko et al., 2005).

Environmental transformations as well as photodegradation experiments for pollutants removal, resulting in the formation of more toxic by-products need more detailed examination. The need in improvement of photothermal bioanalytical FIA methods was realised. The FIA-AChE-TLS bioassay, due to the fast and selective response, has found its application in different environmental matrices as a screning test and an early warning system for contamination with organophosphate pesticides. It was our goal to optimize the detection of OP compounds in real samples (fruits and juices). For this purpose we exploited the use of different oxidant and reducing agents to reach fast (5 min) and sensitive response (few ppbs) in monitoring OP polluted environmental matrices.

A lack in literature reports regarding safe removal of OPs compounds and their transformation products and comparison of different degradation techniques was noticed.That way it was also our aim to study photodegradation (Xenon light source with spectral band ranging from 200 nm through whole visible range, photolysis – λ=254 nm, TiO_2 photocatalysis - λ=355 nm) and ozonation processes of OPs in terms of by-products and their toxicity. In fact, several formed by-products were identified employing gas/liquid chromatography combined with mass spectrometry, but no mechanism of formation was studied. We were mostly interested in compounds, which caused a decrease in AChE activity. The information about the overall anti-ChE toxicity of irradiated or ozonated samples was obtained using bioanalytical FIA method. All treated samples, even at the half of initial concentration or/and when the starting compound was completely degraded, retained a high level of toxicity, and the enzyme activity was drastically decreased.

2 THEORETICAL BACKGROUND

2.1 Organophosphorus compounds

Today, over 500 compounds are registered worldwide as pesticides, or metabolites of pesticides. Pesticides can be classified according to their chemical nature (e.g. inorganic, organonitrogen, organohalogen,…), or their specific biological activity on target species (herbicides, fungicides, acaricides, insecticides,…). Organophosphorus compounds are a massive and highly diverse family of organic chemicals, with many uses, but with the growing importance in pests control as insecticides, acaricides, nematocides, and helmithicides. The acute lethality of OP pesticides can be attributed primarily to their ability to inhibit acetylcholinesterase (AChE), an enzyme vital for normal nerve function.

The term, organophosphorus insecticides, means all insecticides that have the phosphorus atom in the structure. The term phosphates refers to analogs of phosphoric acid, H_3PO_4, in which one phosphorus atom is bound to a tetrahedral array of four oxygen atoms, resulting in highly reactive materials, with short residual activity. Far more numerous, and for agricultural uses more stable and safe handling, are the sulfur-containing organophosporus compounds, especially those with a P=S moiety, the so-called phosphorothionates/phosphorothioates. But as like carboxylic acids, the two classes of organophosphorus compounds – derivatives of phosphoric acid (P=O – phosphates and P=S – phosphorothionates) can form subclasses of amides, esters and thioesters.

As mentioned earlier, many of the organophosphorus (OP) insecticides are phosphorothionates (lipophilic), which are characterized by one thiono moiety (P=S) and three -OR groups attached to a phosphorus atom. The respective oxons are more polar, characterized by double bond between phosphorus and oxygen atom (P=O), resulting in considerably more potent AChE inhibitors (Chambers and Levi, Edt., 1992). Inhibition of AChE by OP compounds is an irreversible process best described as a transesterification or transphosphorylation, reactions, where OP competes with the normal substrate of AChE, acetylcholine (ACh), at the catalytic center of serine-hydroxyl group. Since the transphosphorylation reaction relies on interaction of the P atom with an unshared pair of electrons of the oxygen in serine-hydroxyl group, electrophilicity of the P atom (in oxons is higher) is critical.

The linkage between these two classes of thio- and oxo-OPs is the chemical characteristic of conversion of P=S analogs (more stable and lipid soluble) to the corresponding P=O analogs (more toxic), which occurs in tissues. After absorption in the body, OP undergoes many transformation reactions. Since they are mostly lipophilic compounds (P=S) in order to facilitate penetration through the skin, reactions of transformation are primarily directed toward formation of more polar conjugates (P=O) (Jokanović, 2001). They can be activated in vivo by monooxygenases, particulary cytochrome P450 system and flavin-containing monooxygenases (FMO). This oxidation is referred to as lethal synthesis, since after that bioactivation, OP's become stronger AChE inhibitors.

This process which occurs in natural environment stimulated interest in following the characteristic of oxon's inhibition power by the use of biosensors.

2.2 Biosensors and bioassays for determination of organophosphorus compounds

2.2.1 GENERAL

An alternative to ease the analysis in routine of environmental and industrial samples seems to be the biosensors development. A biosensor is made of two distinct elements: a biological recognition element (e.g. antibodies, enzymes, receptors and microbial cells) and, in close contact, a signal transduction element (e.g. optical amperometric, acoustic or electrochemical) connected to a data acquisition and processing system (Mello et al., 2002; Patel, 2002).

Biosensors can be classified according to the type of involved active biological component and the mode of signal transduction. The main biological materials used in biosensor technology are the couples enzyme/substrate, antibody/antigen and nucleic acids/complementary sequences. Depending on the method of signal transduction, biosensors can be further divided into different groups: electrochemical, optical, thermometric, piezoelectric or magnetic (Velasco-Garcia et al., 2003).

Biosensors for the detection of organophosphorus compounds are mainly based on enzymes, in particular acetylcholine esterase (AChE) and butyryl cholinesterase (BChE), that are the determinant of pesticide concentrations in samples. The biosensor response is in complete dependence of the enzyme activity or inhibition. However, other enzymes have also been used, e.g. tyrosinase and alkaline phosphatase. A recent exception is the use of hydrolytic activity of organophosphorus hydrolase to determine the concentration of organophosphorus pesticides (Marty et al., 1995; Mulchandani et al., 2001; Patel, 2002). The set-up is normally based on flow injection analysis (FIA). The enzymes are generally bound covalently or non-specifically to a variety of surfaces, the reaction of the pesticides in samples with the immobilised enzymes causes inhibition depending on the type of pesticide and its concentration (Patel, 2002).

The large variety of biosensors for the detection of organophosphorus and carbamate pesticides, their biological materials, mode of transduction, analytes, matrix, and detection limits are summarized in Table 1.

Table 1: *Comparison of different types of biosensors used for the detection of OPs and carbamates*

ANALYTE	*APPLICATION*	BIOCOMPONENT	*TRANSDUCER*	DETECTION LIMIT	*COMPARISON*	REF.
paraoxon **captan**	*contamined water*	AChE (electric eel) GST (human placenta)	*Optical* *optic fiber* *Xe lamp, band pass* *400 nm - GST product* *500 nm - AChE product*	0-2 ppm		**Choi et al., 2003**
OP **Carbamates**	*vegetables* *(onion, iceberg lettuce,salad)* *10-25 g / 1 ml acetone* *and 9 ml PBS (pH 8.0)*	BChE (horse serum) AChE (electric eel)	*Optical* *TLS*	< 10 ppb, BChE < 5 ppb, AChE	*GC/MS*	**Pogačnik and Franko 2003**
paraoxon-ethyl **chlorpyrifos-ethyl oxon**	*water miscible* *organic solvents -* *ethanol, acetonitrile*	AChE (*Drosophila melanogaster*)	*Amperometric* *screen printed* *AChE imm. on PVA SbQ*	in 5% acetonitrile $1.91*10^{-8}$ M - paraoxon $1.24*10^{-9}$ M - chlorpyrifos		**Andrescu et al., 2002**
OP	*synthetic sample* *oxidation* Br_2 *in 2 v/v% Ethanol*	AChE (electric eel)	*Potentiometric*	10^{-11} M - diazinon after oxid.		**Lee et al., 2002**
OP (paraoxon) **Carbamates**	*infant food* *10 g mixed with* *10 ml PBS (pH 7.5)*	AChE (electric eel) human AChE (synthetic gene in Pichia pastoris)	*Amperometric* *screen printed elctr.* *printed on PVC, electr.* *pretreatment with* *1 v/v% Tween 20*	< 5 ppb (paraoxon)	*GC/MS, LC/MS* *(prior SFE, LLE)*	**Schulze et al., 2002**
paraoxon	*orange juice,* *peach and apple* *baby food* *50 g in 100 ml isooctane* *oxidation NBS*	AChE (electric eel)	*Amperometric* *disposable AChE-PB-PEI* *screen printed*	20 ppb - parathion 1 ppb - paraoxon		**Shulze et al., 2002**

… continuation of Table 1

ANALYTE	*APPLICATION*	BIOCOMPONENT	*TRANSDUCER*	DETECTION LIMIT	*COMPARISON*	REF.
paraoxon **carbofuran**	*tap water* *orange juice*	AChE BChE	*Amperometric* *3 electr. system* *Ag (RE), Pt (AE),* *WE - biosensor,* *photolithografic Cu track*	10^{-10} M - paraoxon 10^{-11} M - carbofuran		**Albareda-Sirvent 2001**
chlorpyrifos and its metabolites	*water samples* *in 4 v/v% acetonitrile*	AChE (electric eel)	*Amperometric*	24 ppb - chlorpirifos oxon		**Jeanty et al., 2001**
chlorpyrifos-ethyl oxon	*organic solvents (0-30%)* *acetonitrile,ethanol, DMSO*	AChE *(Drosophila melanogaster)*	*Amperometric screen printed* *AChE imm. on PVA SbQ*	in 5% acetonitrile $2.5*10^{-10}$ M		**Montesinos et al., 2001**
OP **Carbamates**	*multicomponent samples*	AChE (electric eel) OPH (recombinant *E.coli*)	*AChE imm. on* *silicagel pH electr.* *OPH in column*	discriminative method		**Simonian et al., 2001**
OP	*organic samples* *oxidation with Br_2 in ACN*	AChE	*batch system, direct* *photometric analysis*	$10*10^{-10}$ M paraoxon		**Ah Kim et al., 2000**
parathion	*bovine blood* *oxidation with Br_2 fumes*	AChE	*batch system, direct* *photometric analysis*			**Arufe et al., 2000**
diazinon **fenthion** **dichlorvos**	*organic solvents* *(0,001-100%)* *ethanol, propanol* *cyclohexanone, benzene*	AChE (electric eel)	*Amperometric* *disposable AChE-PB-PEI* *modified graphite electr.* *thiocholine-hexacianoferate (III)*	$0.5*10^{-6}$ M - dichlorvos $0.8*10^{-6}$ M - diazinon $1.0*10^{-6}$ M - fenthion		**Wilkins et al., 2000**
OP **Carbamates**	*organic solvents (50 v/v%)* *hexan : chloroform*	BChE (horse serum) ChO (*Alcaligenes sp.*)	*Amperometric* *O_2 gas diffusion electr.*	0.5 ug/L - carbaryl, ethyl parathion		**Campanella et al., 1999**

… continuation of Table 1

ANALYTE	*APPLICATION*	BIOCOMPONENT	*TRANSDUCER*	DETECTION LIMIT	*COMPARISON*	REF.
paraoxon	*synthetic sample*	OPH (*Pseudomonas diminuta*)	*pH sensitive FET*	$1*10^{-6}$ M		**Schoeniger group, 1999**
N-methyl carbamates	*fruits, vegetables* *50 uL sample juice* *dropped on the electr.*	AChE (electric eel) BChE (horse serum)	*Amperometric* *screen printed* *RE - silver paste* *WE - platinum paste* *modified by Co (II)* *phthalocyanine and acetylcellulose*	< 0.5 ppb (total pesticide content)	*HPLC/DAD*	**Nunes et al., 1999**
OP (paraoxon, chlorpyrifos, diazinon) Carbamates (carbaryl, carbofuran)	*tap water, orange,* *apple juice* *filtered and pH* *adjusted*	AChE (bovine erythrocytes)	*Optical* *TLS*	0.2 ppb (paraoxon)		**Pogačnik and Franko 1999**
N-methyl carbamates	*vegetables* *(potatoes, carrots, sweet pepper)* *50 uL sample juice* *dropped on the electr.*	AChE (electric eel) AChE (bovine erythrocytes) BChE (horse serum) BChE (human serum)	*Amperometric* *screen printed* *RE - silver paste* *WE - platinum paste* *modified by Co (II)* *phthalocyanine and acetylcellulose*	0.1 ppb - carbofuran, AChE (electric eel)	*LC/UV*	**Nunes et al., 1998**

… continuation of Table 1

ANALYTE	*APPLICATION*	BIOCOMPONENT	*TRANSDUCER*	DETECTION LIMIT	*COMPARISON*	REF.
OP	*synthetic sample* *1% acetone mixture*	AChE (electric eel; bovine erythrocytes; *Torpedo californica; Drosophila melanogaster; Caenorhabditis elegans;* Y408F AChE - mutant *Drosophila melanogaste*)	*UV-Vis* *Ellman reaction*	sensitivity by turns CE<EE<BE<TC<DM<Y408F		**Villatte et al.,1998**
paraoxon	*organic solvents* *(0.01-10%)*	AChE (electric eel) ChO (*Alcaligenes sp.*)	*Amperometric bienzymatic* *AChE in solution* *ChO on O_2 electr.*	in 5% cyclohexane $<10^{-9}$ M		**Fennouh et al., 1997**
paraoxon	*synthetic sample*	ChO (*Alcaligenes sp.*) AChE (electric eel)	*Amperometric* *ChO - Pt electr.* *AChE - nylon net disk*	5.0 ppb		**Cremisini et al., 1995**
paraoxon **carbaryl**	*water, kiwis* *10 v/v % ethanol*	AChE (electric eel)	*Amperometric*	$5*10^{-7}$ M - paraoxon, carbaryl	*UV method*	**La Rosa et al., 1995**
OP	*soil samples* *1 v/v% acetonitrile* *oxidation - Br_2*	BChE (horse serum)	*Potentiometric* *BChE - immobilized on Pall-Biodyne*	35 ppb - diazinon		**Kumaran and Morita 1995**
fenitrothion, **fenamiphos,** **parathion-ethyl,** **carbaryl**	*freezed-dried water*	AChE	*Amperometric* *Pt electr.* *AChE imm. on PVA SbQ*	$1*10^{-10}$ M (paraoxon equivalent)	*LC/DAD* *(SPE, LLE)*	**Marty et al., 1995**
paraoxon **methyl parathion**	*synthetic sample*	AChE OPH	*Amperometric* *Au electr.* *AChE and OPH imm. on electr.*	$0.1*10^{-6}$ M - paraoxon		**Wang et al., 1995**
paraoxon **aldicarb**	*organic solvents -* *hydrophobic - A* *hydrophilic - B*	AChE (electric eel)	*Amperometric* *Pt electr.* *AChE imm. on PVA SbQ*			**Mionetto et al., 1994**

2.2.2 DETERMINATION OF PESTICIDES RESIDUES IN REAL SAMPLES

It has been known for more than 20 years that enzymes are capable of functioning in certain organic media (Mionetto et al., 1994). The choice of solvent is important with respect to enzyme activity. The critical parameter is the amount of tightly bound enzyme water, which is needed for normal functioning of an enzyme and must not be stripped away. Consequently, only very hydrophobic organic solvents that are water-immiscible are appropriate, whereas hydrophilic solvents (mainly alcohols) that are water-miscible strip the water molecules away from the enzyme, resulting in enzyme inactivation. However, it has been noticed by some authors, that the addition of small amounts of polar solvents (1-15 v/v %) can be used as a correction factor, since the activity of the enzyme was slightly enhanced (Fennouh et al., 1997; Wilkins et al., 2000; Montesinos et al., 2001; Andreescu et al., 2002).

Organic solvents are mostly used as extraction media, which are then directly used for inhibition test or prior inhibition, diluted with buffer mixtures. Afterwards, the activity of the enzyme is determined in buffer solutions (Montesinos et al., 2001).

The concentration of pesticides in environmental samples is relatively low lying in ppb-, and rarely in ppm- concentration range. Therefore preconcentration, and oxidation step was introduced by a number of authors, since the oxons formed from thio-organophosphates have stronger effect on biosensor using the same enzyme and comparable experimental conditions. Limits of detection of native and oxidized OP using the same enzyme, AChE from Electric eel, differ for more than three orders of magnitude. (Marty et al.,1995).

Kumaran and Tran-Minh (1992) have studied the enhanced inhibition of AChE after bromine water was added to synthetic seawater spiked with pesticide. Unfortunately, in the research no evaluation of bromine water regarding the enzyme activity was made. Three years later (1995) they have proposed a method to screen for organophosphorus pesticides extracted from soil. The solvent was evaporated, and the residue redissolved in acetonitrile to which bromine water was added in order to enhance the sensitivity of biosensor. The acetonitrile – bromine water mixture was diluted with working buffer prior analysis. The inhibitory power of the bromine water was defined and a suitable concentration was proposed. (Kumaran and Tran-Minh, 1992; Kumaran and Morita, 1995). Similarly, Kim et al., (2000) and Lee et al., (2001) developed a convenient method for oxidation of nine organophosphorus pesticides with 10 molar excess bromine in acetonitrile, within few seconds. The yields of the oxons were 82-100%. Before the measurements of the enzyme inhibition, oxidized and unoxidized OPs were 1000-fold diluted with working buffer (Kim et al., 2000; Lee et al., 2001). Bromine vapors were also used for oxidation of parathion applied on the TLC sheet. The reaction, was completed in 2 min, afterwards inhibitory tests were made with bovine blood samples (Arufe et al., 2000).

N-bromosuccinimide (NBS) has been found as an efficient oxidant resulting in a rapid, and specific conversion of thio-OP to oxons. Herzsprung and co-workers (1990) have reported of a 100% molar conversion of 5 selected thio-OPs in their oxo forms in water samples. The final concentration of NBS was set in the range that no inhibition of the enzyme was noticed, since no reduction compound was used. With a 100-fold preconcentration step even a 0,1 ppb OP concentration can be determined (Herzsprung et al., 1990). Two other research groups also achieved the enhanced sensitivity of biosensor by using NBS. The determination of immobilized enzyme activity, and the residual enzyme activity were measured in buffer solution, whereas the inhibition by pesticides was performed in organic solvents. The inhibition produced by the three insecticides: parathion, fenitrothion, and chlorpyrifos was 5-times higher. (Barcelo et al., 1995; Marty et al., 1995). H. Schulze (2002) and his research group have the first performed the oxidation of real samples including matrix effects. They have optimized the biosensor detection by the oxidation of juices using NBS, which was reduced with ascorbic acid prior extraction. The detection of neurotoxic insecticides in food was performed using a simple isooctane extraction in order to avoid a non-specific inhibition of the enzyme and to preconcentrate the pesticides. Schultze has further improved the detection of OPs by including an activation step based on a cytochrome P450 BM-3 (CYP102 A1) mutant (Schulze et al., 2004). This method however can be better classified as one of the biological ways of oxidation such as enzymatic

oxidations using different enzymes: lignin peroxidase, horseradish peroxidase, chloroperoxidase, and horse heart cytochrome c (Hernandez et al., 1998, Bello-Ramirez et al., 2000).

To the best of our knowledge, bromine and NBS were the only two oxidants forming oxons, used for a better detection of organophosphates by biosensors. However, after oxidation procedure or preconcentration, samples containing OP compounds were incubated with enzyme. A general procedure for determination of OP compounds employing bioassays found in literature (summarized above) range from half an hour to two hours. It is evident, that an optimization in procedures is needed to achieve a fast, selective and sensitivite response in bioassays for OP determination.

However, different approaches of oxidation were developed during years. They were mainly employed for the synthesis of oxons from thio-phosphates. Oxidation was performed on P=S or P=Se moieties with alkyl or *O*-alkyl side chains mostly in organic solvents under elevated experimental conditions. The oxidants and the experimental conditions were:

- dinitrogen tetra oxide in dichloromethane and nitric acid at room temperature for 0,5 h (Michalski et al., 1970; Stec et al., 1971);
- 90% peroxide added to a solution of OP compound in dioxane, heated under reflux for 10 min (Stec et al., 1976);
- acidic dimethyl sulfoxide under reflux for a couple of hours (Luckenbach, 1973; Luckenbach and Kern, 1975);
- dimethyl sulfoxide with the addition of iodine, heated for 4 h at 80°C (Mikolajczyk and Luczak, 1975);
- peroxyacid and OP compound in methylene chloride at 0°C, reaction was completed in seconds (Herriot, 1971);
- *m*-chloroperoxybenzoic acid and OP compound in chloroform or dichloromethane, with reaction times from 2 to 24 h (Bellet and Casida, 1974);
- *m*-chloroperoxybenzoic acid and the OP compound in dry acetone, with reaction taking place for an hour (Segall and Casida, 1982);
- trifluoroacetic anhydride and OP compound in pyridine solution with reaction times of 2 h (Helinski et al., 1990);
- trifluoroacetic anhydride and compound in methylene chloride at room temperature (Bruzik and Stec, 1990);
- dimethyldioxiran in acetone and OP compound in dry dichloromethane, the reaction was completed within 5 minutes (Sanchez-Baeza et al., 1990);
- monoperoxyphtalic acid, magnesium salt added to the compound in dichloromethane, under reflux for 12 hours (Jackson et al., 1992);
- potassium peroxymonosulfate in buffer solution added to OP compound in tetrahydrofuran/methanol solution, the reaction was completed within minutes (Wozniak and Stec, 1999);
- ozone with OP compound in dichloromethane at -75°C (Skowronska and Krawczyk, 1983);
- perfluoro-cis-2,3-dialkyloxaziridine and OP compound in chloroform with the reaction time of few minutes (Terreni et al., 1995; Arnone et al., 1997).

It is apparent, that such oxidation conditions cannot be realized in biosensor determination of OPs, unless some modifications are introduced.

2.3 Photodegradation of organophosphorus pesticides

There are four major causes of pesticide water pollution (Chiron and Fernandez-Alba, 1997):

- pesticide treatment as a consequence of agricultural practices (a concentration range of few ppb),
- rinse water from containers and spray equipments (10-100 ppm),
- wastewater from agricultural industries (10-100 ppm),
- wastewater from formulating or manufacturing pesticide plants (1-1000 ppm).

The last three point sources of pollution may be ideally treated in a small-scale treatment units including physical entrapment, biodegradation and chemical reactions (Chiron et al., 2000).

Unfortunately, entrapment cannot be a final solution, due to low efficiency and high concentration of pollutants and because of the need for complete destruction of entrapped pollutants. Biological treatment techniques are susceptible to toxic compounds that inactivate waste-degrading microorganisms. In such cases, a useful approach is an oxidation pretreatment of pollutants to produce intermediates that are more readily biodegradable. Developments in the field of chemical water treatment have made available several oxidative degradation procedures based on the generation of highly reactive intermediates that initiate a sequence of reactions resulting in the destruction and removal of organic pollutants. They are generally referred to as advanced oxidation processes (AOPs), which can be sorted into two main groups: photochemical processes and ozonation processes. Photochemical processes can be further divided into direct photolysis, photosensitized oxidation and photocatalysis (Burrows et al., 2002).

In the following paragraphs photochemical processes will be presented in general. A more detailed information about pesticides, reactors, kinetics, and formed products are given in Table 2.

2.3.1 DIRECT PHOTODEGRADATION

Exposure of OP insecticides to sunlight results in photolytic degradation. This occurs via direct photolysis, in which the pesticide absorbs the UV radiation, promoting the pesticide to its excited singlet state, which may then by intersystem cross produces triplet state. Such excited state can undergo, among other processes: homolysis, heterolysis, and photoionisation (Burrows et al., 2002).

$$
\begin{array}{lll}
 & h\nu & \rightarrow P\cdot + X\cdot \quad \text{HOMOLYSIS} \\
PX & \rightarrow (PX)^* & \rightarrow P^{-/+} + X^{+/-} \quad \text{HETEROLYSIS} \\
 & & \rightarrow (PX)^{+}\cdot + e^{-} \quad \text{PHOTOIONISATION}
\end{array}
$$

Some OPs absorb radiation fairly strongly in the UV range that reaches the earth, producing sulfoxides, oxons and hydrolytic products (Chambers and Levi, Ed., 1992).

One of the earliest studies regarding direct photolysis was carried out in order to establish the stability of organophosphorus compounds exposed to natural sunlight and to determine the residual duration for predicting the suitability of individual insecticide for tea plants (Chen et al., 1984). Five years later Chukwudebe et al. (1989) observed the formation of *O*-, and *S*- trimethyl phosphates from OPs (parathion, fenthion, methidation, azinphos-methyl, and malathion) exposed to UV light and sunlight. This rose a concern among agricultural specialists, since these photoproducts were well known by the delayed mammalian (oral dose, rat, 15 mg/kg) toxic properties of insecticide commercial products. They were present as minor contaminants formed during the synthesis of active OP compounds. (Chukwudebe et al., 1989).

As a consequence of their continuous widespread use, residuals in water had affected the aquatic environment. The researches for removal the OP compounds during the last decade have indicated that OPs are very much susceptible to irradiation. For the artificial photolytic studies, different light sources (natural summer sunlight, suntest apparatus, Hg and Xe lamps) were used, resulting consequently in different kinetics, mechanisms and by-products, including also the formation of more toxic oxons (Katagi, 1993; Durand et al., 1994; Wan et al.1994).

2.3.2 PHOTOSENSITIZED DEGRADATION

It is based on the absorption of light by a molecule, which than in one possible scenario, transfers energy from its excited state to the pesticide, that can undergo different processes, as the following direct photodegradation:

$$\text{Sens} \rightarrow h\nu \rightarrow (\text{Sens})^* + PX$$

$$\downarrow$$

$$\text{Sens} + (PX)^* \rightarrow P\cdot + X\cdot \quad \text{HOMOLYSIS}$$
$$\rightarrow P^{-/+} + X^{+/-} \quad \text{HETEROLYSIS}$$
$$\rightarrow (PX)^{+}\cdot + e^{-} \quad \text{PHOTOIONISATION}$$

Photosensitization may also involve redox processes, such as the photo-Fenton reaction, which will be presented in the following paragraph. An important advantage of photosensitized photodegradation is the possibility of using light of wavelengths longer than those corresponding to the absorption characteristics of the pollutants (Burrows et al., 2002).

In natural environment it is common that indirect photolysis of OPs occur, in which sunlight is first absorbed by humic and inorganic substances, their activated forms than interact with the pesticide or produce oxygen radicals or peroxides. The most common pathway of OP photolysis involves photooxidation (Chambers and Levi, Edt., 1992). Allmaier and Schmidt (1985) had, on the contrary, proposed that degradation of OPs, in rainwater and soil surface by artificial sunlight, results in hydrolytic products.

The sensitization effects of humic substances and cyclodextrins (cyclic oligosaccharides) was studied in details by Japanese researchers, who suggested that the enhancing effects of photodegradation is attributed to the inclusion effects of cyclodextrins to catalyze the interaction of pesticides with radicals generated by the photosensitizing humic acids, that are trapped in the cyclodextrins. Cyclodextrins have been shown to have an important enhancing effect on the rate of photodegradation of organophosphorus pesticides in water (Kamiya and Nakamura, 1995; Ishiwata and Kamiya, 1999a; Ishiwata and Kamiya, 2000) and in water containing humic substances (Kamiya and Kameyama, 1998; Ishiwata and Kamiya, 1999b; Kamiya and Kameyama, 1998). The sensitization effects of humic substances depends on the binding affinity of pesticides to the radical source of the humic material. It was also found that paramagnetic metal ions inhibit the degradation of organophosphorus pesticides sensitized by humic acids (Kamiya and Kameyama, 2001). Basic factors dominating the metal-ion effects were clarified on the basis of the fluorescence quenching as well as radical scavenging abilities of metal ions complexed with humic substances.

2.3.3 DEGRADATION BY REACTION WITH THE HYDROXYL RADICAL (HO·)

Some of the most frequently used AOPs involve molecules that upon photolysis generate the hydroxyl radical (HO·). This can be achieved by:

- addition of <u>hydrogen peroxide</u> that undergoes homolysis upon irradiation:

  $H_2O_2 + h\nu \rightarrow 2HO\cdot$

- photolysis of <u>ozone</u>, either with generation of atoms of singlet oxygen that then react with water to generate

  $HO\cdot: O_3 + h\nu \rightarrow O_2 + O(^1\Delta)$

$O(^1\Delta) + H_2O \rightarrow 2\,HO\cdot$

or which react directly with water to produce hydrogen peroxide:

$O_3 + H_2O + h\nu \rightarrow O_2 + H_2O_2$

followed by homolysis to generate hydroxyl radicals (Burrows et al., 2002).

- Fenton-type systems using Fe^{2+} or Fe^{3+} and H_2O_2 producing hydroxyl radicals HO· (Penuela and Barcelo, 1998):

$Fe^{2+} + H_2O_2 \rightarrow Fe^{3+} + HO\cdot + OH^-$

$Fe^{3+} + H_2O_2 \rightarrow Fe\text{-}OOH^{2+} + H^+$

$Fe\text{-}OOH^{2+} \rightarrow HO_2\cdot + Fe^{2+}$

$Fe^{3+} + HO_2\cdot \rightarrow Fe^{2+} + O_2 + H^+$

$HO\cdot + Fe^{2+} \rightarrow Fe^{3+} + OH^-$

$HO\cdot + H_2O_2 \rightarrow H_2O + HO_2\cdot$

- Radiolysis of water:

$H_2O \sim> H^+ + HO\cdot + e^-(aq)$,

where the HO·radical can then react either by:

electron transfer: $HO\cdot + P \rightarrow OH^- + P\cdot^+$

abstraction: $HO\cdot + PH \rightarrow H_2O + P\cdot$

or addition to aromatic rings: $HO\cdot + P \rightarrow P\text{–}OH\cdot$

OPs rapidly decompose using a photoassisted Fenton reaction ($Fe^{3+}/H_2O_2/UV$). They are completely mineralized within few minutes, forming acids (HCl, HNO_3, H_3PO_4, H_2SO_4) and gases (CO_2, NH_3).

In the case of methyl parathion, the initial oxidant attack was oriented on the P=S group forming 4-nitrophenol, paraoxon, dimethyl phosphate and oxalate (Pignatello and Sun, 1995). Photodegradation studies of OP commercial products have shown an inhibition effect, mostly due to protective effect of inert materials, from which commercial products are made of. Complete loss of pure OPs occurred in most cases in less than 30 min under the acidic photo-Fenton advanced oxidation process using fluorescent blacklight UV irradiation (300-400 nm). Considerable mineralization over 120 min occurred in most cases as evidenced by the appearance of inorganic ions and the decline in total organic carbon (TOC) of the solution. The examples with little or no loss of TOC (malathion, glyphosate and disulfoton) are of concern because of the possibility that toxic byproducts are formed (Huston and Pignatelo, 1999).

Doong and Chang (1998) studied the photodegradation of five OPs in the presence of H_2O_2 and heterogeneous/homogeneous Fenton system. The addition of iron compounds (Fe^0, Fe^{2+}) enhanced the degradation and resulted in nearly complete removal of pesticide. The efficiency of degradation was given as the disappearance of pesticide. The by-products were not analyzed. They further investigated the photodegradation of parathion in water in the presence of TiO_2, and oxyanions produced during chlorination processes. These were shown to act as electron scavengers, enhancing the degradation in the sequence $ClO_2^- > IO_3^- > BrO_3^- > ClO_3^-$. Some possible intermediates, including also diethyl phosphoric acid were mentioned, but not quantified (Doong and Chang, 1998).

Phorate was almost completely destroyed (>95%) by photolytic ozonation. The initial step of the photolytic ozonation of phorate is considered to be the breakage and subsequent oxidation of the P=S double bond by hydroxyl radicals to form various reaction intermediates: phoratoxon, phorate sulfoxide and others, which were identified, but not quantified. The reaction rate was defined as the removal rate constants of phorate, and the formation rate constants of sulfate, phosphate, and carbonate (Ku and Lin, 2002).

Recently, Hirahara and co-workers (2003) studied the photodegradation products of fenthion in an aqueous solution by UVB irradiation (280–320 nm radiation) using rose bengal as photo sensitizer, and a known generator of singlet oxygen ($^1O_2$). The major photoproducts were identified as fenthion sulfoxide, 3-methyl-4-methylthiophenol (MMTP), dimethyl phosphorothioate and 3-methyl-4-methylsulfinylphenol (MMSP).

2.3.4 PHOTOCATALYTIC DEGRADATION

Generally, the photocatalytic degradation can be defined as a cyclic photo process in which the pesticide photodegrades, but spontaneous regeneration of catalyst occurs to allow the sequence to continue indefinitely until all the substrate is destroyed.

When TiO_2 absorbs radiation, which encompasses energy higher than the corresponding band gap (3.1 eV), electron-hole pairs are generated on the surface of TiO_2. The holes are either trapped by surface hydroxyl group to yield hydroxyl radical that attacks and destroy organic pesticide or recombines with electrons and inhibit the photocatalytic reaction process:

$$TiO_2 + h\nu \rightarrow TiO_2 (e_{cb-} + h_{vb+})$$
$$h_{vb+} + H_2O \rightarrow \cdot OH + H^+$$
$$e_{cb} + h_{vb+} \rightarrow TiO_2$$

In an oxygenated solution, O_2 may adsorb on the surface of titanium dioxide preventing the recombination process by trapping electrons resulting from the formation of superoxide radical anion and hydrogen peroxide (Mengyeu et al. 1995; Doong and Chang, 1997).

$$O_2 + e_{cb-} \rightarrow O_2^{—}\cdot$$
$$O_2^{—}\cdot + H^+ \rightarrow HO_2\cdot$$
$$HO_2\cdot + HO_2\cdot \rightarrow H_2O_2 + O_2$$
$$O_2^{—}\cdot + HO_2\cdot \rightarrow O_2 + HO_2^{—}\cdot$$
$$HO_2^{—}\cdot + H^+ \rightarrow H_2O_2$$

Hydrogen peroxide functions as an intermediate during the photocatalytic oxidation of OP with TiO_2. The concentration of oxygen decreases with the accumulation of H_2O_2. During the irradiation, the concentration of H_2O_2 reaches maximum, further irradiation results in a lower peroxide concentration. A decrease of H_2O_2 at longer irradiation times is a consequence of a faster reaction between the degradation products and H_2O_2 or the reaction of H_2O_2 with positive holes and electrons.

$$2\ h_{vb+} + H_2O_2 \rightarrow \cdot O_2 + 2\ H^+$$
$$2\ e_{cb-} + 2\ H^+ + H_2O_2 \rightarrow 2\ H_2O$$

The adsorption on the TiO_2 surface depends also on the pH of the solution. The surface of a TiO_2 particle is completely hydroxylated and has zero overall charge at pH ~ 6.6. As the pH is lowered, the number of protonated sites increases as does the overall positive charge on the particle. At high pH, the number of oxy-anion sites increases and the particle becomes negatively charged. These surface changes will directly affect surface adsorption and subsequent reactivity (O'Shea et al. 1997).

TiO_2 is nowadays one of the most widely used photocatalysts for pesticide destruction. However, before this procedure is proclaimed as a general and trouble free method it is required that the mechanism, and the forming new compounds are known in details. In fact, the assessment of pollutant disappearance in the early steps is not sufficient, since the heterogeneous catalysis may produce a variety of organic intermediates, which can be more toxic.

Oxidant attack of the hydroxyl radical on phosphorothiolates occurs firstly on the P=S bond resulting in the formation of oxon derivatives. The continuous attack of hydroxyl radicals on aromatic OPs leads to the rupture of P-O bond, with consequent formation of phenols. These are further degraded in quinonidal structures, and different trialkyl and dialkyl phosphorothioates or phosphate esters. All intermediates are, as the catalysis proceeds, subsequently mineralized into CO_2, NO_3^-, $H_2PO_4^-$, and SO_4^{2-} (Konstantinou and Albanis, 2003). The proposed photocatalytic degradation pathway is presented in Figure 1.

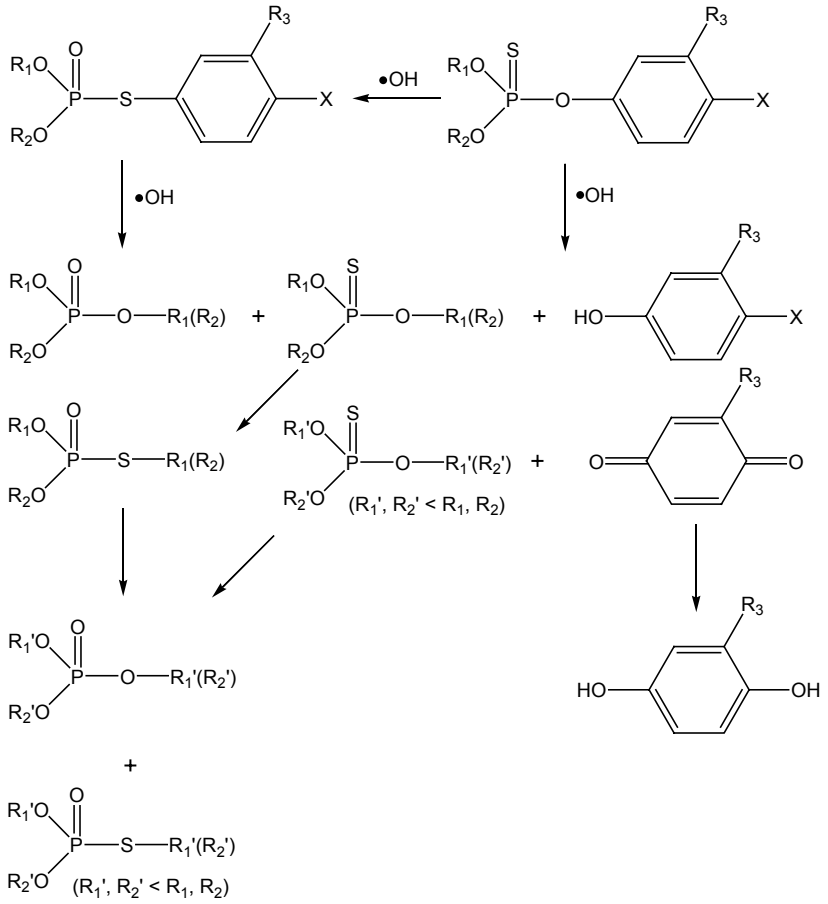

Figure 1: *Photocatalytic degradation pathways and main transformation products of aromatic organophosphorus insecticides in aqueous TiO_2 suspensions (Konstantinou and Albanis, 2003: 330).*

A number of photocatalytic studies were performed, varying the initial concentration of pesticide, amount of catalysts, airflow, type of artificial light source, pH, concentration of sensitizers, ions, time of exposure and other parameters, measuring only the remaining pesticide concentration, and/or the concentration of formed ions. However, very little attention has been devoted to the formation of intermediates. Organophosphates, which were degraded using TiO_2 and varying the catalytic parameters are: malathion (Muszkat et al. 1995), monochrotophos (Hua et al. 1995), dichlorvos, monocrotophos, parathion, and phorate (Mengyue et al., 1995), phorate, methamidophos, malathion, diazinon, and EPN (Doong and Chang, 1997), monochrotophos (Ku and Jung, 1998), dimethoate and azinphos-methyl (Dominguez et al., 1998), methamidophos (Malato et al. 2000), dichlorvos (Naman et al., 2002). These studies may be considered to be of limited importance, since nowadays the formation of by-products is of major concern.

Some authors, however, have over-crossed problems arising from qualitative and quantitative determination of by-products, and have proposed their tentative identification.

The photocatalytic removal of fenitrothion in TiO_2 suspension has been studied. Several intermediates of the photocatalytic photodegradation have been identified. These subsequently underwent mineralization (Kerzhentsev et al. 1996). The phosphonates DMMP and DEMP were readily decomposed by TiO_2 photocatalysis over a range of concentrations and solution pH. Mechanistic considerations imply that hydroxyl radicals were involved in the degradation of DMMP to methylphosphonic acid (O'Shea et al. 1997). When photocatalysts ($FeCl_3$, TiO_2) were employed the highly stable chlorpyrifos (30 days) was degraded in 15-27 minutes forming TCP, *O*-ethyl-*O*-(3,5,6-trichloro-2-pyridyl) phosphorothioate and chlorpyrifos-oxon (Penuela and Barcelo, 1997). Mansour and co-workers (1999) have found that when diazinon was irradiated in a water/soil suspension, it was isomerized to a product containing –S–(P=O)– group instead of the original –O–(P=S)–. The other two products were also diazoxon and hydroxy diazinon. Konstantinou et al. (2001) reported on the

photocatalytic degradation of OPs in aqueous TiO_2 suspension using simulated sunlight from a xenon lamp. The major photoproducts of photodegradation of ethyl bromophos and dichlofenthion were identified from the corresponding GC–MS (EI) fragmentation patterns, indicating oxidation and photohydrolysis pathways. Photocatalytic decomposition of fenthion and parathion was recently investigated employing SPME for monitoring their degradation products. The authors found the oxon analogues (paraoxon, fenoxon) of both insecticides being the primary products derived from the oxidizing attack of (·OH) and the substitution of sulfur by oxygen on the P=S bond. In the case of fenthion the oxidative process leads to the production of fenthion sulfoxide and fenthion sulfone as well as the fenoxon analogues. In both cases, the formation of the respective phenols from each insecticide (4-nitrophenol from ethyl parathion and 3-methyl-4-methylthiophenol from fenthion) was observed, as a consequence of splitting of the phosphorus–phenoxy bond. Measurable amounts of different alkyl phosphorothioate esters have also been identified, which is in agreement with other photocatalytic degradation studies (Sakkas et al. 2002). Kouloumbos and co-workers (2003) have studied the photocatalytic degradation of diazinon in TiO_2 aqueous suspensions and identified primary hydroxy derivates indicating that the mechanism of degradation was based on hydroxyl radical attack. The initial oxidative pathway of the degradation of diazinon involved the substitution of sulfur by oxygen on the P=S bond, cleavage of the pyrimidine ester bond, and oxidation of the isopropyl group.

2.4 Ozonation of organophosphorus compounds

Ozone, due to its powerful oxidizing potential has been applied efficiently to drinking water treatment and wastewater treatment. When it is transferred from the gaseous to liquid phase, it can react in two different ways: as an initiator of free radicals formed by the decomposition of ozone ($OH^{\cdot}$, $OH_2^{\cdot}$) or as a direct oxidation reagent (Laplanche et al., 1984). In the literature (Laplanche et al., 1984) different reaction schemes are proposed: for phosphorothioates (parathion, diethylchlorophosphate), a cycloaddition of ozone occurs on the double bond P=S before the breakdown of the molecule; for phosphorodithioates (malathion, phosalone, *O,O*-diethylphosphorodithioate), a competitive reaction between cycloaddition on P=S and electrophilic attack on the second sulfur atom (P–S–R) takes place; whereas for phosphoroamidates (dimefox, hexamethylphosphorotriamide), the electrophilic attack on the nitrogen dominates.

Application of ozone for OPs destruction was performed on diazinon (Ku et al., 1998), pirimiphos-methyl (Chiron et al., 1998), and two nerve agents VX {*O*-ethyl *S*-[2-(diisopropylamino) ethyl] methylphosphonothioate} and GD (pinacolyl methyl phosphonofluoridate) (Wagner et al., 2000), and phorate (Ku and Lin, 2002). The degradation efficiency of diazinon and phorate was evaluated by the formation of minerals (sulphate, nitrate, phosphate, and carbonate). Pirimiphos-methyl degrades under ozone treatment to several compounds. There are three major pathways including: N-oxime formation, N-dealkylation, and oxidation of methyl groups. The routes are followed by the induced hydrolysis. The VX and GD nerve agents behave totally different under the same experimental conditions. While VX ozonation resulted in several oxidation products, the GD was completely resistant to ozone and did not degrade or transform.

The efficiency of ozone in degradation of OPs is well known, however the stability and the toxicity of their intermediates have not been adequately evaluated. In a recent paper ozonated water was successfully employed for washing vegetables in order to remove residual pesticides (Wu et al., 2007a,b). The authors claimed, that, “Ozonation is a safe and promising process for the removal of the tested pesticides (diazinon, parathion, methyl-parathion, and cypermethrin) from aqueous solution and vegetable surface under domestic use.” (Wu et al., 2007a). It should be expected, that even without toxicological measurements, when oxons are formed in ozonated samples of OPs, the toxicity would be 100-1000 times higher than that expected from the parent compound.

2.5 Identification of by-products

Oxon derivatives appear to be the first products formed during AOPs of OPs since the difference between those intermediates and the parent compounds is only the substitution of sulfur by oxygen. But as the degradation proceedes, oxons, being relatively resistant, degrade further. Mineralisation is a target of all AOPs, but the results of several studies have suggested the formation of small, resistant and toxic compounds, like *O*-, and *S*- trimethyl phosphates, which were recognized as mammalian toxic substances (Chuckwudebe et al., 1989).

Underestimation of the toxicity of by-products is mainly the result of either very low concentrations, which need preconcentration step, including LLE, SPE, SPME, or their high polarity, resulting in low extraction yields from water. The intermediates often bear several hydroxy groups, which decrease their volatility, rendering GC analysis innappropriate (Chiron et al. 2000). Derivatisation with acidic BF_3-MeOH has one major drawback. The drastic experimental conditions may generate unrealistic by-products (Chiron and Fernandez-Alba, 1998). Among chromatographic methods GC/MS, using electron-ionisation and/or chemical-ionisation is particularly suitable and widely used in the identification of by-products. However, LC/MS is gaining in application, since polar, nonvolatile compounds could be analyzed directly, without derivatisation.

The problem remains when only partial degradation is envisaged, then toxicity testing becomes necessary (Chiron et al. 2000). To our knowledge only Dzyadevych et al. (2002) have investigated the toxicity of formed photoproducts using two toxicity test when studying the degradation of methyl parathion: a bioassay test (Lumistox) and conductometric biosensor technique (Dzyadevych et al. 2002, Dzyadevych and Chovelon 2002).

Table 2: *Comparison of different types of photosystems used for OP photodegradation experiments.*

ANALYTE	***PHOTOSYSTEM***	**ADITIVES**	***PHOTOREACTOR***	**KINETICS**	***MINERALIZATION / BY-PRODUCTS***	**REF.**
fenthion	*UVB*	$^1O_2$, rosebengal generator L-histidine and sodium azide as scavengers	*fluorescent UVB light 280 nm < l < 320 nm*		*photodegradation pathway and photoproducts given*	**Hirahara 2003**
diazinon	*UV/TiO_2*		*4/15W black blue lamps 300 nm < l < 400 nm*		*photodegradation pathway and photoproducts given*	**Kouloumbos et al., 2003**
phorate	*UV*	O_3 / p-nitrophenol, hydroquinone, riboflavine	*15 W low-pressure Hg lamp l = 254 nm*	various	*PO_4^{3-}, SO_4^{2-}, CO_3^{2-}*	**Ku and Lin 2002**
dichlorvos	*TiO_2, ZnO/UV, Vis* *TiO_2, V_xS_y/UV, Vis*	H_2O_2, pH, O_2	*150 W medium-pressure Hg lamp l = 365 nm*		*Cl^-* *photodegradation pathway and photoproducts given*	**Naman et al., 2002**
fenthion	*UV/TiO_2*		*Suntest CPS+*	0.0099/min-0.6383/min	*photodegradation pathway*	**Sakkas**
parathion			*xenon arc lamp 1500 W l > 290 nm*	0.012/min-0.2352/min	*and photoproducts given*	**et al., 2002**
bensulide, chlorpyrifos, EPN, diazinon, fenitrothion, fenthion, isofenfos, isoxathion, malathion, parathion-ethyl, tolchlorofos	*artificial sunlight*	cyclodextrins (a, b, g), humic acids	*artificial sunlight 250 W UV lamp*	max 45% increased k in humin + CyDb	*remaining pesticide %*	**Kamiya et al., 2001**
chlorpyrifos, cyanophos, diazinon, fenchlorfos, fenitrothion, iprobenfos, parathion, MPP	*UV*	humic acids, paramagnetic metals --> rate-retardation effect Cr(III)<Co(II)<Mn(II)<Cu(II)	*500 W UV lamp*		*TOC*	**Kamiya and Kameyama 2001**

… continuation of Table 2

ANALYTE	***PHOTOSYSTEM***	**ADITIVES**	***PHOTOREACTOR***	**KINETICS**	***MINERALIZATION / BY-PRODUCTS***	**REF.**
dichlofenthion	*UV/TiO_2*		*Suntest CPS+*	0.0456/min	*photodegradation pathway*	**Konstantinou**
bromofos ethyl			*xenon arc lamp 1500 W*	0.068/min	*and photoproducts*	**et al.,**
bromofos methyl			*I > 290 nm*	0.0195/min	*given for dichlofenthion*	**2001**
parathion ethyl				0.0456/min	*and bromofos methyl*	
parathion methyl				0.0346/min		
fenthion	*sunlight simulator/CO_3^{2-}*	lake water, bicarbonate, nitrate	*sunlight simulator Suntest CPS max 765 W/m^2*	0.0195/min-0.0384/min	*photodegradation pathway and photoproducts Given*	**Huang and Mabury 2000**
commercial products of pesticides	*pre-industrial solar reactor/ TiO_2*		*30 W/m^2 for 2 h around noon*		*TOC*	**Malato et al., 2000**
iprobenfos	*Vis*	poly (3-octylthiophene-2,5-diyl) film, O_2, Fe^{2+}	*500 W ultra-high-pressure Hg and W lamp 400 W high-pressure Hg lamp 8.1-0.62*10^{16} photons/ l s*		*photodegradation pathway and photoproducts given*	**Wen, et al., 2000**
alachlor, aldicarb,atrazine azinphos-methyl, captan, carbofuran, dicamba, disulfoton, glyphosate, malathion, methoxychlor, metolachlor, picloram,	*UV*	Fe (III), H_2O_2	*16 fluorescent black lamps, 14 W 300 nm < I < 400 nm $1.2x10^{19}$ photons/l s*	(1.6-3.8)10^4/s	*Cl^-, PO_4^{3-}, SO_4^{2-}, NO_3^- formate, oxalate, acetate TOC*	**Huston and Pignatello 1999**
diazinon	*UV*	water/soil	*124 W high-pressure Hg lamp I > 290 nm*		*photodegradation pathway and photoproducts given*	**Mansour et al., 1999**

… continuation of Table 2

ANALYTE	***PHOTOSYSTEM***	**ADITIVES**	***PHOTOREACTOR***	**KINETICS**	***MINERALIZATION / BY-PRODUCTS***	**REF.**
azinphos-methyl dimethoate	*artificial sunlight/TiO2*	Fe^{3+}	*400 W solar spectral distribution*		*remaining pesticide %*	**Dominguez et al., 1998**
methamidophos	*UV*	H_2O_2, Fe^0, Fe^{2+}	*100 W medium-pressure lamp*	0.019/min-0.021/min	*remaining pesticide %*	**Doong and**
malathion			*253 nm < l < 578 nm*	0.0039/min-0.012/min		**Chang**
diazinon				0.0025/min-0.011/min		**1998**
phorate				0.020/min-0.026/min		
EPN				0.0026/min-0.013/min		
parathion	*$UV/TiO_2/H_2O_2$*	O_2, N_2, oxyanion oxidants	*100 W medium-pressure lamp*	0.012/min-0.017/min	*photodegradation pathway*	**Doong and**
	$UV/Fe^0/H_2O_2$	$ClO_2^->IO_3^->BrO_3^->ClO_3^-$	*253 nm < l < 578 nm*	0.010/min-0.011/min	*and photoproducts*	**Chang**
	$UV/Fe^{2+}/H_2O_2$			0.011/min-0.012/min	*given*	**1998**
bensulide, chlorpyrifos, EPN,	*artificial sunlight*	humic acids, commercial,	*artificial sunlight*	0.009/day-0.067/day No HA	*remaining pesticide %*	**Kamiya**
diazinon, fenitrothion,		extracted from soil,	*250 W UV lamp*	0.013/day-0.083/day HA		**and**
fenthion, isofenfos,		humic acids-sodium salt				**Kameyama**
isoxathion, malathion,						**1998**
parathion-ethyl, tolchlorofos						
monochrotophos	*UV/TiO_2*	pH, O_2, N_2	*15 W black blue fluorescent llamp*	0.057/min-0.108/min, O_2	*CO_2*	**Ku and Jung**
			l = 365 nm	0.002/min-0.006/min, N_2		**1998**
methamidophos	*UV/TiO_2*	H_2O_2	*100 or 450 W*	0.051/min-0.054/ min	*remaining pesticide %*	**Doong and**
phorate	*UV/H_2O_2*		*medium-pressure Hg lamp*	0.054/min-0.055/ min		**Chang,**
diazinon	*$UV/TiO_2/H_2O_2$*		*253 nm < l < 578 nm*	0.024/min-0.025/ min		**1997**
malathion				0.017/min-0.026/ min		
EPN				0.008/min-0.011/ min		

… continuation of Table 2

ANALYTE	*PHOTOSYSTEM*	ADITIVES	*PHOTOREACTOR*	KINETICS	*MINERALIZATION / BY-PRODUCTS*	REF.
carbofuran	*UV/TiO_2*	TiO_2, H_2O_2, O_3, water, soil	*124 W high-pressure Hg lamp*		*photodegradation pathway*	**Mansour**
diazinon		humic acids, natural water	*I > 290 nm*		*and photoproducts*	**et al.,**
isoproturon		methanol, humic acids			*given*	**1997**
methamitron						
terbuthylazine		humic acids, O_2, N_2		0.021/h-0.11/h		
pendimethalin		humic acids				
dimethyl methyl phosphonate (DMMP)	*UV/TiO_2*	O_2, pH	*16 black-light phosphor lamps* *I = 350 nm*	0.03/min	*CO_2, PO_4^{3-} photodegradation pathway*	**O'Shea et al.,**
diethyl methyl phosphonate (DEMP)				0.02/min	*and photoproducts given*	**1997**
fenitrothion	*UV/TiO_2*		*125 W UV-lamp,* *$1.6x10^{17}$ photons/s* *I > 340 nm*		*CO_2, $H_2PO_4^-$, SO_4^{2-}, NO_3^- pathway and photoproducts given*	**Kerzhentsev et al., 1996**
monochrotophos	*UV/TiO_2*	O_2, H_2O_2 / Cl^-, ClO_4^-, NO_3^-, SO_4^{2-} Cu^{2+}	*20 (or 10) black light fluorescent tubes* *300 nm < I < 420 nm*		*remaining pesticide %*	**Hua et al., 1995**
parathion	*UV*	cyclodextrins (a, b, g)	*220 W high-pressure Hg lamp*	0.127/h-0.033/h	*remaining pesticide %*	**Kamiya**
paraoxon		b-CyD promotion	*I > 290 nm*	0.185/h-0.274/h		**and**
		effect on paraoxon and inhibition on parathion				**Nakamura, 1995**
dichlorvos	*UV/TiO_2*	H_2O_2, pH, O_2, Fe(III)	*375 W medium-pressure Hg lamp*		*PO_4^{3-}*	**Mengyue**
monochrotophos			*I > 300 nm*			**et al.,**
phorate, parathion						**1995**

… continuation of Table 2

ANALYTE	***PHOTOSYSTEM***	**ADITIVES**	***PHOTOREACTOR***	**KINETICS**	***MINERALIZATION / BY-PRODUCTS***	**REF.**
malathion/ commercial product	*sunlight/TiO_2*	natural sunlight		~ 0.012/min	*remaining pesticide %*	**Muszkat et al., 1995**
metolachlor methyl-parathion	*UV*	Fe^{3+}, H_2O_2	*fluorescent black lamp 300 nm < I < 400 nm $1x10^{18}$ photons/l s*		*HCl, NH_3, HNO_3, CO_2, H_3PO_4, H_2SO_4 photodegradation pathway and photoproducts given*	**Pignatello and Sun 1995**
fenitrothion	*UV*		*125 W high-pressure Hg lamp I ~ 254 nm*		*photodegradation pathway and photoproducts given*	**Durand et al., 1994**
butamiphos	*UV, Vis*	phosphate buffer, 2% acetone, river water, Et_2O	*500 W xenon arc lamp I > 290 nm*	0.239/min-0.032/min	*photodegradation pathway and photoproducts given*	**Katagi, 1993**
methyl parathion, fenthion, methidation, azinphos methyl, malathion, acephate	*UV sunlight*	in benzene	*UV / 5 Sylvania BL-40 fluorescent light natural sunlight*		*tentative identification of by-products*	**Chukwudebe 1989**
bromofos, iodofenfos	*artificial sunlight*	rainwater, soil	*3 TL 40/47 day-light lamp 1 TL 40/12 UVA lamp 1 TL 40/09 UVB lamp*		*main degradation products 4-bromo-2,5-dichlorophenol 2,5-dichloro-4-iodophenol*	**Allmaier and Schmid 1985**
36 pesticides OP, organochlorine, triazine, carbamate, pyrethroid	*UV pesticides on glass plates*		*RUL 3000 lamps I = 300 nm*	$265.2*10^{-7}$/s (dichlorvos)- $9.3*10^{-7}$/s (DDE) OP>carbamate>triazine> organochlorine>pyrethroid	*remaining pesticide %*	**Mao Chen et al., 1984**

3 EXPERIMENTAL - GENERAL

3.1 Materials

The pesticides and their metabolites used were at least 95% pure, so no further purification of the chemicals were needed. Diazinon, malathion, malaoxon, azinphos-methyl, chlorpyrifos were provided from RDH, isomalathion was purchased from Institute of Organic Industrial Chemistry (Poland) (98.4%), 2-isopropyl-6-methyl-4-pyrimidinol (IMP) from Aldrich, chlorpyrifos-oxon (94.5%) from Dr. Ehrensdorfer, 3,5,6-trichloro-2-pyridinol (99.4%) from RDH, 1,2,3-benzotriazin-4(3*H*)-one (98.0%) and diethyl maleate (97%) from Aldrich.

For the oxidation studies different oxidants were used: *N*-bromosuccinimide – NBS (Fluka), cerium ammonium nitrate - CAN and *m*-chloroperoxybenzoic acid – *m*CPBA were kindly provided from Faculty of Chemistry and Chemical Technology (University of Ljubljana, Ljubljana, Slovenia), iodine from RDH, potassium iodide from Lachema, potassium hydrogen monopersulfate - Oxone from Merck, 30% hydrogen peroxide from Carlo Erba, Arekina (sodium hypochlorite with 6% active chlorine) from Šampionka Renče (Renče, Slovenia). Reduction was achieved using ascorbic acid from Kemika Zagreb (Zagreb, Croatia).

Solvents used for extraction methods were obtained from different suppliers: ethyl acetate from Carlo Erba, hexane from RDH, which were dried over sodium sulfate – anhydrous purchased from RDH.

For the biosensor measurements acetylcholinesterase (AChE) from electric eel (950 IU mg^{-1}), acetylthiocholine iodide (ASChI), 5,5'-dithio-bis(2-nitrobenzoic acid) (DTNB), pyridine-2-aldoxime methiodide (2-PAM), controlled-pore glass (CPG 240, 80-120 mesh) were purchased from Sigma Chemicals, 25% glutardialdehyde, di-potassiumhydrogenphosphate, 3-aminopropyltriethoxysilane were obtained from Merck.

The organophosphate pesticides used and produced during this work can be presented by the following structural formulas (Fig. 2):

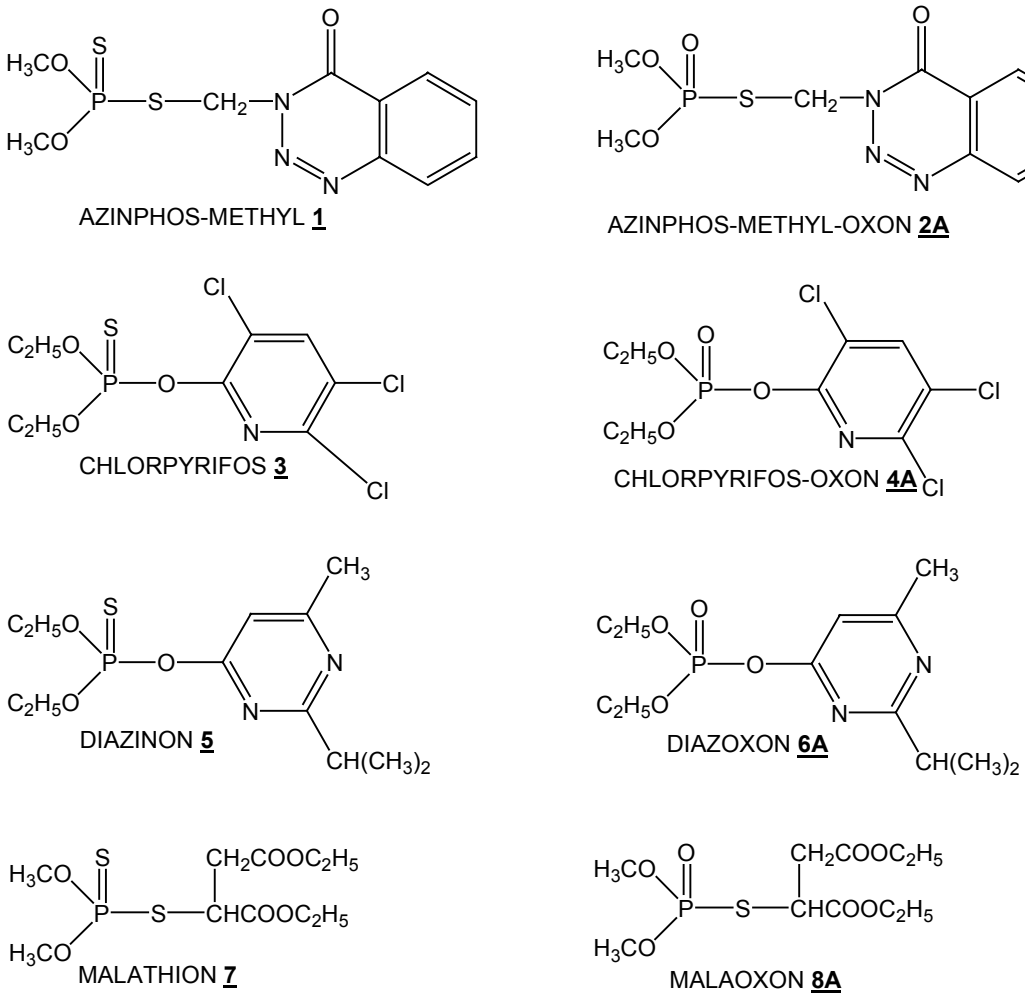

Figure 2: *The chemical structures of studied compounds.*

3.2 Extraction of pesticides

Two different extraction techniques were used during the study - liquid-liquid extraction (LLE) and solid phase extraction (SPE). SPE (100 mg Strata C18) retain a mass of solute (analyte plus retained contaminants) that is equivalent to approximately 5% of sorbent mass (in our case 5 mg). Thus SPE was not used in juice analysis, due to low reproducibility of extracted samples (Chapters: 4.1.2.2, 4.2.2.2, 4.3.2.2, 4.4.2.5.4, 4.5.2.6). Instead, LLE method was developed and was used for oxidation studies in apple juice and in chlorpyrifos degradation study (Chapters: 4.1.2.2, 4.5.2.6) to avoid break-through volumes or/and to retain more polar compounds.

3.3 Pesticide analysis

Pesticides were analyzed by several chromatographic techniques:
- gas chromatograph with electron captured detector and/or flame ionization detector (HP 6890 GC-ECD/FID)- chapter 4.1.2.3;
- gas chromatograph with mass spectrometry detector (Varian, Saturn 2100T GC-MS) – chapters: 4.1.2.3, 4.2.2.2, 4.3.2.2, 4.4.2.5.3, 4.5.2.5. Compounds collected in Table 3 were identified according to their mass spectra;
- high performance liquid chromatograph with diode-array detector (HP 1100 HPLC-DAD) – chapters: 4.2.2.2, 4.4.2.5.1, 4.5.2.4.1;
- liquid chromatograph with mass spectrometry detector (Applied Biosystem Q-Trap 3200 LC-MSD) – chapter 4.5.2.4.1;
- liquid chromatograph for ion chromatoghraphy with conductive detector(Shimadzu LC10Ai pump, operation module Shimadzu CBM10A and conductive detector Shimadzu CDD-6A; IC-CDD) – chapter 4.4.2.5.2.

Table 3: *Compounds identified according to mass spectra, listed by numbers, names, characteristic ions and chemical structures*

Compound name and index	Characteristic ions (m/z)	Chemical structure	Compound name and index	Characteristic ions (m/z)	Chemical structure
1 azinphos-methyl	160 (100%), 132 (84%), 104 (30%), 77 (85%)	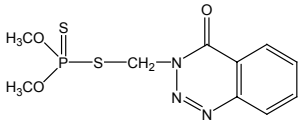	**2A** azinphos-methyl-oxon	160 (100%), 132 (75%), 104 (28%), 77 (72%)	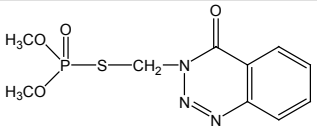
3 chlorpyrifos	316 (34%), 314 (47%), 199 (88%), 197 (91%), 97 (100%)	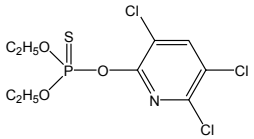	**4A** chlorpyrifos-oxon	300 (37%), 298 (52%), 272 (48%), 270 (73%), 199 (71%), 197 (77%)	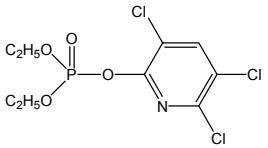
5 diazinon	304 [M^+] (47%), 179 (100%), 152 (70%), 137 (98%)	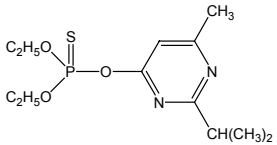	**6A** diazoxon	288 [M^+] (41%), 273 (77%), 152 (56%), 137 (100%)	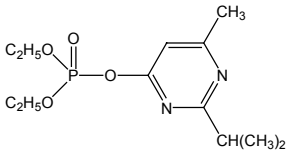
7 malathion	331 [M^+] (16%), 285 (31%), 173 (90%), 127 (100%);	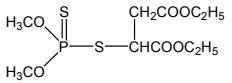	**8A** malaoxon	315 [M^+] (15%), 268 (27%), 173 (30%), 127 (100%), 99 (43%)	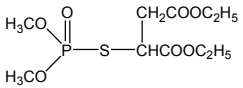
9A isomalathion	331 [M^+] (3%), 283 (42%), 173 (90%), 127 (100%), 99 (37%);	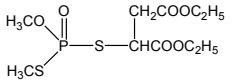	**10A** dimethoxyphosphinyl)oxo - butanedioic acid diethyl ester	315 [M^+] (3%), 269 (10%), 173 (100%), 127 (70%), 99 (27%)	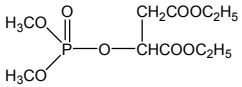
11A *O,O,S*-trimethyl phosphorothioate [OOS(O)]	156 [M^+] (49%), 110 (100%), 79 (63%)	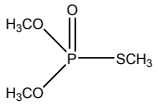	**12A** *O,O,S*-trimethyl phosphorodithionate [OOS(S)]	172 [M^+] (97%), 125 (78%), 93 (100%), 109 (25%), 79 (32%)	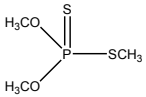
13A O,S,S-trimethyl phosphorodithioate [OSS(O)]	172 [M^+] (60%), 125 (100%), 79 (97%), 47 (90%)	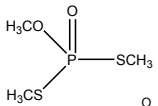	**14** 2-butenedioic acid (Z) diethylester – diethyl maleate	127 (50%), 99 (100%)	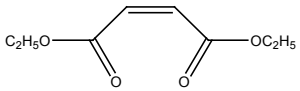
15 2-butenedioic acid (E) diethylester – diethyl fumarate	127 (100%), 99 (56%)	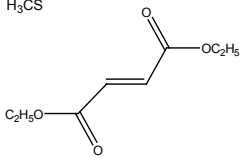	**16** butanedioic acid diethylester	129 (75%), 101 (100%)	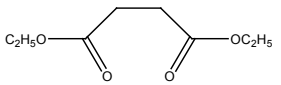

17 sulphanyl butanedioic acid diethyl ester	132 (60%), 104 (60%), 59 (55%), 45 (100%)	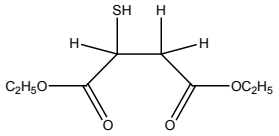	**18** hydroxy butanedioic acid diethylester	145 (25%), 117 (100%), 89 (51%), 71 (83%)	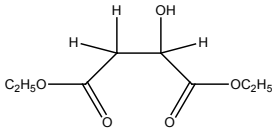
19 2,3-dihydroxy butanedioic acid diethylester	160 (70%), 132 (100%), 104 (35%), 87 (25%)	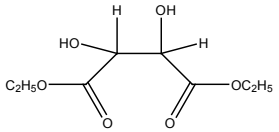	**20** hydroxy butenedioic acid diethylester	141 (28%), 127 (100%), 99(22%)	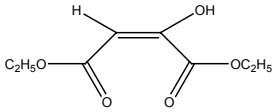
21 *cis*-2-hydroxy-3-sulphanylbutenedioic acid diethylester	220 (46%), 174 (75%), 146 (100%)	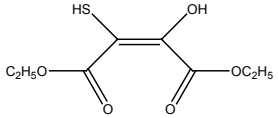	**22** diethyl methylsulfonyl-succinate	252 [M^+] (48%), 206 (76%), 178 (83%), 132 (100%), 103 (31%)	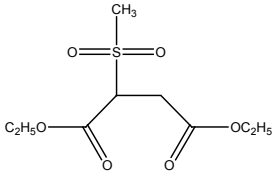
23 1,2,3 benzotriazin-4(1*H*)-one	147 [M^+] (100%), 104 (20%), 92 (62%), 76 (52%)	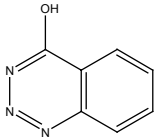	**24** 2-methyl-1,2,3 benzotriazin-4(1*H*)-one	162 [M^+] (20%), 148 (32%), 133 (56%), 105 (48%), 77 (100%)	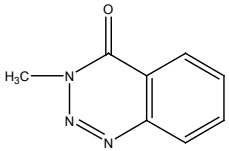
25 benzamide	121 [M^+] (68%), 105 (90%), 77 (100%)	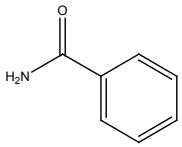	**26** 3,5,6-trichloro-2-pyridinol	201(26%), 199 (87%), 197 (91%) [M^+], 173 (29%), 171 (91%),169 (100%)	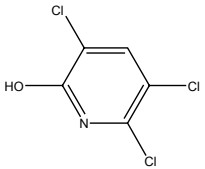
Notes:					
thio-OP	weak AChE inhibiting compound	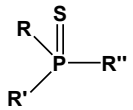	**oxo-OP**	powerful AChE inhibiting compound marked with index **A**	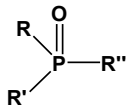

3.4 Calibration curves

According to the type of matrix and concentration levels, different range of pesticide concentration were measured and appropriate calibration curves were calculated. A detailed presentation is given under each of sub-chapters (4.1.2.4, 4.2.2.2, 4.3.2.2, 4.4.2.5.1, 4.4.2.5.2, 4.4.2.5.3, 4.5.2.4.1).

3.5 Biosensor characteristics

3.5.1 SOLUTIONS USED FOR BIOSENSOR STUDIES

0.05 M phosphate buffer containing 45 mM NaCl and 12 μM $MgCl_2$ (pH 8.0) was prepared by dissolving 8.7 g of K_2HPO_4, 2.6 g of NaCl and 6.4 mg $MgCl_2$ x $3H_2O$ in 1 L of deionised water. The pH was adjusted to 8.0 with 37% HCl.

The substrate acetylthiocholine iodide (ASChI) solution was prepared by dissolving 5 mg of ASChI in 3 ml of phosphate buffer and 1 ml of DTNB solution. DTNB solution was prepared by dissolving 4 mg of DTNB in 10 ml of phosphate buffer. The solution was prepared prior analysis and kept on ice to avoid non-enzymatic hydrolysis.

Pyridine-2-aldoxime (2-PAM) was used as a regenerator of inhibited enzyme and was prepared in 4 mM concentration in phosphate buffer.

Pesticide working solutions were prepared daily to avoid decomposition.

3.5.2 ENZYME IMMOBILIZATION

Several immobilization techniques could be appropriate for the purpose of this work. However, a simple cross-linking with glutaraldehyde and binding to the activated controlled porosity glass according to immobilization procedure described in literature (Pogačnik and Franko, 1999, 2001a,b, 2003) was chosen.

The procedure is as follows:
Pre-cleaning step: 2 g of CPG-240 was boiled in 5% nitric acid for 30 min. The CPG-240 was filtered on a glass filter, washed with deionised water and dried in an oven at 95°C.
Aminoalkylating step: the pH of 3-aminopropyltriethoxysilane was adjusted to 3.5 with hydrochloric acid. The dried CPG-240 glass was added, and the mixture was kept at 75°C on a water bath for 150 min, the flask being swirled every 15 min. The alkylamination process was repeated to ensure complete activation of the glass.
Cross-linking: the cross-linking agent, a solution of glutaraldehyde was prepared in phosphate buffer. Alkylamino glass was added to glutaraldehyde-buffer solution in a vessel, which was put under reduced air pressure for 15 min in order to remove air from CPG-240. The treated glass was washed well with deionised water.
Enzyme-immobilization: 50 μL of AChE from electric eel was dissolved in a cold (4°C) phosphate buffer (0.1 M, pH 6.0) and added to the pre-treated glass. Nitrogen was bubbled through the solution

at 4°C for 2.5 h. The immobilized enzyme was washed first with cold phosphate buffer and then with cold water to ensure the removal of any unlinked enzyme. The beads were stored at 4°C in phosphate buffer (pH 6.0).

No decrease in activity of the stock immobilized enzyme was observed after storage for 4 months. The immobilized enzyme was packed into a bioanalytical column as needed.

3.5.3 DETERMINATION OF ENZYME ACTIVITY

The enzyme activity was assayed according to Ellman reaction (Ellman et al., 1961). Acetylthiocholine iodide (ACSChI) was applied as the enzyme substrate with 5,5-dithio-bis-2-nitrobenzoic acid (DTNB) as a chromogenic reagent. The product of enzymatic reaction is 5-thio-2-nitrobenzoate with absorption maximum at 410 nm (in buffer solution) and was detected optically. The substrate solution was prepared by dissolving 5 mg of ACSChI in 3 ml of phosphate buffer and mixing it with 1 ml of DTNB solution (4 mg DTNB dissolved in 10 ml of phosphate buffer). The solution was prepared fresh for each set of experiments and kept on ice to avoid non-enzymatic hydrolysis.

3.5.4 THE BIOANALYTICAL FIA SET-UP WITH TLS AS A DETECTION UNIT

The flow-injection analysis manifold used in this work consisted of an IC pump, two injection valves, a reactor with immobilized enzyme and the detection unit. The carrier phosphate buffer (pH 8.0) was pumped through the system at flow rates from 0.5 ml min^{-1}. To determine the initial enzyme activity (a_0) in the bioanalytical column the substrate was injected through the first injection valve equipped with a 20 µL injection loop (for approximately 5-times). This was followed by injection of the sample containing the pesticide through the second injection valve with 200 µL injection loop. The determination of final enzyme activity (a_r) was carried out by another injection of the substrate through the first injection valve (for approximately 5-times) and calculation of remaining enzyme activity according to the formula (i), where a_r and a_0 are averages of four signal intensities (when five injections were made, the first intensity was not considered):

$$A = a_r / a_0 \qquad \text{(i)}$$

Each bioanalytical column was used for several determinations of the pesticide as long as the activity of the enzyme dropped to 90%, than a reactivation using 2-PAM was performed. When the reactivation with 2-PAM could not reach the initial activity, it was replaced with the fresh one. Around 10 mg of the immobilized enzyme was generally filled in the bioanalytical column, making the biosensor analysis more repeatable, since the initial activity was all the time the same. The biosensor was daily calibrated with 500 ppb malaoxon (Figure 3), which express a 50% inhibition and was afterwards reactivated with 2-PAM. With this a reliable intercheck of the system was introduced.

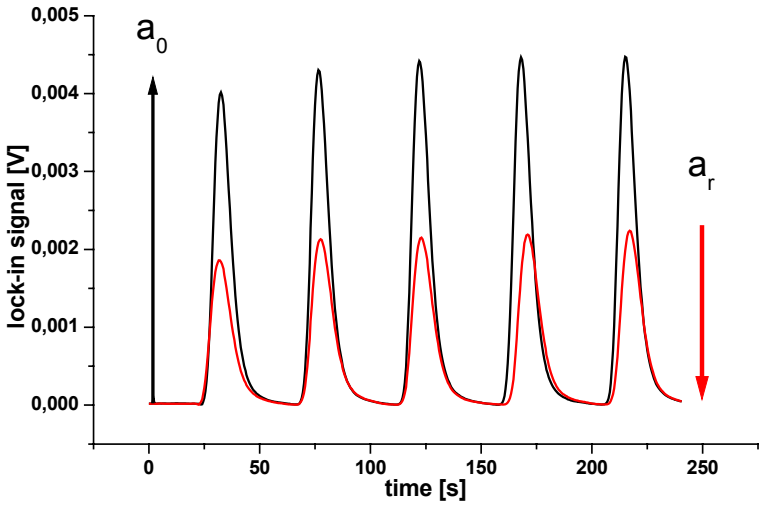

Figure 3: *The evolution of TLS signals before (active AChE) and after inhibition (inhibited AChE) with 500 ppb malaoxon.*

A dual-beam thermal lens spectrometer (TLS) was used as the detection unit. The Argon-ion laser (Ar+) operating at 488 nm (250 mW) was the excitation source and the helium–neon laser (He–Ne) provided the probe beam at 632.8 nm (7 mW). A variable-speed mechanical chopper modulated the pump beam from the argon ion laser at 10 Hz. A collinear propagation of the pump and the probe beams was obtained by a dichroic mirror. The change in the probe beam intensity was monitored by a photodiode, which was fed into a lock-in amplifier with a time constant (1 s). The output of the photodiode was fed into a lock-in amplifier with a time constant (300 ms) (Pogačnik and Franko, 2003). In Figure 4, there is a graphical representation of TLS system for the detection of pesticides used in our laboratory.

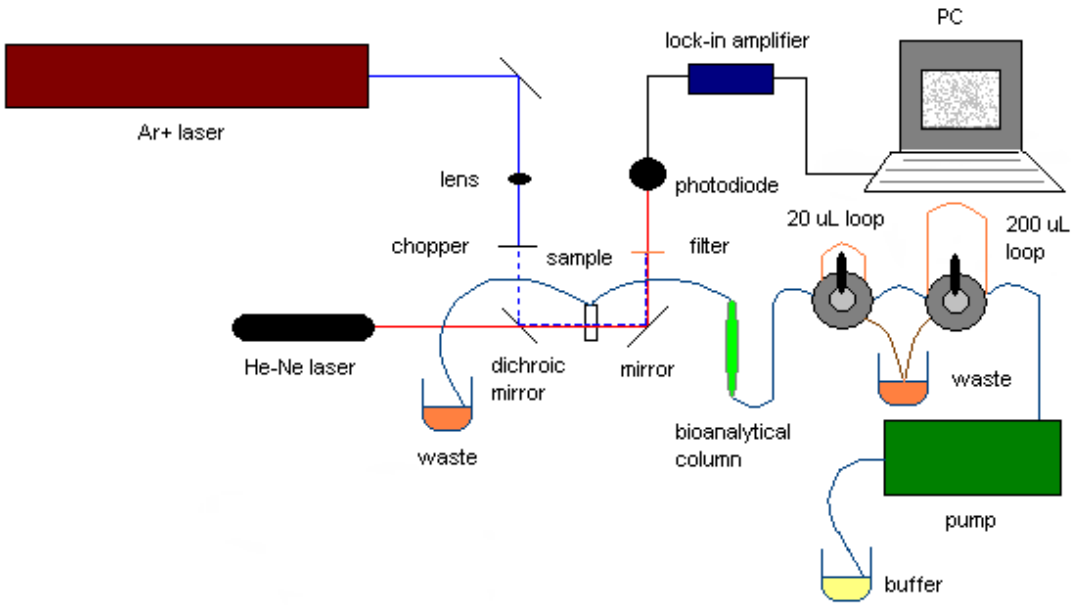

Figure 4: *A schematic diagram of the bioanalytical FIA set up with TLS as a detection unit.*

4 RESULTS AND DISCUSSION

4.1 Oxidation as a pre-step in determination of organophosphorus compounds by AchE-TLS bioassay (Bavcon Kralj et al., 2006)

4.1.1 INTRODUCTION

The biosensors and related bioanalytical techniques are nowadays an alternative for approaching the large amount of daily-based analysis in pesticide residues, which have been covered by the employment of highly sophisticated and time-consuming chromatographic techniques. In most bioassays for organophosphorus pesticides, the inhibition of enzymatic activity, in particular acetylcholine esterase (AChE) and butyrylcholine esterase (BChE), is most frequently exploited (Mello and Kubota, 2002). Generally, the amount of detected pesticides is reported as a cumulative concentration of all present AChE inhibiting compounds, expressed in equivalents of pesticide used for calibration (usually paraoxon).

Several biosensor/bioassay set-ups are based upon flow injection analysis (FIA) for the reasons of optimization, reduction of time, and higher reproducibility (Dornelles Mello and Kubota, 2002; Patel, 2002; Marty et al., 1995). The performance of AChE-FIA assays was further improved, and LOD's lowered by introducing a highly sensitive method of optical detection relying on thermal lens spectrometry (TLS) developed in our laboratory (Pogačnik and Franko, 1999; 2001; 2003).

OPs and their metabolites in environmental matrices are generally present in small quantities (ppb-, rarely in ppm- concentration range). Therefore, the extraction of these compounds from solid matrices or their preconcentration from aqueous media is frequently needed and requires the use of organic solvents, depending on the solubility of extracted pesticide or group of pesticides (Mionetto et al., 1994; Fennouh et al., 1997; Wilkins et al., 2000; Montesinos et al., 2001; Andreescu et al., 2002). Furthermore, the detection of thio-OPs, which are due to agricultural practice the dominant form of OPs in environmental matrices, requires oxidation of thio-OPs into their oxo analogues, because the thio-OPs are much weaker inhibitors or do not inhibit AChE at all. For this purpose bromine (Kumaran and Tran-Minh 1992; Kumaran and Morita 1995; Kim et al., 2000; Lee et al., 2002) and *N*-bromosuccinimide (NBS) (Marty et al., 1995; Herzsprung et al., 1990; Barcelo et al., 1995; Schultze et al., 2002, 2003) were introduced as selective and rapid oxidants to enhance inhibition in determination of thio-OPs by biosensors. H. Schulze and his research group have developed the first biosensor method for the detection of phosphorothionates in food. They used NBS as an oxidizing reagent (Schultze et al., 2002, 2003, 2004). However the complete assay could not be performed in less than 2 h (Schultze et al., 2003).

Other methods of oxidations were also developed till now, but were mainly intended for synthesis of oxons from thio-phosphates (Chapter 2.2.2). It is therefore evident that modifications of existing oxidation methods are needed to avoid false negative results and provide an adequate means for a rapid routine bioanalytical assay as is required in methods for low cost screening of large number of samples.

The aim of our work was thus to search for a rapid, sufficiently effective and specific conversion of selected thio-OPs into oxo-OPs (Figure 2), which could be performed without any preconcentration or extraction step and under normal laboratory conditions in order to enable determination of thio-OPs by the FIA-AChE bioassay with TLS detection.

4.1.2 EXPERIMENTAL

4.1.2.1 Oxidation procedure

Pesticide stock solutions were prepared by diluting approximately 10 mg of pesticide in 10 mL of ethanol. Standard pesticide stock solutions were held in refrigerator until used. Working solutions were prepared daily by diluting 1 mL of standard stock solution in ethanol to 100 mL of water or apple juice. Working solutions of 10 ppm were then further diluted to desired concentrations as needed.

Oxidants and solutions of reducing agents were prepared daily. The volumes of the analytes, oxidants and reducing agents solutions were always in 1 : 1 : 1 volume ratio. In the oxidation experiments, the pesticide concentration ranged from 300 ppb to 10 ppm, the concentration of oxidants was varied to obtain different pesticide to oxidant molar ratios (from 1:1, 1:2, 1:5, 1:10, 1:50, 1:100, 1:500, to 1:1000), whereas the concentration of reducing agent was always set 10 – times higher than the oxidant concentration. The oxidation reaction was allowed to proceed for 5 min only, and was quenched by the addition of a reducing agent.

4.1.2.2 Extraction of pesticides

For the GC analysis of samples two different extraction techniques were used - liquid-liquid extraction (LLE) and solid phase extraction (SPE). LLE extraction was used for oxidation studies in apple juice to avoid exceeding break-through volumes. SPE cartridges (100 mg Strata C18) are specified to retain a mass of solute (analyte plus retained contaminants) that is equivalent to approximately 5% of sorbent mass (in our case 5 mg). Thus SPE was not used in juice analysis, due to low reproducibility. Previously developed LLE method (Bavcon et al., 2003) was used instead.

SPE method was used for extraction of pesticides from water samples. General procedure was as follows: cartridge conditioning step: 3 mL of ethyl acetate, 3 mL of methanol, 5 mL of deionised water; sample load: 10 mL of water samples; analyte elution: 3 mL of ethyl acetate; preconcentration step on rotary evaporator. Samples were then rediluted either in ethyl acetate (GC-MS) or in hexane (GC-ECD; GC-MS).

As mentioned, LLE was generally used for extraction of apple juice samples. 10 mL of oxidant solution was added to a 10 mL sample of spiked apple juice, and after 5 min 10 mL of reducent solution was added. After that, an aliquot of 10 mL was taken and extracted with ethyl acetate (60 mL) with the addition of 50 mL Na_2SO_4 water solution (10%). The organic phase was separated and dried over anhydrous Na_2SO_4, evaporated to dryness; the residue was redissolved in 1 mL hexane and analyzed by GC/ECD and GC/MS.

4.1.2.3 Analysis of pesticides

Ethyl acetate and hexane extracts were analyzed by gas chromatography coupled with electron capture detector GC-μECD (HP 6890) and gas chromatography – mass spectrometry (Varian, Saturn 2100T). A non-polar SPB-1 column (100% polydimethylsiloxane; 30 m × 0.53 mm; film thickness 3 μm) was used for separation in GC-μECD system, whereas a CP-Sil 8 CB low bleed/MS column (5% phenyl - 95% methylpolysiloxane, 30 m × 0.25 mm; film thickness 0.25 μm) was used in the GC-MS system. Temperature programme was the same in both systems: injector was held at 220 °C, oven temperature started at 80 °C, and was increasing with a gradient of 10 °C min^{-1} till 290 °C and maintained constant for 5 min. The injection volume was in all cases 1 μL, the exception was only in case of azinphos-methyl. Due to low sensitivity to this pesticide 2 μL of extracts were injected in GC-MS. In all cases two replicates were performed. The target and qualifier ions of OPs analyzed by GC-MS are summarized in Table 4.

Table 4: *List of target and qualifier ions for formed oxo-OPs*

Organophosphate	*Target ion*	Qualifier ions	
	77	**132**	**160**
Azinphos-methyl-oxon **2A**	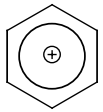	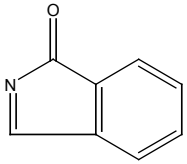	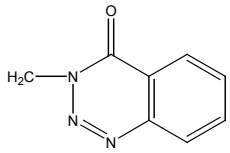
	197	**270**	**298**
Chlorpyrifos-oxon **4A**	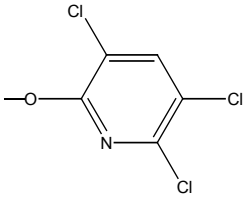	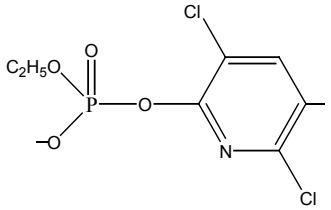	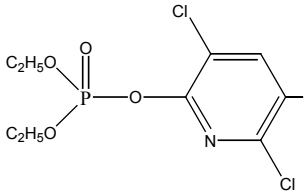
	137	**273**	
Diazoxon **6A**	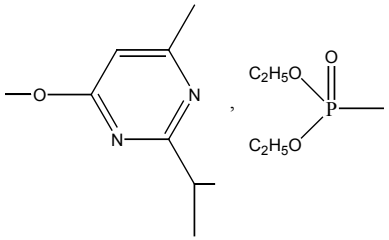	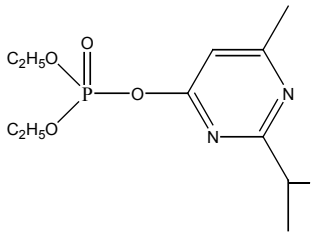	
	99	**127**	**268**
Malaoxon **8A**	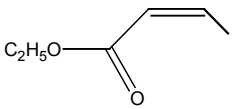	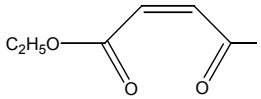	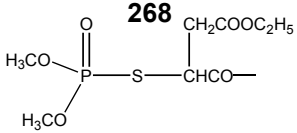

4.1.2.4 Calibration curves

For the oxidation studies in water samples, a SPE extraction was used. The respective extraction recoveries were: (92 ± 10) % for azinphos methyl, (88 ± 4) % for chlorpyrifos, (89 ± 2) % for diazinon, (93 ± 5) % for malathion, and (95 ± 10) % for malaoxon. The r-square values of individual regression lines ranged from r^2 = 0.9867 for malaoxon to r^2 = 0.999 for malathion. When the oxidations were performed in apple juice, which is a far more complex matrix than water, the SPE gave low recoveries and irreproducible results. For this purpose a liquid-liquid extraction was performed yielding the respective extraction recoveries: (45 ± 2) % for chlorpyrifos, (66.5 ± 0.3) % for diazinon, (97 ± 3) % for malathion, and (93 ± 9) % for malaoxon. The r-square values of individual regression lines ranged from r^2 = 0.9934 for malaoxon to r^2 = 1.000 for diazinon. Despite the low recoveries in case of some pesticides, e.i. chlorpyrifos and diazinon, the described method enabled the determinations with the RSD in the range of 5-15%.

4.1.3 RESULTS AND DISCUSSION

4.1.3.1 Testing different oxidants

To investigate the efficiency of oxidation in matrices such as water and fruit juice several oxidants (NBS, sodium hypochlorite, peroxide, CAN, mCPBA, iodine and Oxone) and pesticides (azinphos-methyl, chlorpyrifos, diazinon and malathion) in different molar ratios (from 1:1, 1:2, 1:5, 1:10, 1:50, 1:100, 1:500, to 1:1000 pesticide : oxidant molar ratio) were tested in order to determine the most appropriate ratio. Since the kinetics of oxidation is favorable in acidic conditions (reaction within 5 min), the pH of oxidant solution was corrected to pH 2.0 with acids, peroxide with perchloric acid, CAN with nitric acid, Oxone is acidic by itself, whereas in the case of NBS (pH 5.3), sodium hypochlorite and iodine pH was not corrected.

The comparison of data obtained from GC-MS chromatograms and spectra showed that an efficient conversion into oxons in water samples was achieved using NBS and hypochlorite in the molar ratio of 1:10. No conversion into oxons was noticed using oxidants from 1:1 to 1:10 in juice samples, due to naturally present reducing compounds. Thus a higher molar ratio (1:50) was used, yielding satisfactory results in case of NBS and hypochlorite. By increasing the concentration of oxidants, which were not efficient at lower concentrations, a disappearance of formed oxons compared to amounts expected from stoichiometry was observed (Table 5).

Table 5: *The oxidation efficiency of selected oxidants (molar ratios are given in brackets beside each oxidant) on thio-OPs (column in italics) conversion to oxo-OPs (column in bold) in apple juice*

Oxidant / OPs	*Remaining diazinon*	Formed diazooxon	*Remaining malathion*	Formed malaoxon	*Remaining chlorpyrifos*	Formed chlorpyrifos-oxon
NBS (1:50)	*4%*	**det. ↓**	*0%*	**det. ↑**	*15%*	**det. ↑**
NBS (1:100)	*0%*	**n.d.**	*0%*	**det. ↓**	*0%*	**det. ↓**
NBS (1:500)	*0%*	**n.d.**	*0%*	**det. ↓**	*0%*	**det. ↓**
NBS (1:1000)	*0%*	**n.d.**	*0%*	**det. ↓**	*0%*	**det. ↓**
CAN (1:50)			*68%*	**n.d.**		
H_2O_2 (1:50)			*82%*	**n.d.**		
H_2O_2 (1:500)	*100%*	**n.d.**			*100%*	**n.d.**
I_2 (1:50)			*90%*	**n.d.**		
***m*-CPBA (1:50)**			*35%*	**n.d.**		
Oxone (1:50)			*77%*	**n.d.**		
Oxone (1:500)	*66%*	**n.d.**			*72%*	**n.d.**
hypochlorite (1:50)	*21%*	**det. ↑**			*28%*	**det. ↓**

Notes:
det. ↑ – maximal signal area of detected oxon
det. ↓ – signal area of detected oxon in decrease
n.d. – oxon not detected

This can be explained by the consecutive oxidation of the oxons, resulting in the formation of more polar compounds, which were not efficiently extracted in ethyl acetate and therefore not detected by GC-MS. At oxidations using lower pesticide:oxidant molar ratio (1:50 and lower), this phenomenon was not observed.

Chromatograms of samples from oxidation of malathion to malaoxon using various oxidants are collected in Figure 5, and show that the only efficient oxidant in case of malathion was NBS.

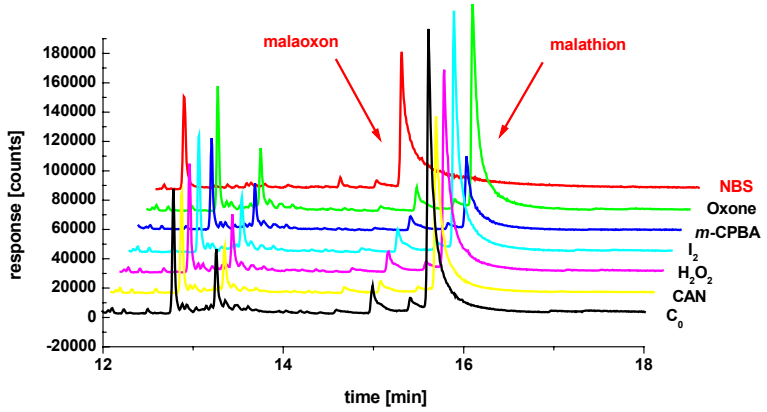

Figure 5: *GC-MS chromatograms of malathion oxidation to malaoxon by various oxidants*

Similar results were obtained with other OPs (data not shown). The only exception was noticed in case of diazinon, which expressed promoted hydrolysis under experimental conditions governed by

the low pH of the juice (pH 3.2). For this purpose, the use of sodium hypochlorite, which was corrected to basic pH 12.0; seemed to be an alternative to avoid induced hydrolysis (Figure 6). In fact, diazinon is a particularity, since it is susceptible to acidic hydrolysis, whereas the majority of OPs are hydrolyzed in basic pH, like most esters (Chambers and Levi, Eds.,1992).

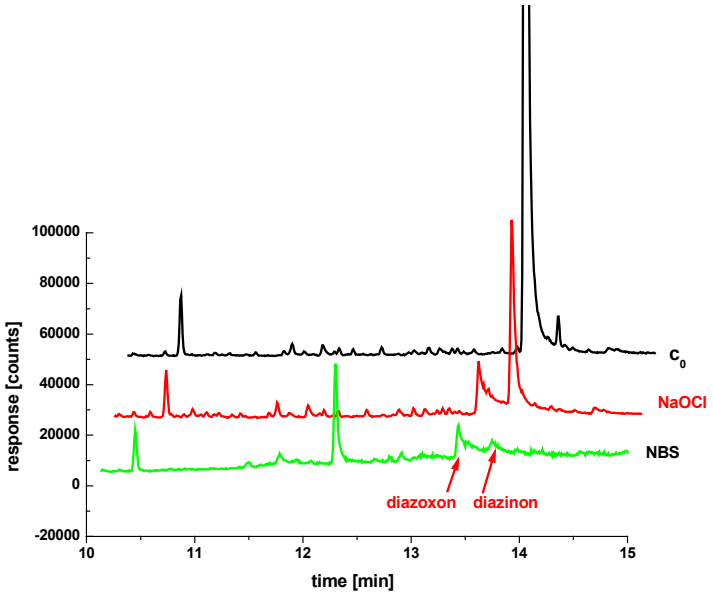

Figure 6: *GC-MS chromatograms of diazinon oxidation to diazoxon by NBS and sodium hypochlorite*

4.1.3.2 The effect of pH and reducing agents on oxidation efficiency in apple juice

Since the AChE bioassay should be performed in neutral-basic pH range (7.4 – 8.0); a correction of pH is needed prior to analysis of acidic juices (pH 3.2). In this experiment the oxidation efficiency after the use of three different reducing agents was determined before and following the adjustment of juice's pH. The experiment was run in natural apple juice (pH 3.2) and pH corrected apple juice (pH 7.4), using a final concentration of malathion of 9.0 ppm. The concentration of NBS was 50-times higher, whereas the concentrations of ascorbic acid (pH 3.2), sodium ascorbate (pH 7.2), and glucose (pH 6.6) as reducing agents were 500-times higher compared to the malathion concentration. Glucose was chosen as a substitute for ascorbic acid or ascorbate, since it is normally present in juices and should thus not interfere with the bioassay. Sodium hydroxide was used to correct the pH of apple juice. As can be seen in Figure 7 the effect of pH of reducing agents is negligible, whereas the effect of the pH of matrix, thus apple juice, is far more important. Since the oxidations are favorable in acidic conditions, the corrections of pH prior to bioanalytical measurements should be done after the oxidation.

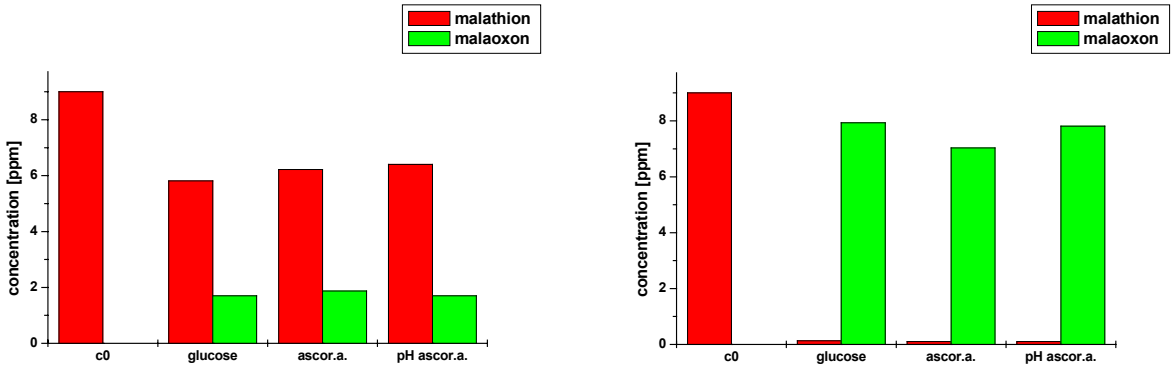

Figure 7: *The conversion of malathion to malaoxon in pH corrected apple juice (pH 7.2) – left and in natural apple juice (pH 3.2) – right*

4.1.3.3 The effect of oxidation procedure on the AChE-bioassay

Prior to inhibition measurements with AChE bioassay, NBS as an oxidant and ascorbic acid as a reducing agent were tested as potential inhibitors of AChE. Their presence resulted in no decrease of enzyme activity (Figure 8).

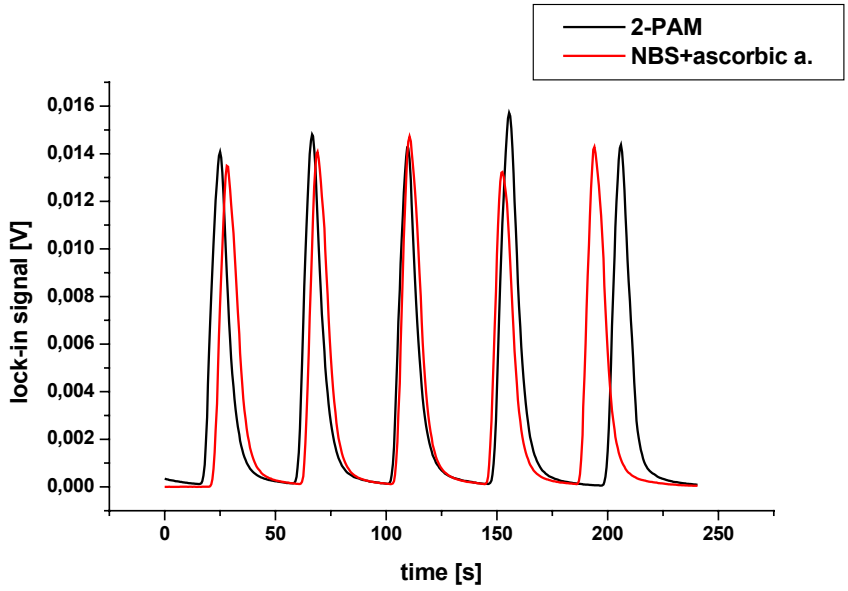

Figure 8: *The effect of NBS and ascorbic acid on the activity of AChE*

To evaluate the suitability of the described AChE - bioassay for detection of phosphorothionates (thio-OPs), samples spiked with the selected thio-OPs (azinphos-methyl – 15.4 ppm, chlorpyrifos – 20.8 ppm, malathion – 9 ppm) were oxidized with NBS. The oxidized samples were split in two. One part was chromatographically separated on the GC-MS system to check for the quantitative conversion of the thio-OPs into the oxo-OPs, which was satisfactorily achieved in 5 min. The second part of the sample was checked for the inhibitory power of the formed oxo-OPs on the AChE enzyme. No decrease in activity of the enzyme due to native thio-OPs substances was observed, whereas a complete inhibition was achieved when the oxidized samples were injected into the bioanalytical column. To obtain a reasonable inhibition curve supplementary dilutions of samples were needed, since oxons are far more powerful inhibitors.
After the oxidation inhibitions of AChE activity from 10 to 80 % were observed for chlorpyrifos in 35 – 350 ppb concentration range, for malathion in 100 – 1000 ppb concentration range, and for azinphos-

methyl in the 12.5 – 100 ppb concentration range (Figure 9). The lower limits of given concentration ranges are also representing the LOD values for determination of corresponding pesticides, which are in all cases well below the maximal residue limits for OPs in foodstuffs (Official Gazette of RS, 13 and 54,1999).

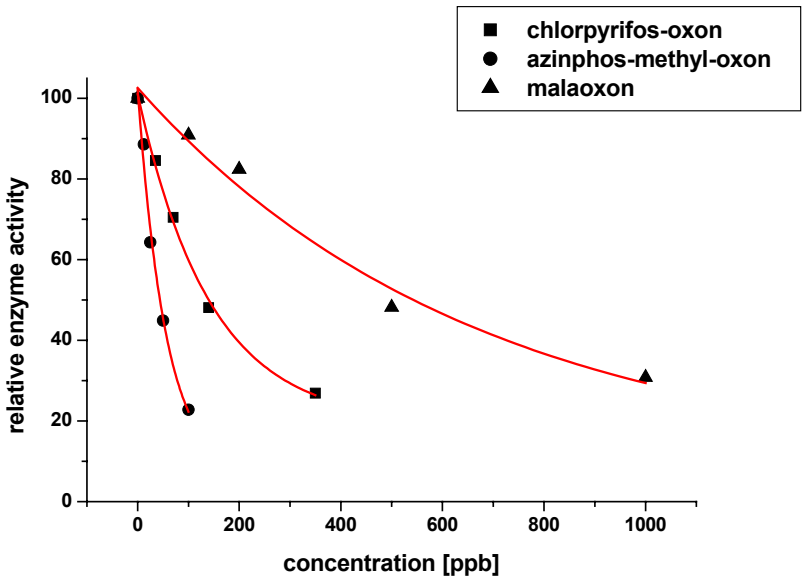

Figure 9: *Inhibition curves for detection of malathion, chlorpyrifos and azinphos-methyl after oxidation to their respective oxons by the FIA AChE-TLS bioassay*

4.1.4 CONCLUSIONS

The oxidation with different commonly used oxidants (NBS, sodium hypochlorite, *m*-CPBA, Oxone, CAN, iodine water, hydrogen peroxide) and reducing agents (glucose, ascorbic acid) has shown that a reliable, rapid and selective oxidation of phosphorothionates (model compounds: malathion, diazinon, chlorpyrifos, azinphos-methyl) to their respective oxons (malaoxon, diazoxon, chlorpyrifos-oxon, azinphos-methyl-oxon) can be achieved with NBS and sodium hypochlorite within five minutes. The oxidizing and reducing agents were directly added to water or juice. Time of analysis was therefore reduced in contrast to previously reported oxidation procedures, since no preconcentration, extraction or other analytical step was needed. The AChE bioassay based on the investigated oxidation procedure enables determination of thio-OPs in the ppb concentration range in less than 15 minutes.

4.2 Photodegradation of organophosphorus insecticides – investigations of products and their toxicity using gas chromatography-mass spectrometry and AChE-thermal lens spectrometric bioassay (Bavcon-Kralj et al., 2007)

4.2.1 INTRODUCTION

The extensive use of pesticides to enlarge the production in agriculture and the intensive development of new chemicals has dramatically increased the variety and quantities of agrochemicals present in environment. The natural degradation pathway of OPs applied on field includes mainly homogeneous and heterogeneous hydrolysis, which is enhanced by the presence of dissolved metals, humic substances, microorganisms and other compounds present in soil (Noblet et al., 1996; Dannenberg and Pehkonen, 1998; Pehkonen and Zhang, 2002). Next among the triggers of OP environmental degradation pathways is the irradiation by sunlight (Pehkonen and Zhang, 2002).

All these natural occurring degradation processes were exploited in research and development of treatments for purification of polluted water. Progress in the field of chemical water treatment resulted in several oxidative degradation procedures based on the generation of highly reactive intermediates that initiate a sequence of reactions resulting in the destruction and removal of organic pollutants. They are generally referred to as advanced oxidation processes (AOPs), which can be sorted into two main groups: photochemical processes and ozonation processes (Burrows et al., 2002).

One of the earliest studies regarding photolysis of OPs has proven the formation of toxic photoproducts, i.e., *O-,* and *S-* trimethyl phosphates, which were till then known as toxic by-products in the synthesis of active OP compounds (Ali and Fukuto, 1982; Chukwudebe et al. 1989). Later photolytic studies of direct OP irradiation under different light sources (natural summer sunlight, suntest apparatus, Hg and Xe lamps) revealed different kinetics, mechanisms, and by-products, including the formation of more toxic oxons (Katagi, 1993; Durand et al., 1994; Bin Wan et al.1994; Zamy et al. 2004). However, the most efficient pathway of OP degradation remains indirect photolysis. The enhanced photosensitizing effects on OPs were studied using humic substances, metal ions, cyclodextrins (Kamiya and Kameyama, 1998, Ishiwata and Kamiya, 1999; Kamiya and Kameyama, 2001). AOPs, which rely on action of hydroxyl radicals (HO·) (Penuela and Barcelo, 1998; Burrows et al., 2002) and photocatalysts (Muszkat et al. 1995, Doong and Chang, 1997, Dominguez et al., 1998), result in complete mineralization of the starting compounds (OPs), but undesired toxic photoproducts are sometimes formed as well (Pignatello and Sun, 1995; Huston and Pignatelo, 1999; Mansour et al. 1999; Doong and Chang, 1998; Ku and Lin, 2002; Hirahara et al. 2003; Konstantinou and Albanis, 2003, Kouloumbos et al. 2003; Derbalah et al. 2004).

To evaluate the progress of toxicity during photocatalytic treatments several assays were employed including *D. magna, S. capricornotum, V. fisheri,* and *Microalgae* (Hincapie et al. 2005, Fernandez-Alba et al. 2002, Farre et al. 2005, Malato et al. 2003). Even though these tests provide information on the overall toxicity, they do not respond specifically to the presence of oxon derivatives and other AChE inhibiting and therefore neurotoxic compounds, which should be of primary concern in removal of OPs. To our knowledge only the photodegradation of methyl parathion was investigated using cholinesterase potentiometric and conductometric biosensors in combination with Lumistox test (*V. fisheri*) to monitor the toxicity of formed methyl-paraoxon (Dzyadevych et al. 2002, Dzyadevych and Chovelon 2002; Dzyadevych et al. 2005). The study was focused on the formation of only one photoproduct (methyl-paraoxon), which was identified using a pure analytical standard. No other photoproducts were detected nor considered in the explanation of biosensor response.
It was therefore the objective of this work to conduct a more general investigation of OPs photodegradation processes by studying the photodegradation pathways of selected representatives of thio-OPs (malathion, azinfos-methyl, chlorpyrifos), and malaoxon as a model oxo-OP compound. The main focus was on the formation of trimethyl phosphate esters and oxons, which are the major sources of induced toxicity, and to combine the results of toxicity tests using FIA-AChE-TLS bioassay

with the identification of transformation photoproducts obtained by GC-MS.

4.2.2 EXPERIMENTAL

4.2.2.1 Photodegradation procedure

The pesticide solutions used for photodegradation studies were prepared daily. To 2-10 mg of each pesticide (malathion, malaoxon, chlorpyrifos, and azinphos-methyl), 250-500 µL of ethanol was added (the final concentration of ethanol was held under 0.5 vol%) and the mixture was then diluted to 250 mL by deionised water. Concentrations of pesticides were as follows: chlorpyrifos – 7 ppm, azinphos-methyl – 30 ppm, malathion – 40 ppm, malaoxon – 31 ppm. The quartz sample cell (10 × 10 × 40 mm) was filled with pesticide working solution and placed in front of the xenon light (125 W Cermax Xenon parabolic lamp) at a distance of 45 cm. The solutions were separately irradiated for a fixed period of time (3.5 min, 7 min, 15 min, 30 min, 60 min or 120 min). Samples were kept at room atmosphere and stirred all the time during the experiment by a magnetic stirrer. The photon irradiance for the range of wavelengths below 410 nm was evaluated by potassium ferrioxalate actinometry (Murov, 1993), and determined to be 2.6×10^{16} $cm^{-2}s^{-1}$.

4.2.2.2 Pesticide analysis

SPE method with 100 mg Strata C18 cartridges was used for extraction of pesticides from water samples. The general procedure included the conditioning step: 3 mL of ethyl acetate, 3 mL of methanol, 5 mL of deionised water; sample load: 1 mL; analyte elution: 1 mL of ethyl acetate. In case of 3,5,6-trichloro-2-pyridinol 2 mL of sample load was used. The pesticide extract was dried on rotary evaporator and redissolved in 200 µL of ethyl acetate. The ethyl acetate extracts were analyzed by gas chromatography – mass spectrometry (Varian, Saturn 2100T) on a CP-Sil 8 CB low bleed/MS column (5% phenyl – 95% methylpolysiloxane, 30 m × 0.25 mm; film thickness 0.25 µm). The injector was held at 220 °C, oven started at 80 °C, and the temperature was increased with a gradient of 10 °C/min till 290 °C and maintained constant for 5 min. The injection volume was in all cases 1 µL, with the exception of samples containing azinphos-methyl. Due to low sensitivity, 2 µL of extracts were injected in GC-MS in the case of this pesticide. The SPE extraction used for the photodegradation studies yielded the following extraction recoveries: (92 ± 11)% for azinphos-methyl, (88 ± 4)% for chlorpyrifos, (93 ± 5)% for malathion, and (95 ± 10)% for malaoxon, 3,5,6-trichloro-2-pyridinol (30 ± 17)%. For quantification purposes a calibration curve in the concentration range from 0.5 ppm to 50 ppm was prepared for each pesticide. The r-square values of individual regression lines ranged from r^2 = 0.987 for malaoxon to r^2 = 0.999 for malathion. All determinations were performed in duplicates with relative errors of 5-15%.

Since the determination of 3,5,6-trichloro-2-pyridinol with GC-MS was unsuccessful (low recovery, high LOD), high performance liquid chromatography – diode array detection technique (HP 1100 HPLC-DAD) was used for this compound. The separation was achieved using C18 Hypersil ODS (Supelco, 150 mm × 4.6, 5 µm) column, kept at 20°C. The injection volume was 75 µL. Eluent (A) was 10 mM ammonium acetate and (B) was acetonitrile (HPLC grade), flow rate 1 mL/min. The gradient elution was as follows: 0 min 90% A and 10 min 70% A. The retention time for the compound was 7.1 min. For quantification purposes a calibration curve in the concentration range from 0.05 ppm to 50 ppm was prepared. The r-square value of the regression line was 0.9993.

4.2.2.3 Toxicity measurements using FIA-AChE-TLS bioassay

The toxicity measurements of irradiated samples (azinphos-metyl, chlorpyrifos, malathion) using FIA-AChE-TLS bioassay were analyzed as such, only samples containing irradiated malaoxon, were all diluted 33-times (300 µL of irradiated sample diluted to 10 mL with deionised water) prior to toxicity bioassay.

4.2.3 RESULTS AND DISCUSSIONS

4.2.3.1 Photodegradation of chlorpyrifos

The degradation curve of chlorpyrifos, with the 13.3 min half life indicates the complete degradation of the parent compound within 120 min of irradiation. The GC-MS identification of chlorpyrifos photodegradation products suggested the formation of only one major product, i.e., chlorpyrifos-oxon – **4A**(Figure 10).

CHLORPYRIFOS

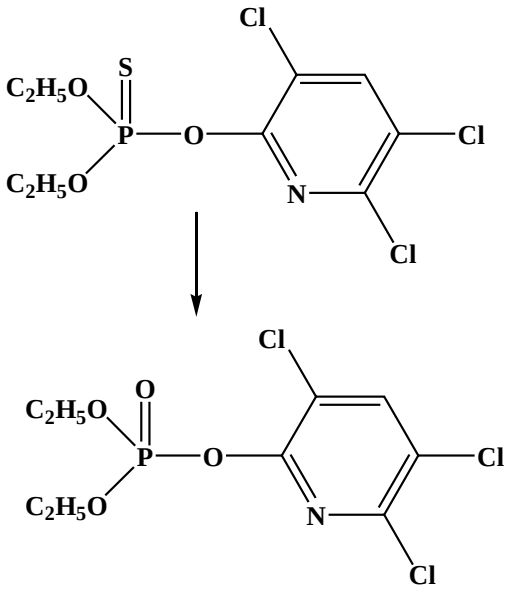

4A, t_r = 15.5 min, (m/z) 298 [M+], 270, 242, 197, 109

Figure 10: *Main photodegradation product of chlorpyrifos*

No other products, such as diethyl phosphate ester or 3,5,6-trichloro-2-pyridinol as a result of bond cleavage were observed in the experiment. The reason could lay in the use of SPE C18 cartridge for extraction, which does not retain compounds of relatively high polarity. It was in fact determined that only 30% of 3,5,6-trichloro-2-pyridinol is retained by the C18 SPE procedure, used. On the other hand, the LOD for this compound on the Varian Saturn 2100T IT-MS (ion-trap MS detector) was relatively high, i.e. 25 ppm, compared to LODs between 0.1 ppm and 0.5 ppm ppm for parent compounds.

The lack of detection of 3,5,6-trichloro-2-pyridinol and observation of only one major product, lead us to additional efforts in search of the pathway of chlorpyrifos transformation. The introduction of twenty-fold preconcentration step, and engagement of other analytical techniques (HPLC-DAD) revealed, that the formation of trichloropyridinol during chlorpyrifos photolysis is small compared to concentration of parent compound. The observed conversion of chlorpyrifos to 3,5,6-trichloro-2-pyridinol, during the 2 h of irradiation was only 0.4% (max at 1 h). The reason for such small amount of cleavage product could be the formation of a variety of chlorpyrifos isomers, including iso-chlorpyrifos, and different *O,O*-diethyl *O*-(di and mono-chloro-2-pyridinyl) phosphorothioates, detected during the experiment. The majority of them are formed in maximal quantity between 15 and 60 minutes of experiment, whereas the formation of chlorpyrifos-oxon is detected already in the first 3.5 minutes of experiment starting from 85%, achieving maximal value at 15 min and decreasing down to 30% at the end of experiment. The formation of chlorpyrifos-oxon, however did not exceed amounts corresponding to 1% of the starting compound throughout the entire experiment. The degradation rate of chlorpyrifos-oxon, determined in a separate experiment on a pure compound was however found the three-times lower

(half life of 42.0 min) compared to chlorpyrifos.

The AChE-TLS bioassay measurements of irradiated samples indicate a 60% decrease of initial AChE activity (Figure 11 – blue line). The reduced activity of the enzyme can be mainly attributed to the formation of chlorpyrifos-oxon, since it was found as the major transformation product and 3,5,6-trichloro-2-pyridinol did not inhibit AChE even at higher concentrations (10 ppm).

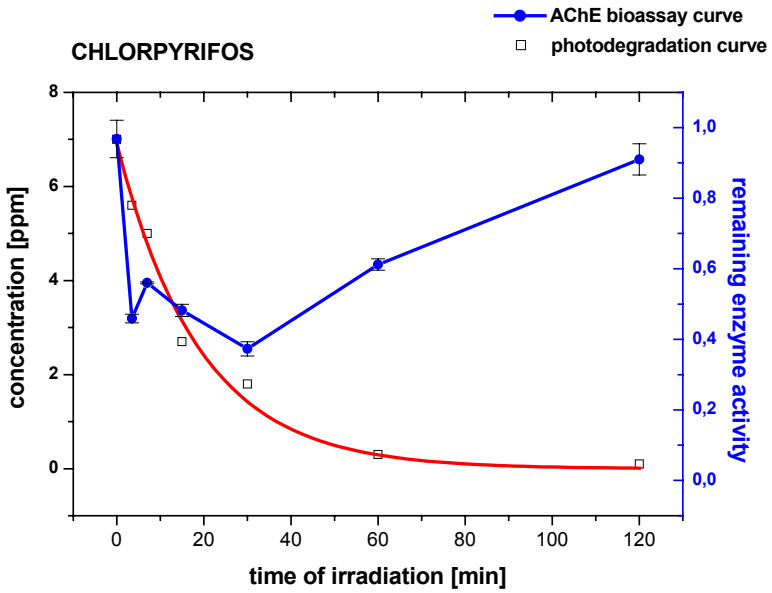

Figure 11: *A first-order degradation curve of chlorpyrifos (squares) and reduced AChE activity (circles)*

With the toxicity measurements of chlorpyrifos-oxon using analytical standard solution, it was possible to compare the 60% decrease of initial AChE activity with the same 60% decrease, which is caused by 100 ppb chlorpyrifos-oxon aqueous solution. This would correspond to only a 1.4% (100 ppb from initial 7 ppm) conversion of thio-OP into oxo-OP. It is further evident that the anti-AChE toxicity increases during the photodegradation process and reaches maximum after 30 min. At 95% degradation efficiency (60 min) the toxic photodegradation products still cause about 40% inhibition of AChE. This can be explained by the formation of different chlorpyrifos isomers of unknown inhibition capacities, and chlorpyrifos-oxon's slower photodegradation compared to parent compound. After 120 min of irradiation the inhibition of AChE was still observed at the LOD level of the method (corresponding to 10 ppb of chlorpyrifos-oxon), which indicates that longer irradiation is required for complete removal of toxic degradation products and confirms the importance of on-line monitoring of toxicity in photodegradation of OPs.

4.2.3.2 Photodegradation of azinphos-methyl

From the obtained GC-MS chromatograms indicating the disappearance of the starting compound a first-order degradation curve can be derived (Figure 12).

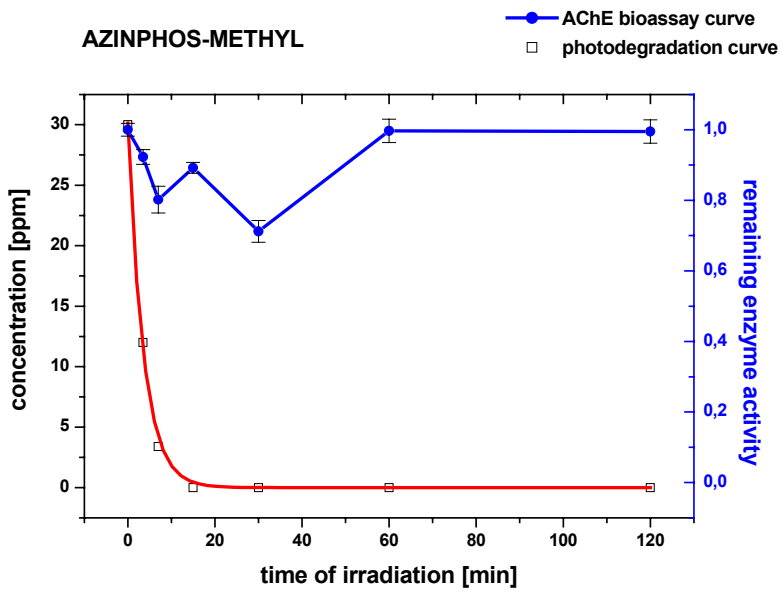

Figure 12: *A first-order degradation curve of azinphos-methyl (squares) and AChE bioassay toxicity curve (circles)*

The calculated half-life for azinphos-methyl from the fitting curve of exponential first order decay was 2.5 min. The complete degradation of the starting compound was achieved within first 15 minutes, but the GC-MS analysis of irradiated samples indicates the formation of several photoproducts. The decomposition of molecule is initiated at the S—C and C—N bonds of the leaving group (Figure 13). The photoproducts **11A, 12A** and **23** indicate the bond cleavage at the methylene-nitrogen bond, whereas the product **24** suggests the bond cleavage at the sulphur-methylene bond. Both products **23** and **24** belong to a family of triazines, which are known pollutants. Since AChE was not susceptible to the inhibiton of **23** and **25** even at very high concentrations (10 ppm and 100 ppm, of each), the 30% induced inhibition in AChE toxicity assay within first 30 min of the experiment (Figure 12) could be attributed to the presence of phosphate esters. Two of them were identified as *O,O,S*-trimethyl ester phosphorodithioic acid – **12A** and *O,O,S*-trimethyl ester phosphorothioic acid **11A** as a result of oxidation of compound **12A**. The maximal formation of **12A** at 15 minutes of experiment was followed by the maximal formation of **11A** at 30 minutes of experiment. At the end of experiment, they were however present only at 10% of maximal amount.

AZINPHOS-METHYL

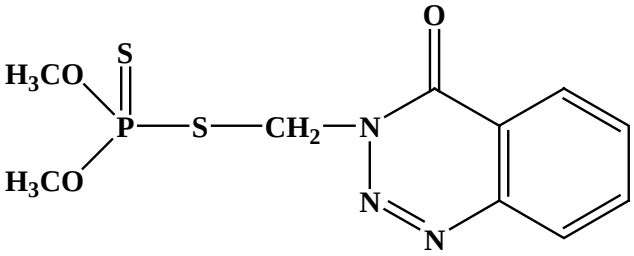

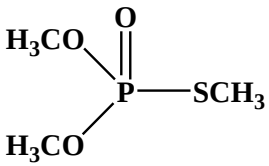

11A, t_r = 5.5 min, (m/z) 156 [M^+], 110, 79

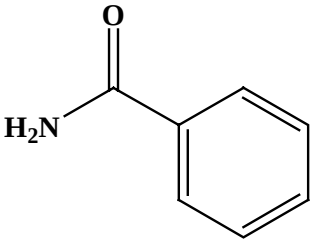

25, t_r = 8.5 min, (m/z) 121 [M^+], 105, 77

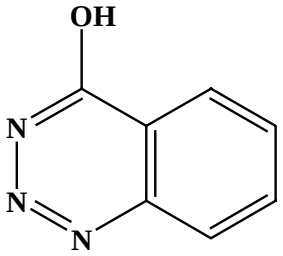

23, t_r =11.4 min, (m/z) 147 [M^+], 104, 92, 76

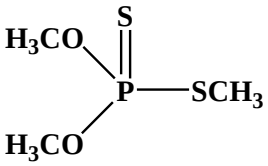

12A, t_r = 6.3 min, (m/z) 172 [M^+], 125, 93

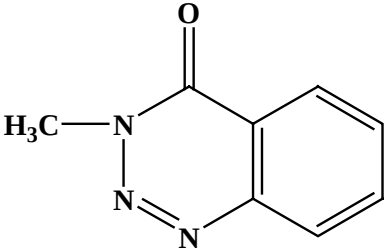

24, t_r = 12.8 min, (m/z) 162 [M^+], 148, 133, 105, 77

Figure 13: *Proposed photodegradation pathway of azinphos-methyl*

The formation of toxic by-products was first noticed by Chukwudebe and his research group. They proposed the formation of the same photoproducts in azinphos-methyl photodegradation labeled as **11A** and **12A**, with the **12A** as the major product (Chukwudebe et al., 1989), which is similar to our observations. The delayed toxic properties of **11A** and **12A** compounds were found to potentiate the acute toxicity of OPs in rats (Talcott et al. 1979; Fouad and Fukuto, 1982; Chukwudebe et al., 1989). The results obtained in AChE-TLS bioassay measurements indicate a 30% decrease of initial AChE activity. The reduced activity of the enzyme can be attributed mainly to formed trimethyl phosphate esters. However, any firm conclusion regarding the toxic effect of particular compound **11A**, and **12A** to AChE, or their mixtures cannot be made. Their physical, chemical and toxicological properties are poorly described. They both exhibit aging of AChE and delayed toxic effects in rats, which died two to eight days after exposure (Talcott et al. 1979; Fouad and Fukuto, 1982). Beside this particularity the acute reference exposure level (REL) for **11A** is 0.5 µg/kg –day (Rice D.W. et al 1997).

4.2.3.3 Photodegradation of malathion

The degradation curve of malathion was similar to that of chlorpyrifos, with the calculated half life of 11.6 min (Figure14). Complete degradation of the starting compound was achieved within 60 min of irradiation. The GC-MS chromatograms of irradiated samples indicate the formation of several photoinduced by-products (Figure 15). The identification of some photoproducts was based on mass spectra and was only tentative.

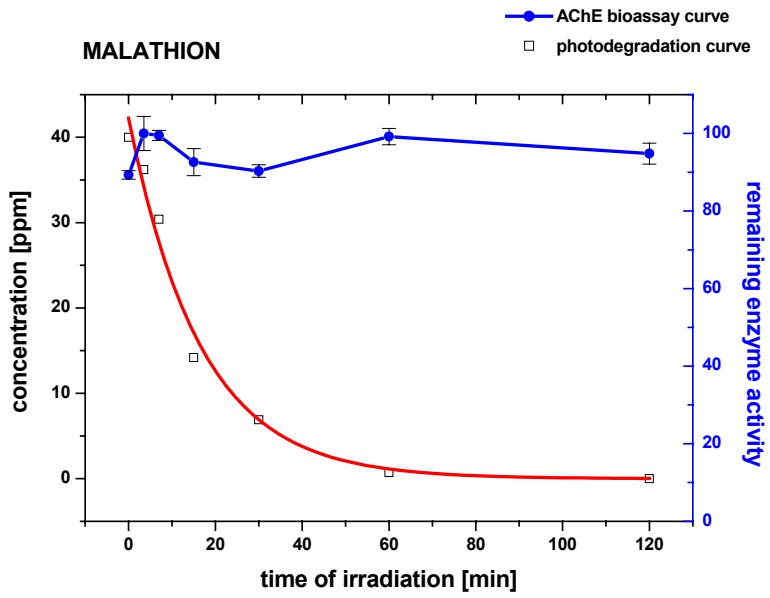

Figure 14: *A first-order degradation curve of malathion (squares) and AChE bioassay toxicity curve (circles)*

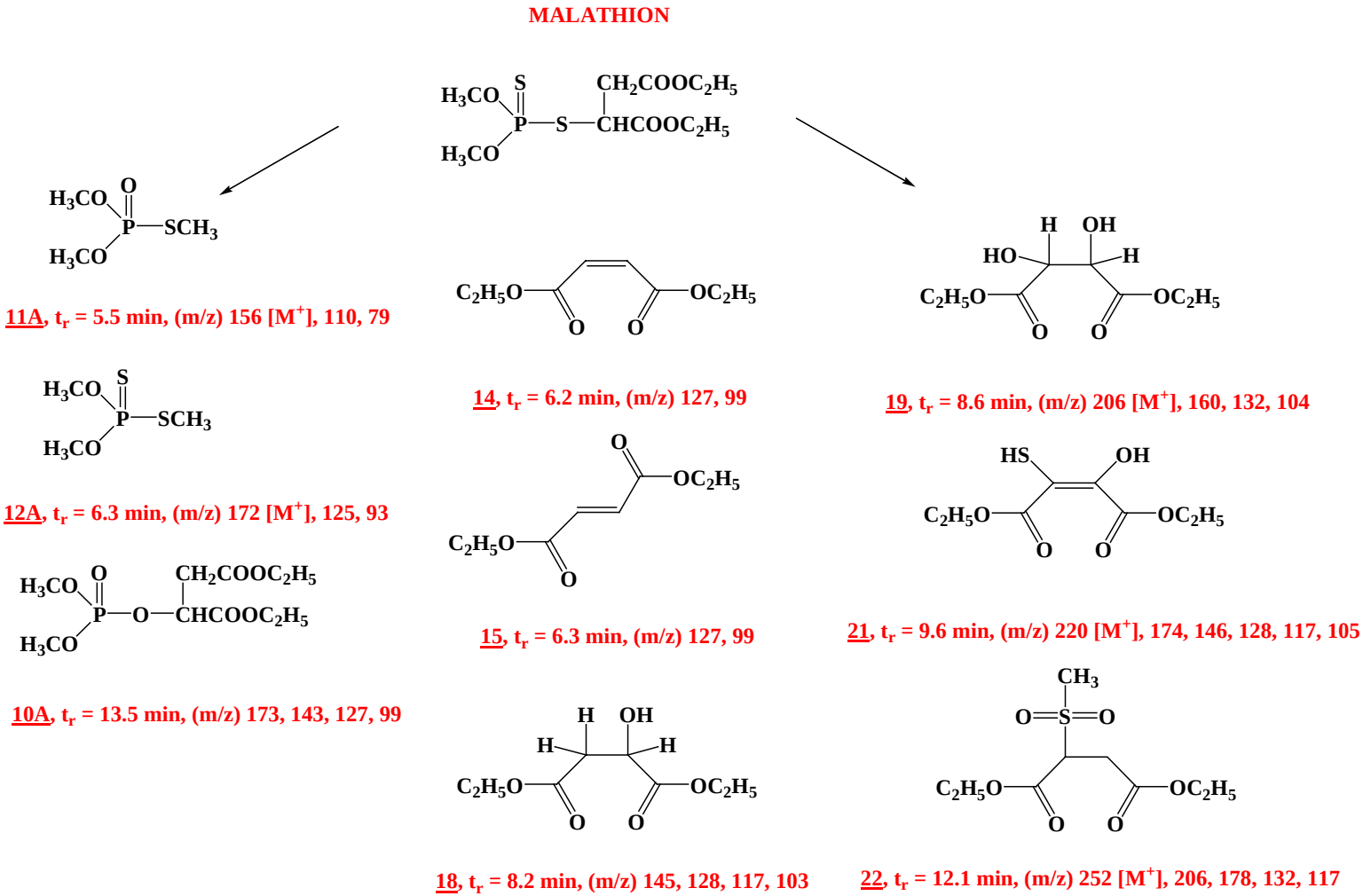

Figure 15: *Proposed photodegradation pathway of malathion*

The majority of them belongs to a family of bute(a)nedioci acid diethyl esters. The other three identified photo-products belong to the family of toxic compounds, all members of phosphate esters' group: phosphorodithioic acid *O*,*O*,*S*-trimethyl ester **12A** and phosphorothioic acid *O*,*O*,*S*-trimethyl ester - **11A** as major compounds and (dimethoxyphosphinyl)oxo - butanedioic acid diethyl ester in traces **10A**. The results are in accordance with some of the products identified after the exposure of malathion to UV or sunlight (Chukwudebe et al., 1989; Pehkonen and Zhang, 2002). In other investigations it was however emphasized that little loss of TOC (total organic carbon) should be of concern because of the possible formation of toxic by-products (Huston and Pignatello, 1999).

The decomposition of molecule is initiated with the cleavage of the P—S and S—C bonds of the leaving group. The cleavage of the P—S bond leads to the formation of diethyl methyl sulphonyl succinate **22** and 2-hydroxyl-3-sulphanyl-2-butene-diethylester **21** or one of its tautomers, whereas the second pathway includes the cleavage of the S—C bond, leading to the formation of different substituted bute(a)nedioic acids diethyl esters (**14,15,18,19**).

Since a standard solution of (10 ppm and 100 ppm) of diethyl maleate (**14** and **15**) - a representative of substituted bute(a)nedioic acid diethyl esters did not inhibit AChE, thus the induced inhibition observed by AChE-TLS bioassay of irradiated samples (Figure 14), can be attributed to the formation of trimethyl phosphates **11A**, **12A** and (dimethoxyphosphinyl)oxo - butanedioic acid diethyl ester **10A**. **12A** was already present in the starting solution, and it was almost completely degraded from 100% at the beginning to 1% at the end of irradiation. The oxidized analogue **11A**, on the other hand, expressed its maximal value at the 7th minute of experiment and was degraded to 30% at the end. **10A** reached the maximal value at the 60th minute of experiment and was degraded to 25% after an additional hour of irradiation. However the maximal detected inhibition, which was on the order of about 10% is considered as the LOD of the AChE bioassay. No firm conclusions can therefore be made regarding the origin of the toxicity of photodegraded samples.

4.2.3.4 Photodegradation of malaoxon

The degradation curve of malaoxon gave the calculated half life of 45.5 min. The degradation of this model oxo-OP compound was not complete after 120 min (only 80% of the initially present compound degraded). The higher resistance toward photodegradation justifies a concern, since similar compounds (like paraoxon) are far more potent AChE inhibitors compared to the parent ones (parathion). The GC-MS chromatograms of irradiated samples indicate the formation of similar photoinduced by-products as those identified in case of malathion photodegradation (Figure 16).

The decomposition of malaoxon molecule is initiated at the P—S or/and S—C bonds of the leaving group. The cleavage of the P—S bond leads to the direct formation of photoproduct, 2-hydroxy-3-sulphanylbutendioic acid diethyl ester **21** or one of its tautomers. The second pathway includes the cleavage of the S—C bond, leading to the formation of different substituted bute(a)ne acids diethyl esters **14-16** and **18-19**. The other two identified photo-products belong to the family of toxic compounds, all members of phosphate esters: phosphorothioic acid *O,O,S*-trimethyl ester **11A** as major compound, and (dimethoxyphosphinyl)oxo - butanedioic acid diethyl ester **10A** found in traces. However, to our best knowledge, there has not been any report regarding the malaoxon photodegradation as a starting compound, thus no comparison of observed degradation products with the literature data could be done.

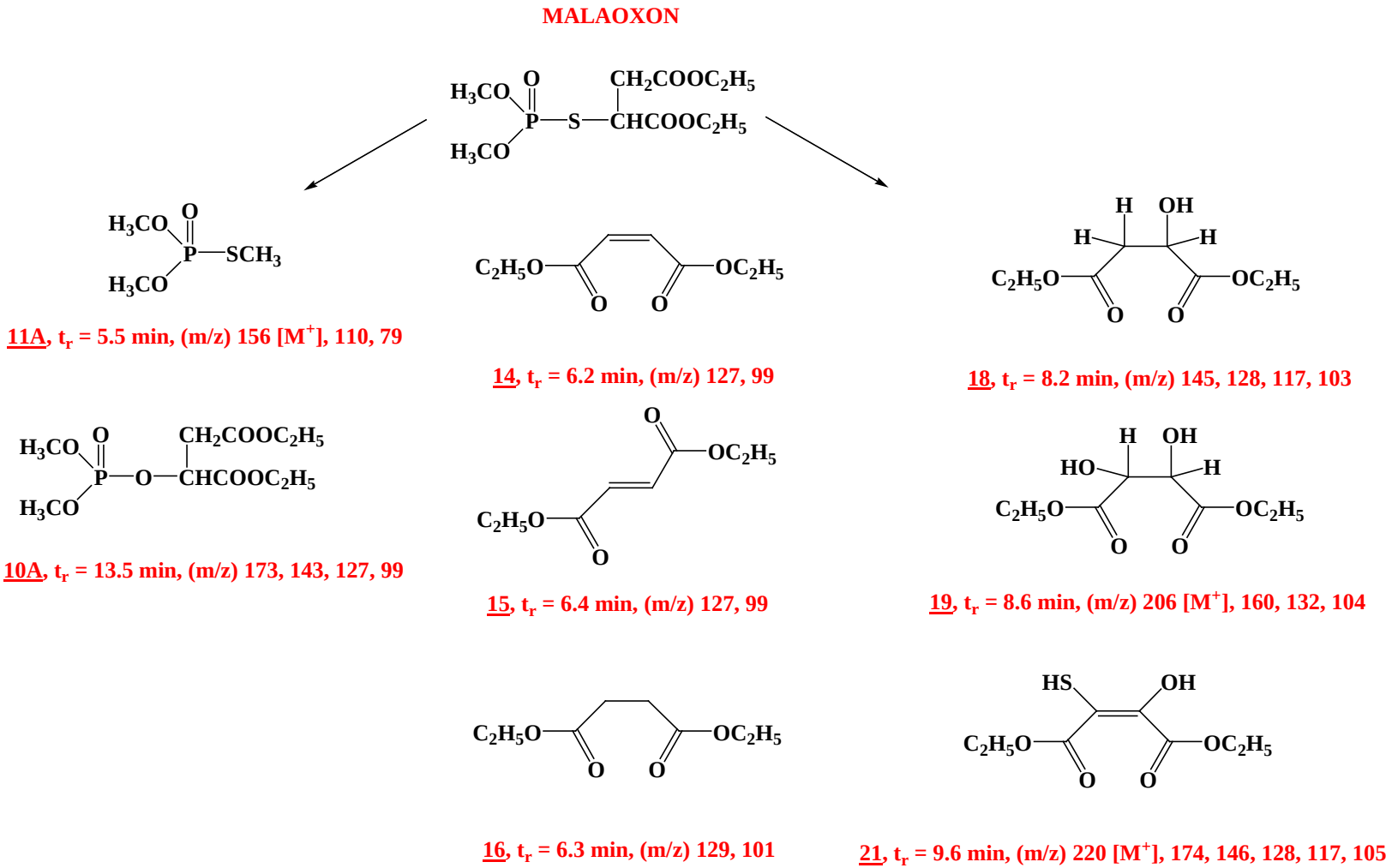

Figure 16: *Proposed photodegradation pathway of malaoxon*

The AChE-TLS bioassay measurements indicate a 20% decrease of enzyme activity within first 7 minutes of irradiation (Figure 17). This can be mainly attributed to the formation of **11A** – a known potent AChE inhibitor, expressing delayed toxicity (Chambers and Levi, Eds., 1992). It was found in up to 4 times higher amount than in the case of malathion. The maximal amount was reached in first 7 minutes of experiment and it was still persistent at 33% of maximal value at the end of experiment. The other identified product was (dimethoxyphosphinyl)oxo - butanedioic acid diethyl ester **10A**, which is expected to inhibit AChE, and is rising throughout the entire experiment. Since no data, regarding its toxicity or its toxicity in combination with **11A** are available in literature, no firm conclusion could be made. It is however important to note that the anti-AChE behaviour of photodegraded samples steadily decreases with the irradiation time, but reaches only about 50% of the initial toxicity exhibited by non-irradiated malaoxon solutions, when the degradation of malaoxon is 80% completed (120 min) as shown on Figure 17.

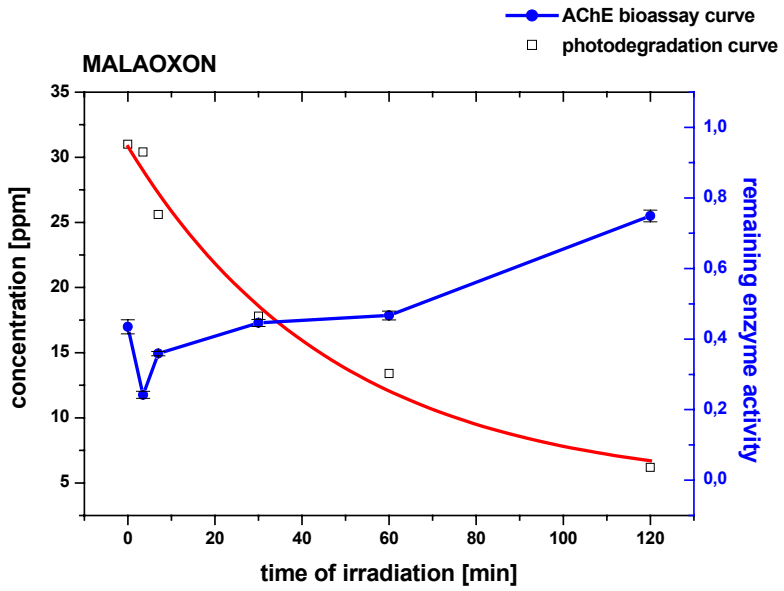

Figure 17: *A first-order degradation curve of malaoxon (squares) and AChE bioassay toxicity curve (circles)*

4.2.4 CONCLUSIONS

Photoreactions of selected thio-OPs (azinphos-methyl, malathion, and chlorpyrifos) belonging to two sub groups of thiono compounds (dithionates and thionates), and a compound from the oxo-OP group (malaoxon), can be described using a first-order kinetic degradation curve. The half lives were as follows: 2.5 min for azinphos-methyl, 11.6 min for malathion, 13.3 min for chlorpyrifos and 45.5 min for malaoxon, which was at the end of 120 min irradiation still present at 20% of the initial concentration. The degradation pathways suggest the susceptibility of P—S and S—C bonds to cleavage. Two AChE inhibiting toxic photo-products, i.e., phosphorodithioic acid *O,O,S*-trimethyl ester and phosphorothioic acid *O,O,S*-trimethyl ester, were identified as a result of P—S—C bond cleavage in case of azinphos-methyl, malathion and malaoxon. In addition, AChE inhibiting oxidation products were noticed through the formation of diethyl (dimethoxyphosphinyl)oxo - butanedioic acid diethyl ester in case of malathion and malaoxon, while chlorpyrifos-oxon was detected as the only photoinduced compound in chlorpyrifos photodegradation under given experimental conditions.

Among compounds, which are not known as AChE inhibitors, different substituted butane and butenedioic acids diethyl esters were identified as photoproducts in case of malathion and malaoxon, while substituted benzotriazines are products of azinphos-methyl photodegradation. With the use of other extraction methods adopted for polar photo-products (SPE on more polar stationary phase), and

other chromatographic instrumentation, like LC-MS, other by-products could be likely identified.

The application of the AChE bioassay has revealed that the anti-AChE toxicity of pesticide solutions subjected to photodegradation does not follow the degradation curves obtained by monitoring the dissaperance of parent compounds. Complete removal of toxic compounds would in general require longer irradiation times compared to those needed for complete removal of parent pesticides. This confirms the need for on line monitoring of OPs' photodegradation by apropriate sensitive and fast response toxicity tests to ensure the complete degradation and removal of any toxic compounds.

4.3 AChE induced toxicity by radiolytic products of malathion, malaoxon, and isomalathion

4.3.1 INTRODUCTION

Several oxidative degradation procedures for the removal of pesticides based on the generation of highly reactive intermediates referred to as advanced oxidation processes (AOPs) were recently considered (Burrows et al., 2002). Ionizing radiation, the most efficient source of active free radicals, seems to be especially useful (Abdel Aal et al., 2001; Trojanowicz et al., 2002; Campos et al., 2003; Trebše and Arčon, 2003; Drzewicz et al., 2004). Besides for the degradation of various pollutants in wastewater treatment, the use of ionizing radiation could also help solving the problem of out-dated agrochemical preparations containing pesticides.

Malathion is a member of phosphorothionothiolates. It is effectively used in pest control as insecticide, acaricide, nematocide etc., and it was also applied in a malaria control program in Pakistan in 1976, where 2,800 spraymen out of 7,500 became poisoned and 5 of them died (Aldridge et al., 1978). After much investigation, it was concluded that the toxicity of the commercial malathion used in the mosquito control program was due to impurities in the manufacture of the technical material, whereas commercial formulations usually contains only trace impurities.

Numerous compounds are found in technical grade formulations of pesticides. In malathion 11 chemicals are routinely detected in its technical formulations (isomalathion, malaoxon, diethyl fumarate, *O,S,S*-trimethyl phosphorodithioate [OSS(O)], *O,O,S*-trimethyl phosphorothioate [OOS(O], *O,O,S*-trimethyl phosphorodithionate [OOS(S)], *O,O,O*-trimethyl phosphorothionate [OOO(S)], diethyl hydroxysuccinate, ethyl nitrite, diethyl mercaptosuccinate, diethyl methylthiosuccinate) (Rice et al., 1997). Some coproducts, especially isomalathion and malaoxon are conversion products of the active ingredient malathion. They arise from unintentional reactions occurring during synthesis or when technical products are stored for extended periods at elevated temperature or exposed to humidity, air or sunlight.

One of the earliest studies regarding inactivation of esterases by impurities isolated from technical malathion showed that compounds [OOS(S)] – **12A**, [OOS(O] – **11A**, [OSS(O)] – **13A**, and isomalathion – **9A** decreased the activity of cholinesterases (Talcott et al., 1979). Acute toxicity of **11A** and **13A** is a result of rapid aging of AChE, where oxime therapy is unlikely to be successful (Clothier et al. 1981). Malathion by itself is slightly toxic via the oral route, with reported oral LD_{50} values of 10 000 mg/kg to 12,000 mg/kg. The acute effects of malathion depend on product purity and the route of exposure, since the commonly present more toxic, essentially equipotent contaminants isomalathion and malaoxon, have approximately 100-fold lower LD_{50} (isomalathion – **9A** 113 mg/kg and malaoxon – **8A** 158 mg/kg) (Rice et al., 1997).

In previous studies regarding the degradation of malathion, the formation of toxic photoproducts was proven, i.e., *O-,* and *S-* trimethyl phosphates, which were till then known as toxic by-products in the synthesis of active compounds (Chukwudebe et al. 1989). Later photolytic studies of malathion including the hydroxyl radical attack resulted in a complete mineralization of starting compounds but little loss of total organic carbon (TOC) should be of concern because of the possible formation of toxic by-products (Huston and Pignatello, 1999).

To evaluate the progress of toxicity during photocatalytic (Fernandez-Alba et al. 2002; Malato et al. 2003; Hincapie et al. 2005; Farre et al. 2005) and radiolytic treatments (Trojanowicz et al., 2002; Zona and Solar 2003; Drzewicz et al., 2004) several assays were employed including *D. magna, S. capricornotum, V. fisheri,* and *Microalgae.* Even though these tests provide information on the overall toxicity, they do not respond speciffically to the presence of oxon derivatives and other AChE inhibiting

neurotoxic compounds, which should be of primary concern in the removal of OPs.

The aim of our work was to examine changes of toxicity, determined by FIA-AChE–TLS bioassay, occuring during γ-irradiation of malathion and its conversion products malaoxon and isomalathion. The main focus was on the identification of trimethyl phosphate esters and oxons, which are the major sources of induced toxicity and their presence at various doses of irradiation. The results obtained by toxicity tests using FIA-AChE-TLS bioassay proved that transient toxic products were formed during radiolytic degradation. The objective of this investigation of malathion and its related compounds formed by radiolytic degradation processes was to study degradation pathways and to find out how the products of these processes may affect the toxicity of irradiated solutions at various doses. A better understanding of pesticide degradation, employing ionizing radiation in waste water treatment, should be of general interest, since even more toxic compounds could be released in the environment.

4.3.2 EXPERIMENTAL

4.3.2.1 Irradiation source

Gamma irradiation was carried out in a cylindrical irradiation space of the ^{60}Co γ-ray panoramic irradiation facility of the Rudjer Bošković Institute, Zagreb, Croatia. The irradiation was carried out at ambient temperature (about 20°C in the chamber) and at dose rate of 7.25 Gy s^{-1} as established by the ethanol – chlorobenzene dosimetry. Fresh pesticide working solutions used for gamma irradiation were prepared daily. Solutions containing approximately 10 μL of each pesticide were diluted to 1 L, resulting in the following concentrations: malathion (11.4 ± 0.2) ppm, malaoxon (19.6 ± 0.6) ppm, isomalathion (7.0 ± 0.3) ppm. No additional amount of solvents (e.g. ethanol) was used to improve the solubility of pesticides. Test tubes containing 10 mL of pesticide working solutions were irradiated in triplicate for each pesticide. The solutions were separately irradiated for fixed periods of time each, with doses in the range from 2.2 to 123.3 Gy. Irradiated samples were extracted with ethyl acetate immediately after irradiation.

4.3.2.2 Pesticide analysis

Solid phase extraction (SPE) method with 100 mg Strata C18 cartridges was used for the extraction of pesticides from water samples. The general procedure included the conditioning step: 3 mL of ethyl acetate, 3 mL of methanol, 5 mL of deionised water; sample load: 10 mL; analyte elution: 3 mL of ethyl acetate. The pesticide extract was dried in a rotary evaporator and redissolved in 1 mL of ethyl acetate. The ethyl acetate extracts were analyzed by gas chromatography – mass spectrometry (Saturn 2100T by Varian) on a CP-Sil 8 CB low bleed/MS column (5% phenyl – 95% methylpolysiloxane, 30 m × 0.25 mm; film thickness 0.25 μm). The injector was held at 220 °C, oven started at 80 °C, and the temperature was increased with a gradient of 10 °C min^{-1} till 290 °C and maintained constant for 5 min. The injection volume was in all cases 1 μL. The SPE extraction used for the radiolysis studies yielded the following extraction recoveries: (85 ± 5)% for malathion, (79 ± 4)% for malaoxon, (76 ± 2)% for isomalathion. For quantification purposes a calibration curve in the concentration range from 0.5 ppm to 20 ppm was prepared for each pesticide. The r-square values of individual regression lines were r^2 = 0.992 for malathion, r^2 = 0.996 for malaoxon, and r^2 = 0.999 for isomalathion. The identification was carried out by analyzing mass spectra of individual compounds (Table 6). For this purpose an additional 150-fold preconcentration was applied.

4.3.3 RESULTS AND DISCUSSIONS

4.3.3.1 Radiolytic degradation of malathion.

Malathion, as an active substance in technical formulations degrades the most easily compared to malaoxon and isomalathion. The radiolytic degradation of malathion can be described as a first-order decay, with the 50% degradation dose of 75.4 ± 3.6 Gy (Figure 18).

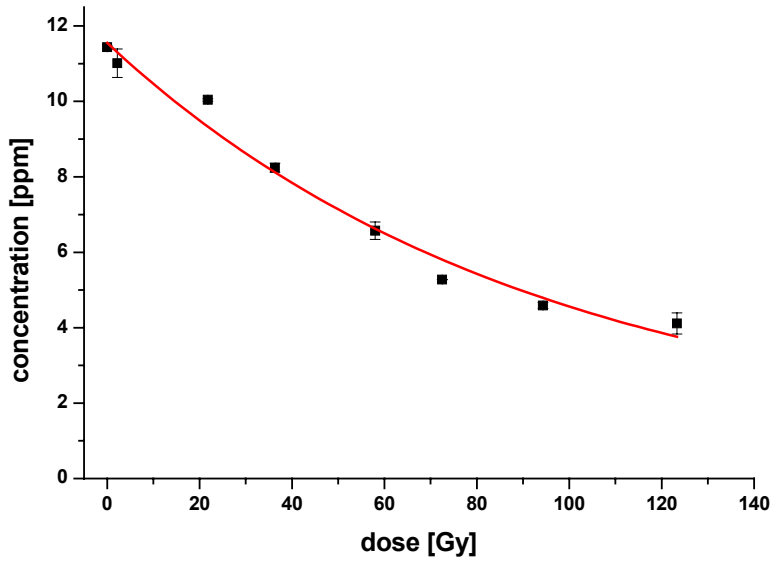

Figure 18: *First order degradation curve of malathion*

Formed oxidizing radicals primarily oxidize double P=S bond in malathion forming 300 ppb of malaoxon. The maximal concentration of malaoxon is found at the dose of 94.3 Gy and could be expressed as a 3% molar conversion malathion to malaoxon. Isomalathion is present in non-irradiated solutions. The 20 % increase in its concentration is only slightly observed (Figure 19).

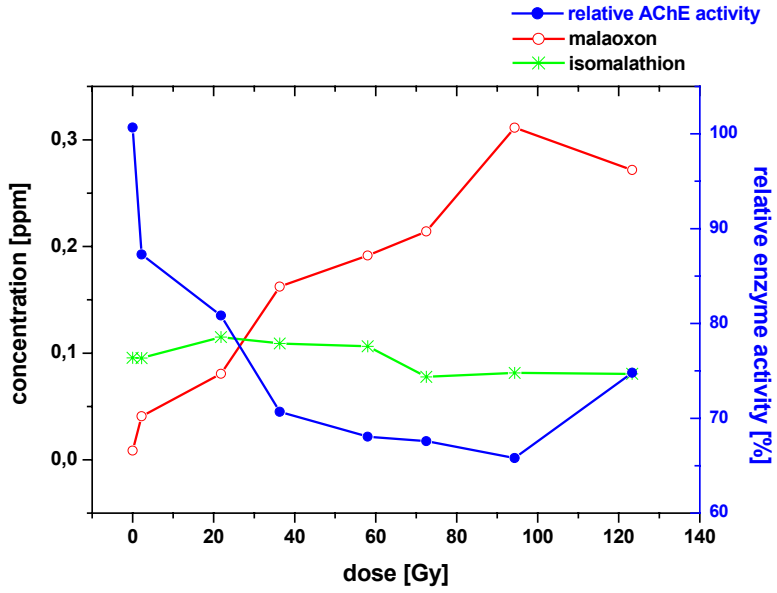

Figure 19: *Comparison of toxicity and development of main malathion degradation anti-AChE compounds – malaoxon and isomalathion*

The additional radical attack resulted in the cleavage of P—S—C bonds of the leaving group. Individual peaks in the mass spectra allowed the identification of several substituted bute(a)nedioic acids diethyl esters and their hydroxy substituted analogs (Table 6).

Table 6: *Detected transformation products of irradiated malathion, malaoxon and isomalathion irradiated samples: product analysis by GC-MS based on retention times (t_R) and their MS spectral characteristics (+ present; - absent, ~ starting compound)*

Photoproduct name and index	**Malathion**	**Malaoxon**	**Isomalathion**
7A malathion	~	-	-
8A malaoxon	+	~	-
9A isomalathion	+	-	~
11A [OOS(O)]	+	+	-
12A [OOS(S)]	+	-	-
13A [OSS(O)]	+	-	+
14 diethyl maleate	-	+	+
15 diethyl fumarate	+	+	+
16 butanedioic acid diethyl ester	+	+	+
17 sulphanyl butanedioic acid diethyl ester	-	+	+
18 hydroxy butanedioic acid diethyl ester	+	+	+
19 2,3-dihydroxy butanedioic acid diethyl ester	+	+	+
22 diethyl methylsulphonylsuccinate	+	+	+

Since isomalathion is present in the starting solution and the increase in its concentration is only 20% (regarding to its initial concentration) at the dose of 21.8 Gy, it could be concluded that the isomerisation is a reaction of minor importance in radiolysis of malathion. The additional radical attack resulted in the cleavage of P—S—C bonds of the leaving group. The maximal observed amounts of buta(e)ndioic acids diethyl esters were at the dose of 72.5 Gy. The consecutive reactions, first cleavage and then hydroxylation were observed as maxima in observed amounts of buta(e)ndioic acids diethyl esters (72.5 Gy) followed by the formation of (di)hydroxy butandioic acids diethyl esters (max 123.3 Gy).

The toxicity of irradiated samples indicates the presence of different anti-AChE toxic photoproducts. Diethyl maleate even in higher amounts (100 ppm) did not cause any decrease in AChE activity, suggesting that all substituted buta(e)nedioic acids diethyl esters and their hydroxy substituted analogs were not presumable AChE inhibitors. However, it is known from the literature that the real cause of anti-AChE activity should be searched in trimethyl esters, malaoxon and isomalathion (Aldridge et al., 1978; Talcott et al., 1979; Clothier et al. 1981). Malaoxon was generated during the irradiation process and its formation curve perfectly fits the toxicity curve (Figure 19). The isomerisation, on the other hand, was only a minor transformation reaction, since a slight increase in isomalathion concentration is only noticed with the dose of 21.8 Gy.

The trimethyl phosphate esters were present in all irradiated solutions of malathion. The [OOS(S)] – **12A** was found only in non-irradiated samples of malathion and could be treated as an impurity of the analytical standard. The [OOS(O)] – **11A** was also present in non-irradiated samples of malathion, but the continuous radical attack caused a rise in **11A** during the experiment. The degradation of **12A** during radiolysis of malathion was very low, and the formation of **11A** is a result of either its oxidation or malaoxon bond cleavage. The amount of [OSS(O)] – **13A** was rising throughout the entire experiment, reaching its maximal observed concentration at the end of experiment.This can be explained as continuous degradation of isomalathion.

The formation of both **11A** and **13A** during γ-irradiation is of concern since both exhibit aging of AChE and delayed toxic effects in mammals, as observed in rats which died two to eight days after the exposure (Talcott et al. 1979; Ali and Fukuto, 1982). Because of this, the acute reference exposure level (REL) for **11A** has been set to 0.5 μg/kg day (Rice et al., 1997). General estimation of anti-AChE compounds present in irradiated solution is impossible, since all five compounds exert different inhibition capacities, and the different synergistic effects could be expected. It is however known, that trimethyl phosphate esters potentiate acute toxicity of malaoxon and isomalathion, but their cholinergic and noncholinergic mechanism of intoxication is not examined closely (Ali and Fukuto, 1982). It could be, however, firmly stated, that the majority of the effect described by the toxicity curve obtained in FIA-AChE-TLS, could be assigned to the formation of malaoxon. As can be seen in Figure 19, the trend line of malaoxon formation can be easily compared to the trend line of remaining AChE activity. The maximal induced toxicity (35 %) was found almost at the end of experiment (94.3 Gy), with the 25% inhibition of enzyme activity at the dose of 123.3 Gy (set as the end of experiment). The effect of isomalathion on AChE inhibition could be neglected, since there is only slight variation of its concentration during the entire experiment.

4.3.3.2 Radiolytic degradation of malaoxon and isomalathion.

The degradation of both compounds can be described as a zero-order decay, with the 50% degradation of the pesticide achieved at the absorbed dose of 110.9 ± 11.1 Gy in case of malaoxon (Figure 20) and 95.2 ± 1.4 Gy in case of isomalathion (Figure 21).

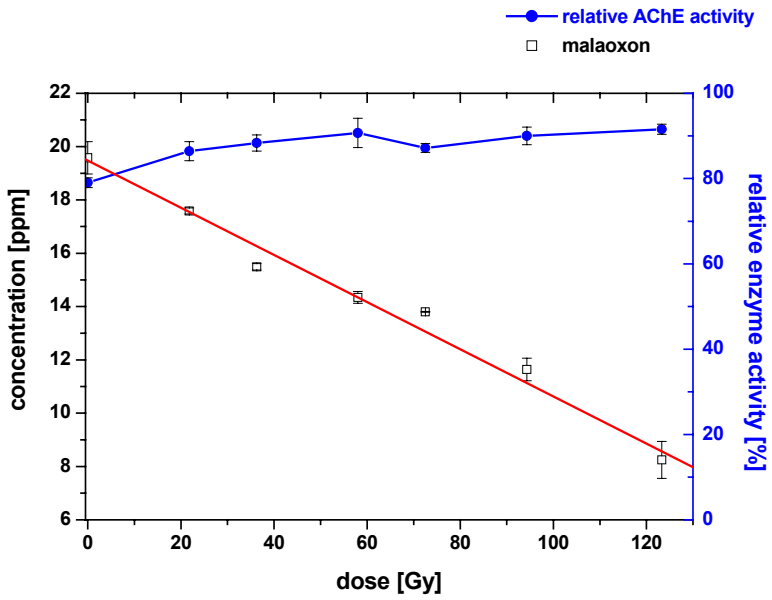

Figure 20: *Zero order degradation curve of malaoxon and its toxicity curve*

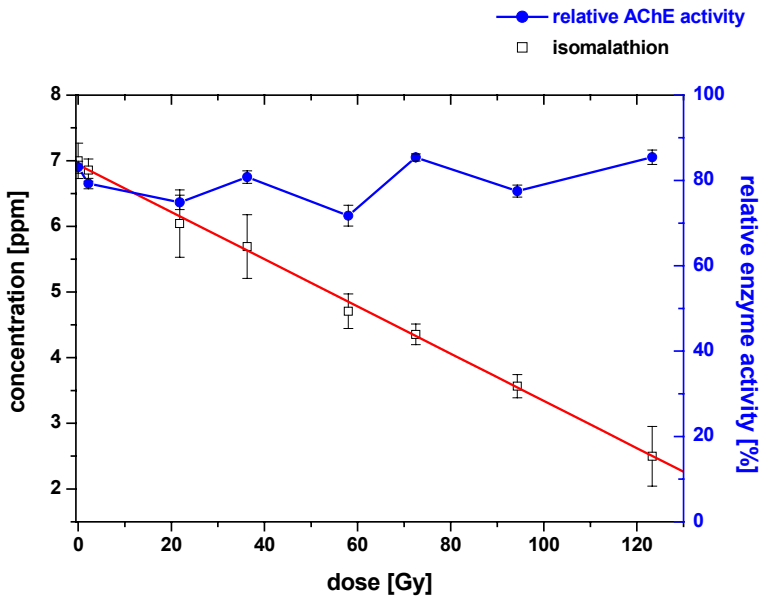

Figure 21: *Zero order degradation curve of isomalathion and its toxicity curve*

The GC-MS analysis of both compounds suggested the formation of several radiation-induced products, that belong to a family of buta(e)nedioic acids diethyl esters and hydroxy analogs which arise as a result of hydroxyl radical attack (Table 6) **(14-19)**. The consecutive reaction of bond cleavage and hydroxylation took place also in case of malaoxon and isomalathion radiolysis. The concentration of **11A** rose with the dose in case of malaoxon (max amount at the end of experiment 123.3 Gy). The maximal amount of **13A** in case of isomalathion was observed at the beginning and was degraded slowly, reaching 10% at the end of the experiment.

The toxicity curve of malaoxon-irradiated samples shows a 10% increase in enzyme activity during the experiment (Figure 20). Irradiated samples were all diluted 100-times prior toxicity measurements. The linear rise in activity of the enzyme throughout the irradiation experiment observed by AChE-TLS bioassay can be attributed mainly to the decrease of malaoxon. However, the increase of only 10% of relative enzyme activity at the 50% degraded starting amount of malaoxon, suggest an expressed synergistic effect between **11A** and malaoxon.

On the other hand, there was a variable trend noticed in AChE toxicity curve in case of isomalathion degradation. Maximal amount of **13A** was noticed at the beginning of the experiment and it was decreased throughout the irradiation experiment. This can be explained as a lower resistance toward hydroxyl radicals in comparison to its analog - **11A** in malaoxon radiation experiments. The variable trend of remaining enzyme activity in case of irradiated isomalathion samples suggested us not only the ability of **13A** to potentiate the toxicity of isomalathion, but also the presence of other non identified anti-AChE inhibitors. As could be seen from toxicity curve in Figure 21, despite the fact that the concentration of the standard compound is 50% of the initial value the initial activity of the enzyme dropped more than 20% almost like in case of non-irradiated samples at the beginning of the experiment. These and other observations inspire us in a continuous research in presented topic.

4.3.4 CONCLUSIONS

Radiolytic degradation of malathion was significantly more efficient (D_{50} 75.4 ± 3.6 Gy) than in case of malaoxon (110.9 ± 11.1 Gy) and isomalathion (95.2 ± 1.4 Gy). The dose profile of degradation of both transformation products followed zero-order decay, whereas malathion degradation could be described as a first-order. The FIA-AChE-TLS bioassay showed a pronounced toxicity of all irradiated

samples. In case of malathion five anti-AChE compounds were identified by GC-MS. Three of them **11A-13A** belong to trimethyl phosphates. Their formation and relative stability (none of them was totally degraded at the end of the experiment) toward γ-irradiation should be of concern since all of them exhibit aging of AChE and delayed toxic effects (Talcott et al. 1979; Ali and Fukuto, 1982). This particularity led the authorities to set up the acute reference exposure level (REL) to 0.5 μg/kg day for **11A** (Rice et al., 1997). The other two products found in radiolytic degradation of malathion were isomalathion and malaoxon. Since there is no information regarding synergistic effects of trimethyl phosphate esters, their cholinergic and noncholinergic mechanism of intoxication, but the presence of malaoxon and isomalathion leads to acute AChE toxicity, their formation should be of public concern. The comparison of trend lines of malaoxon formation and remaining AChE activity led us to the conclusion that the majority of the toxic effect described by the toxicity curve obtained in FIA-AChE-TLS assay could be assigned to the formation of malaoxon. The increased acute toxicity in the presence of trimethyl ester was suggested in case of radiolytic degradation of malaoxon and isomalathion. Among compounds, which are not known as AChE inhibitors, different (hydroxy) substituted butane and butenedioic acids diethyl esters **(14-19)** were identified as radiolytic products in case of all three pesticides. Complete removal of toxic compounds would in general requires longer irradiation times or higher doses compared to those needed for complete removal of parent pesticides. This confirms the need for on line monitoring of OP's degradation by apropriate sensitive and fast response toxicity tests to ensure the complete degradation and removal of any toxic compounds. The FIA-AChE-TLS assay looks promising in that respect.

4.4 Comparison of photocatalysis and photolysis of malathion, isomalathion, malaoxon and commercial malathion – products and toxicity studies

4.4.1 INTRODUCTION

The use of photocatalysts, like TiO_2, has been the subject of intensive studies for more than 20 years for the removal of a large variety of organic and inorganic pollutants from waste waters. However, before it is proclaimed as a general and safe advanced oxidation method (AOM), identification of possible intermediates and performing of toxicity tests is required. The heterogeneous catalysis, in fact, may produce more toxic substances compared to starting materials. Oxidative attack of the hydroxyl radical on the P=S group in phosphorothioates results in the formation of oxon derivates. The continuous oxidation then results in the rupture of P–O or P–S bond of the leaving group (Konstantinou and Albanis, 2003).

There were several studies of OPs degradation employing TiO_2 in the last ten years which included: malathion (Muszkat, et al. 1995), monochrotophos (Hua, et al. 1995), dichlorvos, monocrotophos, parathion, and phorate (Mengyue, et al., 1995), phorate, methamidophos, malathion, diazinon, and EPN (Doong and Chang, 1997), monochrotophos (Ku and Jung, 1998), dimethoate and azinphos-methyl (Dominguez et al., 1998), methamidophos (Malato, et al. 2000), dichlorvos (Naman et al., 2002). In the listed studies authors compared different factors governing the efficiency of photocatalysis in removing the starting compounds, with no attention paid to the analysis of formed by-products. A better insight in qualitative determination of by-products was given in photocatalytic studies of diazinon (M. Mansour, et al. 1999; Kouloumbos, et al. 2003). The authors proposed oxidation of P=S bond and the formation of oxons as primary products, followed by the rupture of P–O bond in the leaving group (Kouloumbos, et al. 2003). Isomerisation took place in irradiated diazinon water/soil suspension, resulting in the formation of isodiazinon (Mansour, et al. 1999). Oxidation and photohydrolysis pathways were proposed also in photocatalysis of ethyl bromophos and dichlofenthion (Konstantinou, et al. 2001). Measurable amounts of different alkyl phosphorothioate esters were also found in agreement with other photocatalytic degradation studies (Sakkas, et al. 2002).

Oxon analogs appear to form during initial steps of photodegradation, but as degradation proceedes, oxons degrade further. Complete mineralisation is the final goal of AOMs, but studies have suggested the formation of smaller, resistant and toxic degradation products. Such compounds include *O*-, and *S*- trimethyl phosphates, which were generally classified as toxic substances in early 80-s. An important consideration is also whether additives in commercial formulations will inhibit the reactions of active pesticide ingredients, in our case OPs. Additives consist of various inert solids, wetting agents and other substances, which are needed to facilitate handling and application.

Among several studies regarding OP degradation, only few deal with commercial pesticide products, their degradation or/and transformation products. This is the reason, why we have chosen malathion, its commercial product (Radotion P-5, Herbos), and two common transformation products, i.e. malaoxon (product of oxidation) and isomalathion (product of isomerisation). According to US National Agricultural Statistics Service (Agricultural Chemical Usage 2005 Field Crops Summary, May 2006) malathion is the most widely applied insecticide in cotton production in terms of total pounds.

Since malathion is still widely used in agriculture and there are rather no information regarding its transformation products, it was our aim to evaluate the photodegradation of malathion, its degradation products malaoxon and isomalathion, as well as its commercial product Radotion during UV photolysis and TiO_2 photocatalysis. The photoprocesses were compared in terms of degradation kinetics (with high performance liquid chromatography – HPLC), product identification (gas chromatography-mass spectrometry – GC-MS), their toxicity (acetylcholinesterase bioassay based on flow injection analysis coupled with thermal lens spectrometry – FIA AChE TLS) and degree of mineralisation (with ion chromatography - IC). The product formation and the degree of mineralization were followed in order

to achieve not only the dissaperance of the starting compound but an environmental safe photodegradation.

4.4.2 EXPERIMENTAL

4.4.2.1 Materials

For the preparation of sol-gel derived TiO_2 films tetraethoxysilane (Acros Organics), ethanol (Riedel-de Haen), and concentrated (65 %) nitric(V) acid (Acros Organics). For TiO_2 sol: titanium (IV) isopropoxide (Acros Organics), ethyl acetoacetate (Riedel-de Haen), 2-methoxyethanol (Fluka), and the triblock copolymer Pluronic F-127 (Sigma) were used.

The commercial product Radotion was 2 years out-dated purposely to contain as much as possible of isomalathion, which is generally formed during storage. The concentration of malathion was 2% instead of 5% in new commercial products, and the molar ratio between malathion and isomalathion was 40:1. Malaoxon was not present in Radotion, but it was formed during photodegradation processes.

4.4.2.2 Sol-gel derived TiO_2 films

Transparent TiO_2-anatase films deposited on both sides of SiO_2-precoated soda-lime glass slides (175 mm x 12.5 mm x 2 mm) were produced by sol-gel processing route described in detail already in our previous publications (Černigoj et al., 2006; Lavrenčič-Štangar et al., 2006).

4.4.2.3 Photocatalytic and photolysis cells, lamps and photoreactor.

The photocatalytic cell consisted of a DURAN glass tube (240 mm, inner diameter 40 mm), which was closed on the lower side with a glass frit and the valve for purging with gas. The effective volume of the glass tube is 250 mL. The spinning basket was made entirely of Teflon and fitted into the photocatalytic cell. Six glass slides with immobilized catalyst were fastened around the axis by the help of two holders. The glass slides and the axis were not joined together. There was a gap of 1.5 mm in between to enable homogeneous mixing of the solution in all segments of the cell. The spinning basket with the immobilized TiO_2 placed in the glass tube could freely rotate around its axis (Figure 22) (Černigoj et al., 2007).

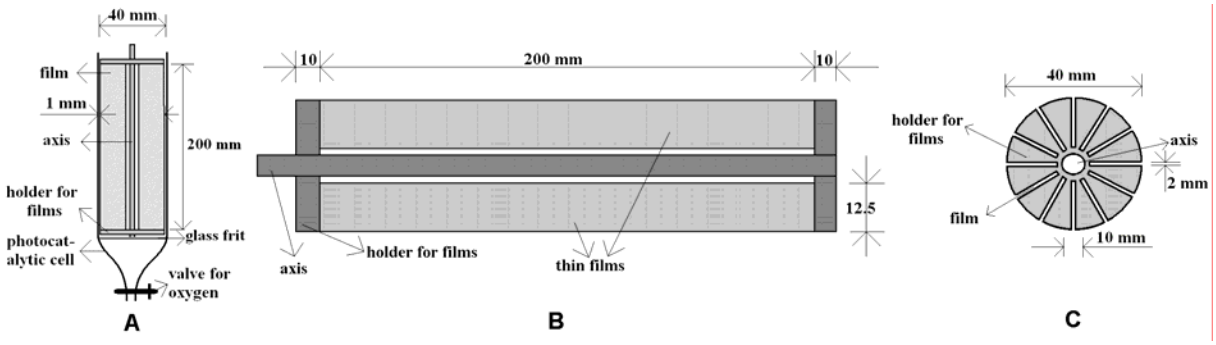

Figure 22: *The photocatalytic cell (A), its longitudinal profile with thin films position (B) and Teflon holder with twelve notches for film fastening (C)*

The photocatalytic activity of the as-prepared TiO_2 films was evaluated in a tailor-made chamber photoreactor using 6 low-pressure mercury fluorescent lamps as a UVA radiation source (CLEO 20 W, 438 mm x 26 mm, Philips; broad maximum at 355 nm). The photocatalytic cell was put in the center inbetween the lamps. The motor on the top of the reactor rotates the spinning basket with the variable speeds (between 0 and 300 rpm).

The cell used in photolysis experiment consists of a QUARTZ glass tube (370 mm, inner diameter 18 mm), which was fastened in the center of photoreactor. One lamp was used for irradiation purpose (Philips UV-C, 15W, 438 mm x 26 mm; maximum at 254 nm).The Teflon tube capped with frit for purging with gas was drawn to the bottom of the cell. The effective volume of the quartz tube is 90 mL. The solutions were constantly purged with oxygen (approx. 1.0 L min^{-1}) during the irradiation, keeping the solution saturated with dissolved oxygen all the time during the irradiation.

4.4.2.4 Photocatalytic and photolysis experiments.

Aqueous solutions containing malathion (14.7 ± 0.1) mg L^{-1}, malathion in Radotion (11.3 ± 0.2) mg L^{-1}, malaoxon (18.0 ± 0.3) mg L^{-1}, and isomalathion (15.7 ± 0.6) mg L^{-1} were irradiated in the presence of 6 glass slides with immobilized sol-gel derived TiO_2. Blank experiments were performed in the same way, but without TiO_2 on the glass plates. Whereas for photolysis in quartz cell, solutions containing malathion (21.2 ± 0.7) mg L^{-1}, malathion in Radotion (12.9 ± 0.2) mg L^{-1}, malaoxon (17.5 ± 0.1) mg L^{-1}, and isomalathion (10.0 ± 0.1) mg L^{-1} were used. Two to four repetitions with each configuration were performed to evaluate the reproducibility of measurements. The solution of OP was purged with oxygen for 15 min in dark before the beginning of the irradiation. During the irradiation 9 mL to 15 mL portions (photolytic and photocatalytic experiment, respectively) of irradiated samples were taken from the cell at different times and analyzed by HPLC, IC, GC-MS and AChE-TLS. The TiO_2-coated slides and the photocatalytic cell were washed with deionised water after the experiment. Before starting the next experiment, the cells were washed and filled with the new solution of OPs. The TiO_2-coated slides showed the same efficiency during the period of 6 months (Černigoj et al., 2007b).

The irradiated samples, taken during the irradiation of Radotion, which forms a heterogeneous mixture, were centrifuged at 7000 rpm for 10 min and then the supernatant was collected for chromatographic analysis. No additional filtration, extraction or centrifugation was needed. All disappearance curves indicated first-order kinetics. Therefore they were fitted as first-order reactions to obtain reaction rate constants and half-life times (Table 7).

4.4.2.5 Analytical procedures

4.4.2.5.1 HIGH PERFORMANCE LIQUID CHROMATOGRAPHY ANALYSIS (HPLC)

The HPLC equipment consisted of a HP 1100 Series chromatograph, coupled with DAD detector. The chromatographic separations were run on a C18 Hypersil ODS column (Supelco, 150 mm × 4.6 mm, 5 µm) using a 70:30 mixture of deionised water and acetonitrile (J.T. Baker). The following retention times were observed: malaoxon 10.7 min, isomalathion 13.1 min, and malathion 22.6 min. The gradient elution protocol was as follows: 0 min 30% acetonitrile; 30 min 70% acetonitrile. The eluent flow rate was 1.0 mL min^{-1}. Injection volume was 100 µL. All the compounds were detected by DAD detector at 202 nm. The r-square values of the regression lines from were 0.9998 for malaoxon, 0.9993 for isomalathion and 0.9998 for malathion.

4.4.2.5.2 ION CHROMATOGRAPHY (IC)

Ion chromatography was employed for the measurements of phosphate and sulphate. The chromatograph consisted of Shimadzu LC10Ai pump, operation module Shimadzu CBM10A and conductivity detector Shimadzu CDD-6A. The ions were separated using a Dionex AS4A-SC-anionic column. The injection volume was 100 µL. Eluent was 1.8 mM sodium carbonate (Fluka) : 1.7 mM sodium hydrogencarbonate (Fluka) at the flow rate 2 mL min^{-1}. The retention time for phosphate was 9.6 min and for sulphate 13.1 min. The r-square values of the regression lines from calibration curves were 0.9913 for phosphate and 0.9995 for sulphate.

4.4.2.5.3 GAS CHROMATOGRAPHY-MASS SPECTROMETRY (GC-MS)

The ethyl acetate extracts were analyzed by GC-MS (Varian, Saturn 2100T) on a CP-Sil 8 CB low bleed/MS column (5% phenyl – 95% methylpolysiloxane, 30 m × 0.25 mm; film thickness 0.25 µm). The injector was held at 270 °C, oven started at 80 °C, and the temperature was increased with a gradient of 10 °C min^{-1} till 290 °C and maintained constant for 5 min. The injection volume was in all cases 1 µL. Internal standard (diazinon, 100 ppb) was employed for the quantification. The r-square values of individual regression lines were r^2 = 0.9951 for malaoxon, r^2 = 0.9967 for isomalathion and r^2 = 0.9962 for malathion. Because of the lack of analytical standard in case of all identified products listed in Table 8, quantification was only relative, based on the internal standard and maximal observed areas of individual compound.

4.4.2.5.4 PESTICIDE EXTRACTION

Solid phase extraction (SPE) method on 100 mg Strata C18 cartridges was used for extraction of pesticides from water samples. The general procedure included the conditioning step: 3 mL of ethyl acetate, 3 mL of methanol, 5 mL of deionised water; sample load: 10 mL in case of photocatalysis and 5 mL in case of photolysis; analyte elution: 5 mL of ethyl acetate. The pesticide extract was dried on rotary evaporator and redissolved in 200 µL of ethyl acetate.

4.4.3 RESULTS AND DISCUSSIONS

4.4.3.1 Photodegradation of malathion and Radotion

From the HPLC chromatograms, indicating the disappearance of the starting compound, first-order degradation curves can be derived with half-live times presented in Table 7.

Table 7: *Calculated half-life times from fitting experimental data to first order decay curves*

photoprocess/($\tau_{1/2}$) [min]	***Malathion***	**Radothion**	***Malaoxon***	**Isomalathion**
photolysis,λ= 254 nm	*5.9 ± 0.1*	8.7 ± 0.3	*27.0 ± 0.9*	8.9 ± 0.1
TiO_2 photocatalysis, λ= 355 nm	*8.3 ± 0.6*	10.8 ± 1.7	*36.5 ± 5.5*	26.7 ± 1.5
photolysis,λ= 355 nm	*2900 ± 230*	420 ± 23	*370 ± 15*	320 ± 11

Malathion was degraded faster in the form of a pure analytical standard than as malathion active ingredient in commercial formulation Radotion. In photolysis (λ 254 nm) experiment, the respective rate constants were 0.117 min^{-1} for malathion, and 0.079 min^{-1} for Radotion. In the case of TiO_2 photocatalysis, the rate constants were lower, 0.083 min^{-1} for malathion, and 0.064 min^{-1} for Radotion. The half-live times in blank photocatalysis experiments were in all cases very high (Table 7). The difference between Radotion and malathion was, however very well pronounced. The 7-times higher degradation rate of malathion in Radotion in comparison with pure analytical standard solution, is the result of the photosensitizing effect of the adjuvants present in the commercial product.

Complete mineralisation is a quite long process. A period of 240 min of irradiation was chosen to monitor two anions, sulphate and phosphate formation during irradiation. Both anions showed different formation patterns in the case of malathion and Radotion degradation. The trend of sulphate formation in photolysis was similar as in the case of photocatalysis. During the photolysis of malathion, 95% of theoretical concentration (expected) of sulphate was noticed (left graph, Figure 23), whereas in photocatalysis 90% of expected sulphate concentration was formed (right graph, Figure 23). Phosphate, on the other hand, was poorly formed in photolysis of malathion. Its concentration scarcely increased up to 10% of stoichiometric concentration at the end of experiment (left graph, Figure 23).

Photocatalysis was, in fact, more efficient with respect to phosphate formation. In a 240 min, 80% of expected phosphate was observed. The phosphate anion is the target ion in OPs degradation, since phosphorus compounds (trimethyl phosphate esters as also OPs by theirselves) express AChE inhibition.

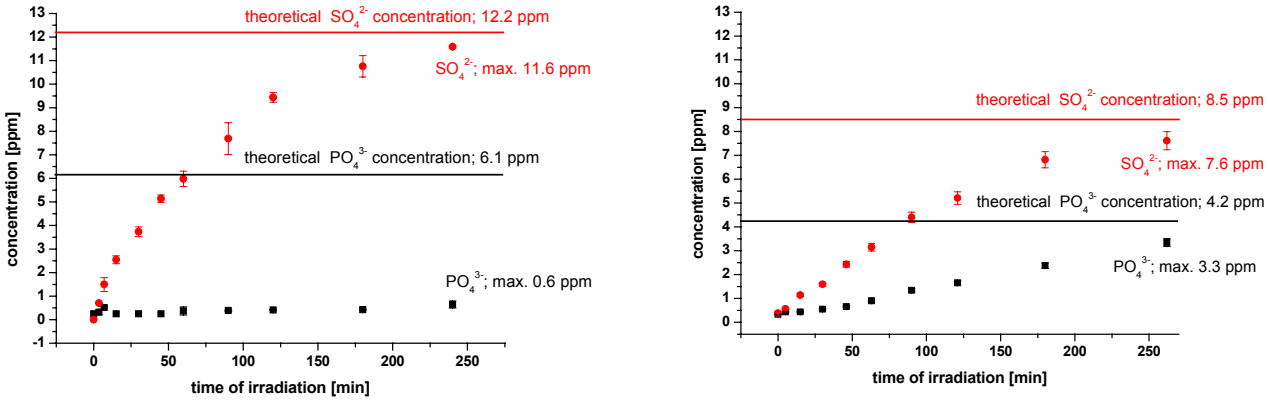

Figure 23: *Formation of sulphate (red circle) and phosphate (black square) in malathion UV photolysis (left graph) and TiO_2 photocatalysis (right graph)*

The measured concentration of sulphate in mineralisation of Radotion was higher than calculated from the molar ratio malathion : sulphate. The reason lays most probably in the presence of other compounds in commercial product, even though the whole mass percentage of organic compound present in Radotion was not higher than 3%. The other 97% was inorganic material, which remained after 1 h of incineration at 500 °C. The trend of formation of both anion species was similar as in case of malathion irradiation. Sulphate was present in 153% in case of Radotion photolysis, and 177% in case of Radotion photocatalysis. Phosphate was in both cases presented in non-irradiated solutions and was poorly formed (16%) in photolysis of Radotion (left graph, Figure 24). Photocatalysis was far more successful and 150% of expected phosphate was measured (right graph, Figure 24).

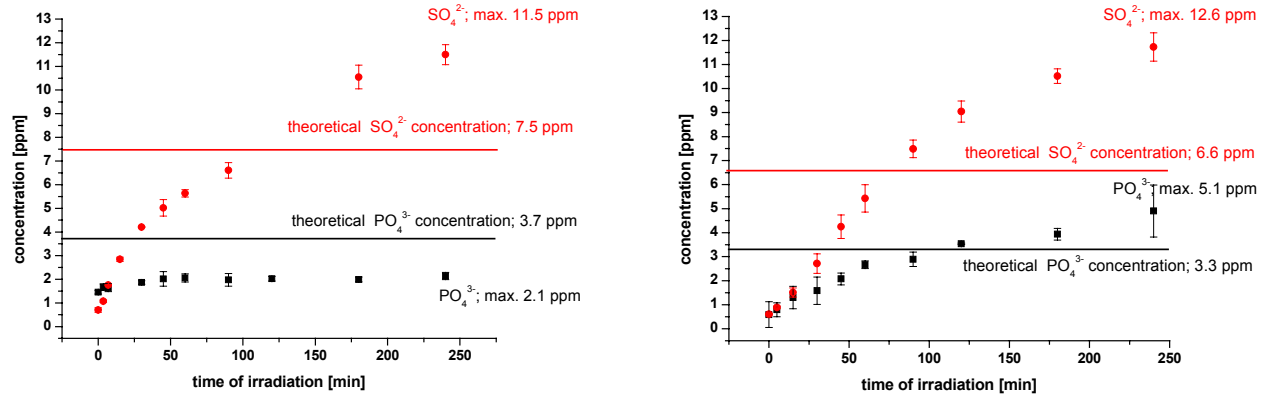

Figure 24: *Formation of sulphate (red circle) and phosphate (black square) in Radotion UV photolysis (left graph) and TiO_2 photocatalysis (right graph)*

In Table 8 several transformation products are listed. They can be divided in two groups; in AChE inhibiting (compound with index A) and AChE non-inhibiting compounds (compounds without index). The type A compounds express inhibiting potentials toward enzyme AChE, whereas the other non-labelled compounds belong to the group of diethyl esters analogs of different buta(e)ne dioic acids. Diethyl maleate was chosen as a representative compound from this group, and was tested on FIA-AChE-TLS bioassay. Even in high concentrations (100 ppm) it did not exhibit inhibiting potential toward the AChE enzyme, and therefore the entire group was treated as AChE non-inhibiting. It is also known from the literature, that AChE inhibiting compounds are members of organophosphorus and

carbamate pesticides (Chambers and Levi, Eds., 1992). Reactions, involving the group of AChE non-inhibiting compounds were isomerisation and oxidation in photolysis and photocatalysis processes. The trans-cis isomerisation of **15** to **14** compound was taking place in photolysis and photocatalysis of both malathion and Radotion. Since **15** was present in maximal amounts at the beginning of the experiment in all experiments, it can be treated as an impurity in production of OPs. The formation of **14** can be thus mainly, a result of isomerisation of **15** present in non-irradiated samples and less a result of OPs degradation. On the other hand **16** was mainly formed during photocatalysis of malathion and Radotion. In case of photolysis, it was present only in irradiated solutions of Radotion, and came from impurities of isomalathion present in Radotion, since **16** was formed during isomalathion photolysis. The hydroxylation of buta(e)ne dioic acids diethyl esters analogs was a result of hydrolysis of malathion or oxidation of AChE non-inhibiting compounds in the presence of hydroxyl radicals. The hydroxy analog **18** was formed during photocatalysis and photolysis of both malathion and Radothion. The dihydroxy analog **19** was, on the other hand, observed only in malathion photocatalysis. It was absent in photocatalysis of malaoxon and isomalathion. Another interesting compound was formed during photolysis of Radotion, i.e. 2-hydroxy-3-sulphanyl butenedioic acid diethyl ester (or one of its isomers or tautomers) – **21**, which was only detected in photolysis of malaoxon, not in photolysis of malathion nor isomalathion. The diethyl methylsulphonylsuccinate – **22** is a typical co-product in commercial malathion formulations (Rice et al., 1997) and was present at highest concentration in non-irradiated samples of Radotion, whereas it was formed during malathion photolysis and photocatalysis.

The far more important group in terms of AChE inhibiting capacity of OP degradation products is the A group because of inhibiting capacity of the AChE enzyme. It includes trimethyl phosphate esters **11A** - [OOS(O]; **12A** - [OOS(S)]; **13A** - [OSS(O)]; **10A** – (dimethoxyphosphinyl)oxo - butanedioic acid diethyl ester; **8A** – malaoxon; **7A** – malathion; and **9A** – isomalathion. They all exhibit potency to diminish the activity of cholinesterases (Talcott et al., 1979). The acute toxicity of **11A-13A** is a result of rapid aging of AChE (Clothier et al. 1981). The toxicity curves obtained from photocatalytic degradation of malathion and Radotion showed an expressed inhibition of AChE enzyme in both cases.

Table 8: *Detected transformation products in irradiated solutions of malathion, Radothion, malaoxon and isomalathion: product analysis by GC-MS based on retention times (t_R) and their MS spectral characteristics (/ absent, ~ starting compound)*

Compound name and index	Type of reaction	Malathion	Radotion	Malaoxon	Isomalathion
7 malathion	TiO_2	~	~	/	/
	UV-C	~	~	/	/
8A malaoxon	TiO_2	30<max<60	max 30	~	/
	UV-C	/	/	~	/
9A isomalathion	TiO_2	max 0	max 0	/	~
	UV-C	*max 0*	*max 0*	/	~
10A (dimethoxyphosphinyl)oxo - butanedioic acid diethyl ester	TiO_2	/	/	/	/
	UV-C	/	*15<max<30*	*max at the end*	/
11A [OOS(O]	TiO_2	max 15	30<max<45	max 0	/
	UV-C	/	/	*max 0*	/
12A [OOS(S)]	TiO_2	max 0	max 0	/	/
	UV-C	*max 0*	*max 0*	/	/
13A [OSS(O)]	TiO_2	/	/	/	0<max<5
	UV-C	/	/	/	*max 0*
14 diethyl maleate	TiO_2	15<max<45	15<max<30	/	0<max<30
	UV-C	*max 45*	*max 30*	*max 60*	*max 30*
15 diethyl fumarate	TiO_2	max 0	max 0	max 0	max 0
	UV-C	*max 0*	*15<max<30*	*max 0*	*max 0*
16 butanedioic acid diethylester	TiO_2	30<max<45	max 30	/	max 0
	UV-C	/	*max at the end*	/	*max 60*
18 hydroxy butanedioic acid diethylester	TiO_2	45<max<60	max 60	/	45<max 60
	UV-C	*45<max<60*	*max 30*	*max at the end*	*max 60*
19 2,3-dihydroxy butanedioic acid diethylester	TiO_2	max 15	5<max<15	/	/
	UV-C	/	/	/	/
20 hydroxy butenedioic acid diethylester	TiO_2	/	/	max 45	/
	UV-C	/	/	/	/
21 2-hydroxy 3-sulphanyl butenedioic acid diethylester	TiO_2	/	/	/	/
	UV-C	/	*max 7*	/	*7<max<15*
22 diethyl(methyl)sulphonyl succinate	TiO_2	15<max<30	max 0	/	5<max<15
	UV-C	*3.5<max<7*	*max 0*	/	*3.5<max<7*

In case of malathion photocatalysis **11A** and **8A** are compounds, that were formed during the experiment (Figure 25, left graph). The maximal concentration of **8A** - malaoxon was measured between 15th (470 ppb) and 60th (630 ppb) minute of the experiment, which agrees very well with the inhibiting trend observed in the toxicity curve. The minimum in AChE activity was between 15th (59.3%) and 60th (62.3%) minute of the experiment. **12A** was present from the beginning and **11A** is

probably its oxidation product as also product of malathion oxidation. Its maximal observed amount was at the 15th minute of the experiment, which matches with the minimum in AChE activity.

There were two AChE inhibiting compound present in Radotion non-irradiated samples; **12A** and **9A** - isomalathion, whereas **11A** and **8A** - malaoxon were formed during photocatalysis (Figure 25, right graph). The maximal amount of **8A** - malaoxon was at the 30th minute (690 ppb) of the experiment. The same is observed in case of **11A**, which expressed maximal concentration between 30th and 45th minutes of experiment. Both observations could be easily linked to expressed AChE inhibition. The minimal relative enzyme activity (64.0%) was noticed at the 30th minute of experiment.

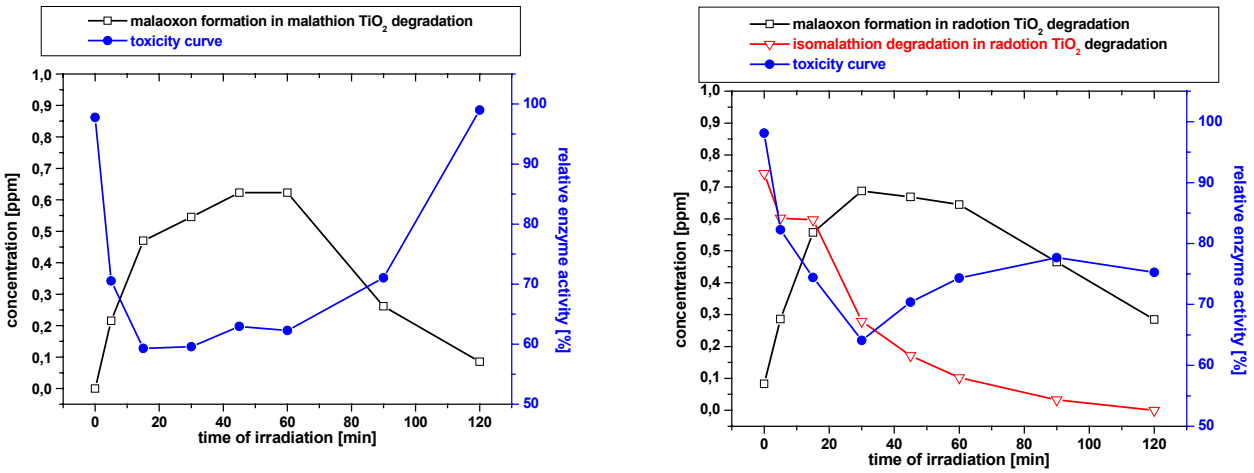

Figure 25: *Toxicity curves in TiO_2 photocatalysis of malathion (left graph) and Radotion (right graph) and formation of AChE inhibiting malaoxon*

In photolytic experiments of malathion any new inhibiting AChE compound was formed; only **12A** and **9A** were present in non-irradiated samples as impurities from the standard. There was no observable induced toxicity in malathion photolysis. The measured 5% of inhibition can be regarded within the RSD of the measurement (Figure 26, left graph).

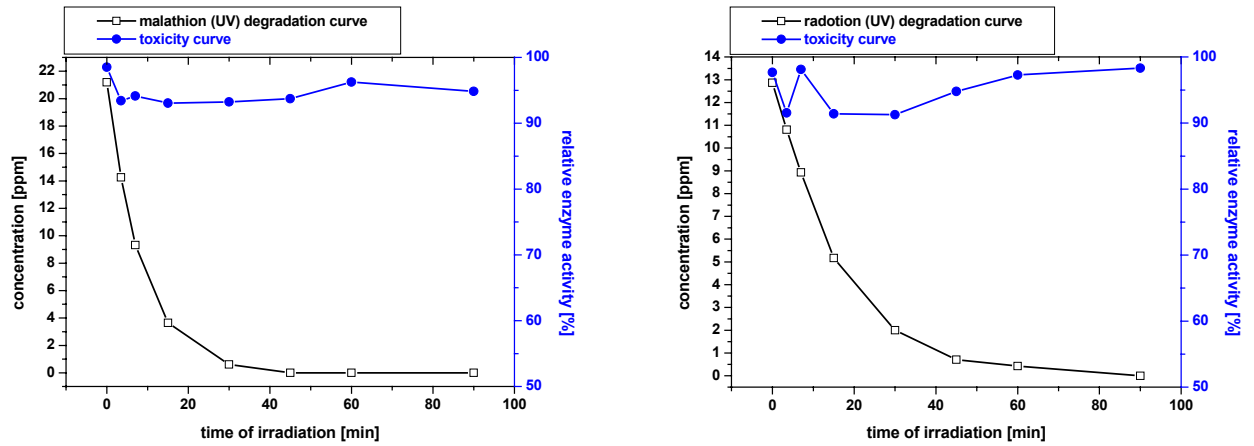

Figure 26: *Toxicity curves (blue circles) and degradation curves (black squares) describing UV photolysis of malathion (left graph) and Radotion (right graph)*

Radotion, on the other hand expressed a 10% decrease in AChE activity, which should be taken into account. The maximal decrease in AChE activity is noticed during the 15th and 30th minute of the experiment (Figure 26 – right graph), and coincides with the presence of (dimethoxyphosphinyl)oxo -

butanedioic acid diethyl ester – **10A** formed during the same period of time. This compound was later on also detected in malaoxon photolysis.

4.4.3.2 Photodegradation of malaoxon and isomalathion

The disappearance of the starting compounds can be described by the first-order degradation kinetics (Table 7). The respective half-life times in photocatalytic experiments were considerably longer than in case of malathion. Up to 4-times slower degradation was observed in case of malaoxon photocatalysis with the rate constant 0.0190 min $^{-1}$ and up to 3-times slower degradation in case of isomalathion with the rate constant 0.026 min $^{-1}$ in comparison to photocatalysis of malathion. Photolysis of isomalathion was, on the other hand, comparable to malathion photolytic degradation, with the rate constant 0.078 min $^{-1}$, whereas malaoxon was also in this case more resistant to degradation. Its rate constant was 0.026 min $^{-1}$, which is 4-times lower than in case of malathion photolytic degradation. The half-live times in blank photocatalytic experiments were in both cases very high but comparable (Table 7).

The mineralisation of phosphorus compounds was negligible in case of malaoxon photolysis (Figure 27, left graph), but it reached 80% in case of malaoxon photocatalysis. The formation of sulphate was similar in both processes. During the photolysis of malaoxon, 77 % of theoretical sulphate concentration (expected) was noticed (left graph, Figure 27), and 89% in photocatalysis of malaoxon (right graph, Figure 27).

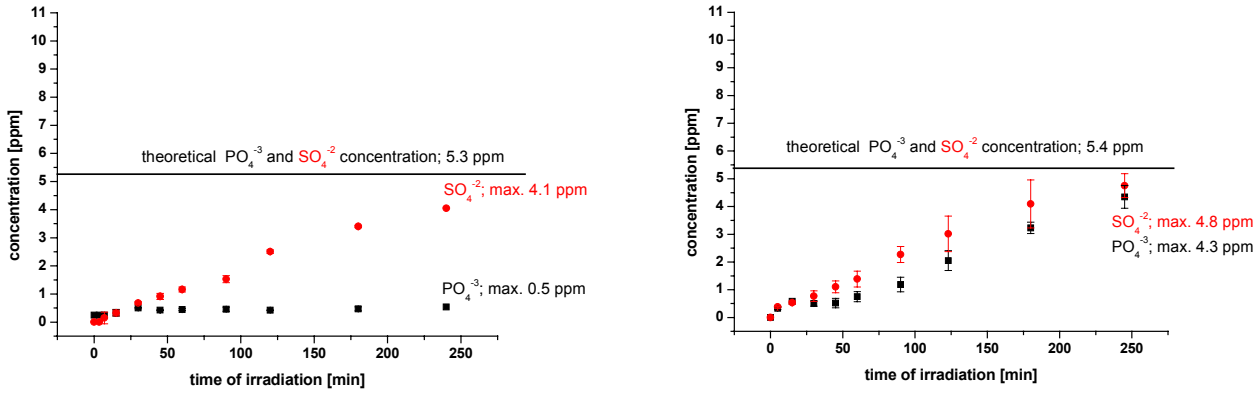

Figure 27: *Formation of sulphate (red circle) and phosphate (black square) in malaoxon UV photolysis (left graph) and TiO_2 photocatalysis (right graph)*

Phosphate was present at only 30% at the end of stoichiometric amount at the end of photolysis of isomalathion (left graph, Figure 28). Photocatalysis was, in fact, more efficient in phosphate formation. In a 240 min of experiment, 93 % of expected phosphate was observed (right graph, Figure 28). Sulphate was formed efficiently in both cases. Total conversion of sulphur containing compounds into sulphate was achieved in 180 min in photolysis (left graph, Figure 28). Photocatalysis of isomalathion, on the other hand resulted in 78% of expected sulphate (right graph, Figure 28).

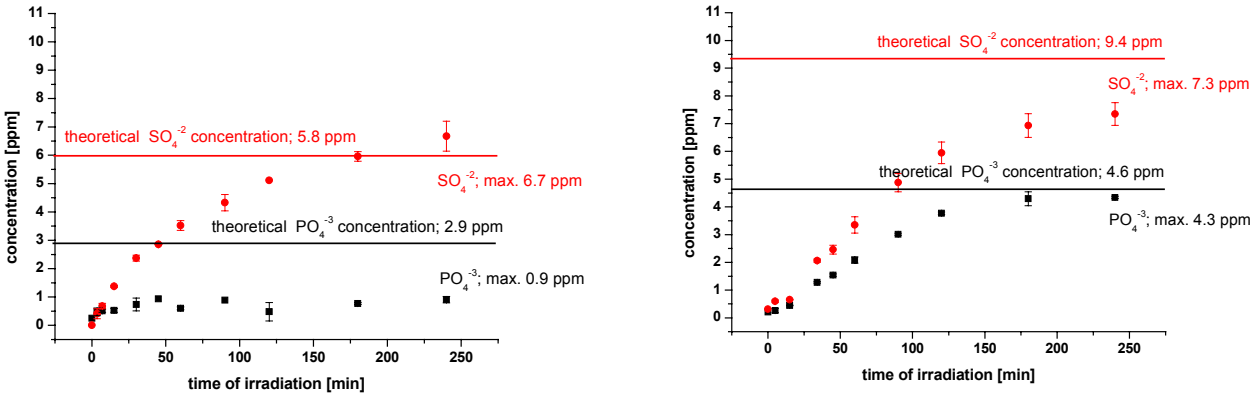

Figure 28: *Formation of sulphate (red circle) and phosphate (black square) in isomalathion UV photolysis (left graph) and TiO_2 photocatalysis (right graph)*

During photolytic and photocatalytic degradation of malaoxon and isomalathion, reactions involving isomerisation and oxidation took place (Table 8). The trans-cis isomerisation of **15** to **14** compound was taking place in photolysis of both malaoxon and isomalathion and in photocatalysis of isomalathion. Since **15** was present in maximal amounts already at the beginning of the experiment in case of both compounds, the formation of **14** must result primarily from isomerisation of **15** present in non-irradiated samples rather than from bond cleavage. However, since **15** is present in pure analytical standards of all three OPs (malathion, malaoxon, isomalathion), its presence could be expected and was also proved in case of technical Radotion. The compound **16** was formed only in photolysis of isomalathion, whereas it was absent in photolysis of malathion and malaoxon. It was also found in photolysis of Radotion, but only due to isomalathion impurities present in Radotion. Compounds from **18-21** were the result of hydroxylation of buta(e)ne dioic acids diethyl esters. The hydroxy analog **18** was present in all irradiated solutions in the middle of experiment, except in case of malaoxon photocatalysis, where it was absent. Following the maxima of observed **18** formation, one can deduce that **18** is the hydroxylated product of **14**. The compound **14** was also absent in photocatalysis of malaoxon, and its formation is mainly observed at the beginning of the experiments in all the other irradiated solutions. The 2-hydroxy-3-sulphanyl butenedioic acid diethyl ester – **21** was only detected during photolysis of malaoxon and Radotion.

In photocatalysis and photolysis of malaoxon and isomalathion no trimethyl phosphate esters were formed. The maximal amounts of **11A** - [OOS(O] in case of malaoxon and **13A** - [OSS(O)] in case of isomalathion were observed in non-irradiated solutions and can be considered as impurities of the standards. The compound **10A**, which was present at the maximal concentration at the end of malaoxon photolysis, was later on also detected during Radotion photolysis.

The toxicity curves for both compounds are in anticorrelation with degradation curves during both processes (Figure 29). No anti-AChE compound was formed during the photocatalysis of malaoxon and isomalathion, thus the relative enzyme activity increased as the compound decreased. The same phenomenon was observed in case of isomalathion photolysis. On the other hand the relative enzyme activity at the end of malaoxon photolysis was only 84%, since the concentration of malaoxon was still 4.4 ppm.

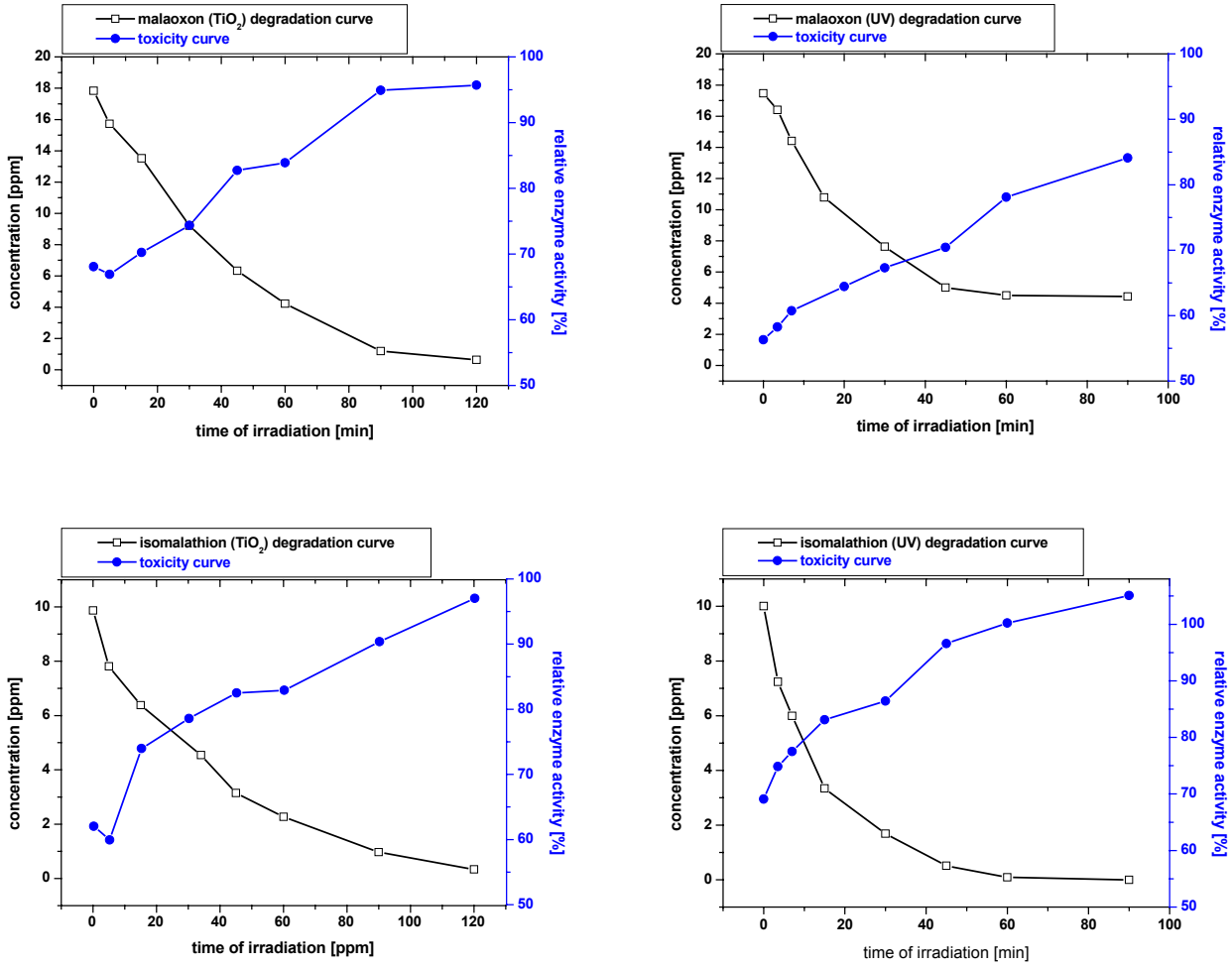

Figure 29: *Toxicity curves (blue circles) and degradation curves (black squares) describing TiO_2 photocatalysis (left side) and UV photolysis (right side) of malaoxon (above) and isomalathion (below).*

4.4.4 CONCLUSIONS

From the HPLC chromatograms, indicating the disappearance of the starting compounds, first-order degradation curves were derived. The half-live times in photolysis experiment indicated the fastest degradation in case of malathion, followed by Radotion and isomalathion, with similar values. The slowest degradation was in case of malaoxon photolysis, with up to 4-times lower rate constant. In photocatalytic experiment the order of precedence was from the fastest degradation noticed in malathion and Radotion photocatalysis, followed by up to 3-times slower degradation of isomalathion and the slowest, up to 4-times lower rate constant in malaoxon photocatalysis. The comparison of photolytic and photocatalytic experiments is difficult, because of totally different nature of photons emitted. The focal point in comparison of both experiments was drawing near as much as possible the rate of disappearance of the starting compound, in our case malathion. On this base the only reasonable difference between processes was the amount of energy required for the same effect. In photolytic experiment only one 15 W lamp was used, whereas in case of photocatalysis six lamps (same dimensions) of 20 W were needed. The energy ratio has given good weight in favor of photolysis.

According to ion chromatography, the formation of sulphate and phosphate showed different patterns. The sulphur in P=S and P—S groups was easily oxidized, forming sulphate anion during both experiments in all four OPs solutions. In fact, more than 75% of theoretically expected amount was

formed during 240 minute of irradiation. Phosphate, the target ion in monitoring the efficiency of OPs degradation, was however formed in amounts of less than 30% of those exected in photolytic experiment. Photocatalysis was in this respect far more efficient. More than 80% of expected phosphate was measured in all for OPs solutions. The mineralisation has resulted advantageous in case of photocatalysis.

Several transformation products were identified based on mass spectra when investigating the fate of degradation products. They were divided in two groups; in AChE inhibiting (index A) and AChE non-inhibiting compounds. The main reactions involving the AChE non-inhibiting compounds were isomerisation and oxidation. The presence of compounds from the A group is directly correlated to the reduced relative activity of the enzyme in toxicity curves. The toxicity curves obtained from photocatalytic degradation of malathion and Radotion showed an expressed inhibition of AChE enzyme in both cases. The formation of malaoxon in both cases perfectly fitted the decreased relative enzyme activity. In photolytic degradation of malathion no new inhibiting AChE compounds were formed, thus the measured 5% of inhibition can be treated as RSD of the measurement. Radotion, on the other hand expressed a 10% decrease in AChE activity. The decrease was noticed during the 15^{th} and 30^{th} minute of the experiment, which could be also covered by the presence of (dimethoxyphosphinyl)oxo - butanedioic acid diethyl ester – **10A** formed in the same period of time. This compound was later on also present in malaoxon photolysis, which also expressed decreased enzyme activity. The expressed toxicity in malaoxon and isomalathion during both processes was inversely proportioned to the degradation curves. The relative enzyme activity in case of malaoxon photolysis was still pronounced at the end of experiment, since it was still present at 20% of initial concentration.

From the obtained data, one can conclude, that the photocatalytic as photolytic degradation of pesticides' active ingredients is a very complex process. The dissapearance of the starting compound is only the first step in the long sequence of safe pesticide management. The slower rate constants in degradation of commercial product as also even more significantly slower rate constants in degradation of toxic by-products (malaoxon and isomalathion) represent a serious public threat. The employment of catalyst (TiO_2) resulted in the formation of toxic compounds, which inhibited the enzyme. Photolysis was in this regard safer. New methods cannot always completely replace the verified older approaches.

4.5 Ozonation and photocatalysis of chlorpyrifos and chlorpyrifos-oxon

4.5.1 INTRODUCTION

Chlorpyrifos, a member of diverse family of organophosphorus compounds (OP) is the only OP insecticide authorized for use in plant protection for the next years (chlorpyrifos, chlorpyrifos-methyl, mancozeb, maneb, and metiram as active substances will be used till 2016; 2005/72/EC amending 91/414/EEC). It is a broad-spectrum insecticide widely used in our environment. Its insecticidial property comes from the bioactivation to chlorpyrifos-oxon in organisms and the ability to inhibit acetylcholinesterase (AChE), an enzyme crucial for normal nerve function (Chambers and Levi, Eds., 1992). However, esterases in biological systems as well as natural occurring hydrolysis degrade both chlorpyrifos and chlorpyrifos-oxon to 3,5,6-trichloro-2-pyridinol (TCP). The acute toxicity depends on the level of exposure to chlorpyrifos, the rate of transformation to chlorpyrifos-oxon and the ability to hydrolyze it to TCP. Chlorpyrifos-oxon is about three orders of magnitude more potent as an inhibitor of AChE as chlorpyrifos (Chambers and Levi, Eds., 1992). The acute toxicity of chlorpyrifos expressed as LD_{50} (oral, male rat) is 82-155 mg/kg (Kousba et al., 2004). *In vitro* incubation of chlorpyrifos-oxon and paraoxon showed similar rates of phosphorylation, a descriptor of the AChE inhibitory capacity (Kousba et al., 2004). The relative toxicity of TCP in comparison to chlorpyrifos was found higher for a soil bacterium in Microtox system (Shemer et al., 2005, Barcelo et al., 1993).

Transformation pathways of chlorpyrifos have been widely studied (Pehkonen and Zhang, 2002). Different transformation products were identified under specific experimental conditions. When photodecomposition in dilute aqueous solutions at different pH values was studied only TCP and *O*-diethyl-*O*-(3,5,6-trichloro-2-pyridinyl) phosphorothioate were identified (Meikle et al., 1983). The environmental phototransformation rates and photochemical half-lives for chlorpyrifos and TCP in water under conditions of variable light intensity were derived from quantum yields, measured at 313 nm. It was calculated that significantly higher quantum yield for TCP (up to 33-times in comparison to chlorpyrifos) and much stronger absorption of troposferic solar radiation caused the degradation of TCP in minutes (4.4-120 minutes) and the degradation of chlorpyrifos in days (31-980 days). Chlorpyrifos is rather stable to phototransformation reactions in the absence of species that catalyze hydrolysis (Dilling et al., 1984). Photodegradation of chlorpyrifos on soil surfaces with UV light (254 nm) demonstrated that three different photochemical processes (hydrolysis – TCP; dechlorination of pyridinol ring and oxidation – chlorpyrifos-oxon) took place simultaneously (Waila et al., 1988). Photodegradation of chlorpyrifos was also followed in a suntest apparatus, with 5% acetone as a photosensitizer, where TCP was found to be the main transformation product, since chlorpyrifos-oxon and dechlorochlorpyrifos were not monitored (Barcelo et al., 1993). When photocatalysts ($FeCl_3$, TiO_2) were employed the highly stable chlorpyrifos (30 days) was in 15-27 minutes degraded forming TCP, *O*-ethyl-*O*-(3,5,6-trichloro-2-pyridyl) phosphorothioate and chlorpyrifos-oxon (Penuela and Barcelo, 1997).

During recent investigations of the toxicity and fate of chlorpyrifos in aqueous systems, the rapid transformation of chlorpyrifos to chlorpyrifos-oxon in chlorinated tap water was observed (Wu and Laird, 2003). Than in 2004, there was a report (Coupe and Blomquist, 2004), that at least three of OPs: chlorpyrifos, malathion and diazinon, were present in source water with enough frequency to indicate their fate to the environment. In finished potable water, however the parent compounds were not detected. This observation could be explained as complete transformations of parent compound into oxons, which are generally not target analytes in the surveys (Duirk and Collette, 2006). The model of chlorpyrifos transformation into chlorpyrifos-oxon and finally in TCP were then developed to forecast the fate of OP pesticides under drinking water treatment conditions using chlorine solution (Duirk and Collette, 2006).
Ozone, on the other hand was efficiently applied to drinking water treatment and wastewater treatment for its powerful oxidizing potential. Its efficiency was exploited on diazinon (Ku et al., 1998), pirimiphos-methyl (Chiron et al., 1998), and two nerve agents VX {*O*-ethyl *S*-[2-(diisopropylamino)

ethyl] methylphosphonothioate} and GD (pinacolyl methyl phosphonofluoridate) (Wagner et al., 2000), and phorate (Ku and Lin, 2002). The first transformation products in ozonation of OPs were always oxons (Chapter 2.4).

Regardless the knowledge, we achieved during years, very fresh papers are published promoting the removal of residual pesticides on vegetables using ozonated water (Wu et al., 2007a,b). Such papers rose our interest and because chlorpyrifos is the only OP insecticide authorized for use in plant protection for the next years, we decided to take it under inspection. It has been skipped from the large investigation of ozonation during the last years and it was thus selected together with its oxon analogue chlorpyrifos-oxon for additional studies. We have noticed a lack in photocatalysis studies regarding chlorpyrifos-oxon. That is why, we cycled the investigations on chlorpyrifos and chlorpyrifos-oxon in terms of kinetics (with high performance liquid chromatography – HPLC), products (gas chromatography-mass spectrometry – GC-MS, liquid chromatography-mass spectrometry) and toxicity studies (acetylcholinesterase bioassay based on flow injection analysis coupled with thermal lens spectrometry – FIA AChE TLS) under ozone and photocatalytic treatment. The use of advanced oxidation processes (AOPs) – ozone and TiO_2 - for treatment of OP polluted waters represents a serious threat if stable by-products are not adequately monitored.

4.5.2 EXPERIMENTAL

4.5.2.1 Materials

Technical chlorpyrifos (Pyrinex 48 EC), with the concentration of 480 g L^{-1} was purchased from Makteshim Chemical Works Ltd., Beer-Sheva, Izrael.
The sol-gel TiO_2 films were prepared as described in 4.4.2.2. Photocatalytic cell, lamps and photoreactor used are described under 4.4.2.3.

4.5.2.2 Ozonation

Aqueous samples were purged with ozone generated by the adjusting power input to a Pacific Ozone (L11-L24) generator at the inlet oxygen gas flow rate of 10 L h^{-1}. The mass flow of generated ozone was calculated from iodometric titration with a standard thiosulphate solution, and it was (1.50 ± 0.1) g h^{-1}.

4.5.2.3 Photocatalytic and ozonation experiments

Aqueous solutions containing standard solution of chlorpyrifos (1.03 ± 0.03) mg L^{-1}, chlorpyrifos-oxon (11.90 ± 0.04) mg L^{-1} were photodegraded with 6 glass slides with immobilized sol-gel derived TiO_2. For ozonation experiment, chlorpyrifos solution was warmed in the water bath (35 ± 5)°C to increase the solubility. The concentration of working solutions were than for chlorpyrifos (2.4 ± 0.3) mg L^{-1}, and for chlorpyrifos-oxon (12.06 ± 0.08) mg L^{-1}. Technical chlorpyrifos (Pyrinex) forms a heterogeneous solution, which was prior experiments filtrated. The working solution was prepared by diluting 98.6 mg of Pyrinex into 1 L of deionised water. The solution of OP was left rotating and purging with oxygen 15 min in dark before beginning of the irradiation. The 15 ml of the samples were taken from the cell at different times during the irradiation and analyzed by HPLC, GC-MS and AChE-TLS.

4.5.2.4 Analytical procedures

4.5.2.4.1 LIQUID CHROMATOGRAPHY ANALYSIS (LC)

The HPLC-DAD equipment consists of a HP 1100 Series chromatograph, coupled with DAD detector for the kinetics studies. The identification of formed by-products LC-MSD instrument was employed. The chromatographic separations were run on a monolith column C18 Merck, Purospher STAR (250

mm x 4.6 mm, 5 µm). The injection volume was 75 µL. Eluent (A) was 10 mM ammonium acetate and (B) was acetonitrile (HPLC grade), flow rate 0.6 mL min^{-1}. The gradient elution was as follows: 0 min 90% A; 20 min 70% A; 60 min 30% A; 70 min 10% A. The retention times for 3,5,6-trichloro-2-pyridinol was 24.8 min, for chlorpyrifos-oxon 57.5 min, and for chlorpyrifos 74.9 min. For quantification purposes a calibration curve in the concentration range from 0.05 ppm to 20 ppm was prepared. The r-square values of the regression lines were in all cases > 0.999.

For the identification of formed by-products LC-MSD (Applied Biosystem Q-Trap 3200) instrument was employed. The chromatographic separations were the same as run HPLC-DAD instrument, for easier comparison of obtained chromatograms. The instrument (temperature 400°C) was from the beginning till 25th minute of each injection (50 µL) run in negative mode (IS (ionization source) –4500 V; DP (declustering potential) –50 V; EP (entrance potential) –10 V) to confirm *O,O*-diethylphosphorothioate, *O,O*-diethylphosphate and TPC and/or their related transformation products. Whereas, the analysis of the second part (from 25th minute till 85th minute) was run in positive mode (IS (ionization source) +5500 V; DP (declustering potential) +25 V; EP (entrance potential) +5 V), when both chlorpyrifos-oxon and chlorpyrifos were identified.

4.5.2.4.2 GAS CHROMATOGRAPHY-MASS SPECTROMETRY (GC-MS)

The ethyl acetate extracts were analyzed by GC-MS (Varian, Saturn 2100T) on a CP-Sil 8 CB low bleed/MS column (5% phenyl – 95% methylpolysiloxane, 30 m × 0.25 mm; film thickness 0.25 µm). The injector was held at 270 °C, oven started at 80 °C, and the temperature was increased with a gradient of 10 °C/min till 290 °C and maintained constant for 5 min. The injection volume was in all cases 1 µL.

4.5.2.4.3 PESTICIDE EXTRACTION

Solid phase extraction (SPE) method with 100 mg Strata C18 cartridges and liquid-liquid extraction (LLE) were used for extraction of pesticides from water samples. The general SPE procedure included the conditioning step: 3 mL of ethyl acetate, 3 mL of methanol, 5 mL of deionised water; sample load: 10 mL; analyte elution: 5 mL of ethyl acetate. In order to catch also more polar compounds LLE was employed. For 10 ml of samples, 25 ml of ethyl acetate was added. The extraction mixture was than shaked for 30 min, and separated in the funnel. The ethyl-acetate extracts were dried over sodium sulphate and evaporated on rotary evaporator. Dry samples were than redissolved in 200 µL of ethyl acetate or acetonitrile.

4.5.3 RESULTS AND DISCUSSIONS

Chlorpyrifos-oxon is a potent AChE inhibitor (Kousba et al., 2004). Prior toxicity bioassay of ozonated or irradiated samples, analyses of diluted water samples containing chlorpyrifos-oxon in the concentration range from 50 - 500 ppb were done, and toxicity curve was derived (Figure 30).

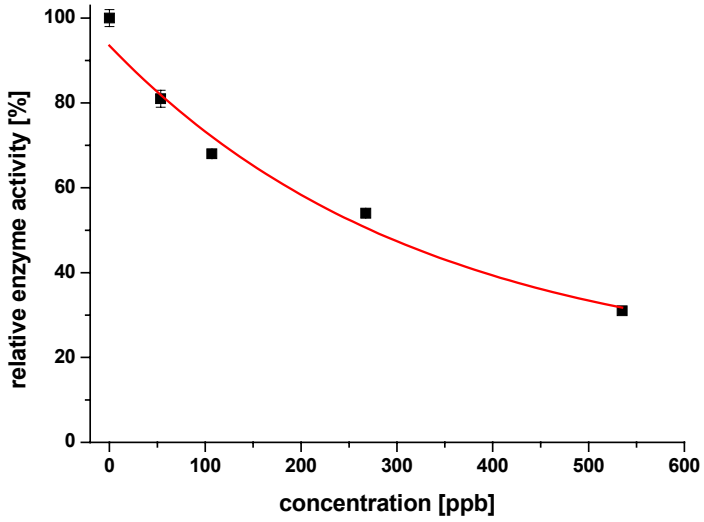

Figure 30: *Relative inhibition of AChE (in FIA-AChE-TLS bioassay setup) in dependence of chlorpyrifos-oxon concentration in spiked water samples.*

The setup for chlorpyrifos-oxon detection in our FIA-AChE-TLS was enough sensitive to detect less than 50 ppb of chlorpyrifos oxon in samples. It was possible, thus, to monitor less than 5% of transformation from chlorpyrifos into chlorpyrifos-oxon during ozonation or photocatalysis.

A cycloaddition of ozone on the double bond P=S before the breakdown of the molecule was expected from the literature (Laplanche et al., 1984), since chlorpyrifos is a member of phosphorothioates (as parathion and diazinon are). But, to our knowledge, there are no data regarding the kinetics of transformation to chlorpyrifos-oxon, nor its stability / susceptibility to further ozone attacks. It was noticed, that in pure analytical standard solution of chlorpyrifos the conversion into chlorpyrifos-oxon was rapid. In 15 minute a total conversion into oxon was observed (Figure 31 – left). When technical product (Pyrinex) was ozonated, the picture was almost the same, except the conversion was slower compared to pure analytical standard, and it was achieved in one hour (Figure 31 – right).

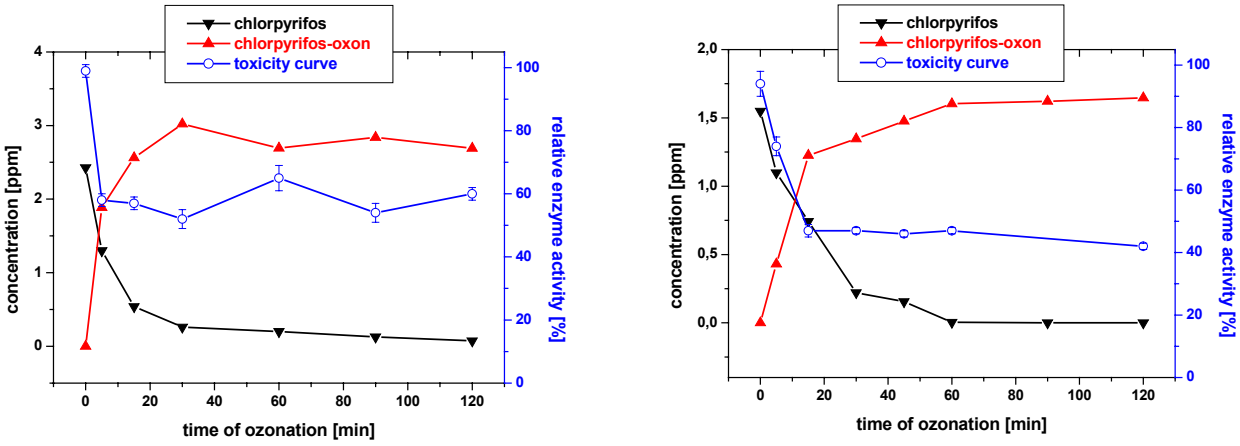

Figure 31: *Ozonation of pure analytical standard solution of chlorpyrifos (left) and technical chlorpyrifos – Pyrinex (right). The disappearance curve of chlorpyrifos is black (▼), the formation curve of chlorpyrifos-oxon is red (▲), the toxicity curve is blue (○) represented by the right scale.*

The ozonated samples were prior FIA-AChE-TLS bioassay diluted. The samples containing pure analytical standard chlorpyrifos were (2.4 ± 0.3) diluted 10-times. The relative enzyme activity,

according to chlorpyrifos-oxon toxicity curve (Figure 30), was expected to be around 55% in case of complete transformation to chlorpyrifos-oxon, and it was (Figure 31 - left). The same was observed in case of Pyrinex ozonation. The samples were prior bioassay 4-times diluted. Regarding the initial concentration of chlorpyrifos in Pyrinex (1.5 ± 0.2), the expected relative enzyme activity in total conversion to chlorpyrifos-oxon was 40% (Figure 30), and it was (Figure 31 - right).

Since the concentration of formed chlorpyrifos-oxon did not drop with additional ozonation process, it was thought, that ozone is rather unsuccessful in oxon degradation. The concerning fact was proved, by ozonation of higher amounts of chlorpyrifos-oxon analytical standard under same experimental conditions. In fact, in two hours only 21.5% of the starting compound was degraded, and the relative enzyme activity increased for 6% (Figure 32). The samples were prior analysis diluted 50-times (Figure 32), which perfectly fits the toxicity curve obtained (Figure 30). Chlorpyrifos-oxon was further degraded (9.4 %) into TCP (Figure 32). The other hydrolysis product was also diethyl phosphate identified by LC-MS at RT 3.6 in negative mode, with m/z 153 (M-H), and 125 (M-C_2H_5).

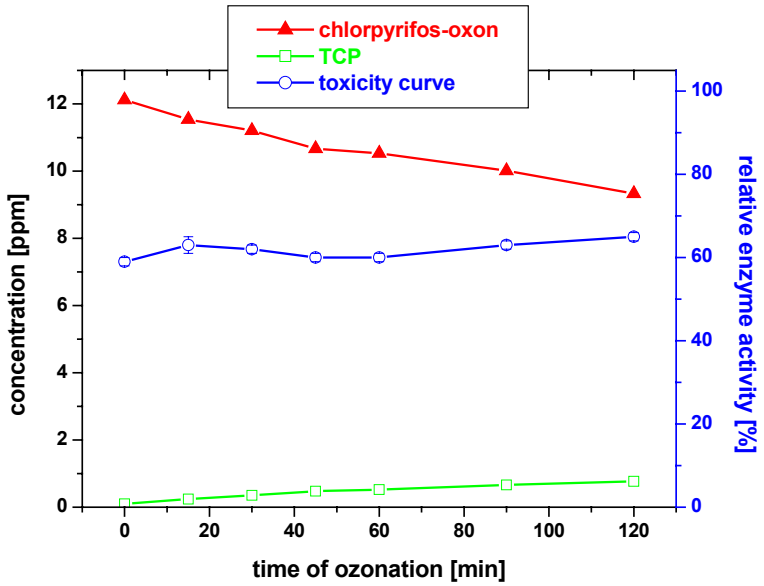

Figure 32: *Ozonation of pure analytical standard solution of chlorpyrifos-oxon. The disappearance curve of chlorpyrifos-oxon is black (▼), the formation curve of TCP is green (□), the toxicity curve is blue (○) represented by the right scale.*

Several authors have dealt with chlorpyrifos photodegradation (Waila et al., 1988; Barcelo et al., 1993; Penuela and Barcelo, 1997), but any degradation study was devoted to chlorpyrifos-oxon. In our case the degradation half-live times were (15.0 ± 0.8) min for chlorpyrifos and (27.7 ± 1.3) min for chlorpyrifos-oxon. The degradation kinetics totally depends upon experimental conditions used. However, it could be noticed, that anyway it took more than twice to degrade chlorpyrifos-oxon, since the kinetics followed first order in both cases (Figure 33). For the bioassay chlorpyrifos irradiated solutions were not dilute and were analyzed as such. The maximal observed amount of chlorpyrifos-oxon (236 ppb) in chlorpyrifos photocatalysis was at 30th minute of the experiment and caused 38% inhibition (Figure 33- left). The inhibition perfectly fits the toxicity curve (Figure 30) indicating, that any other anti-AChE toxic by-product was formed.

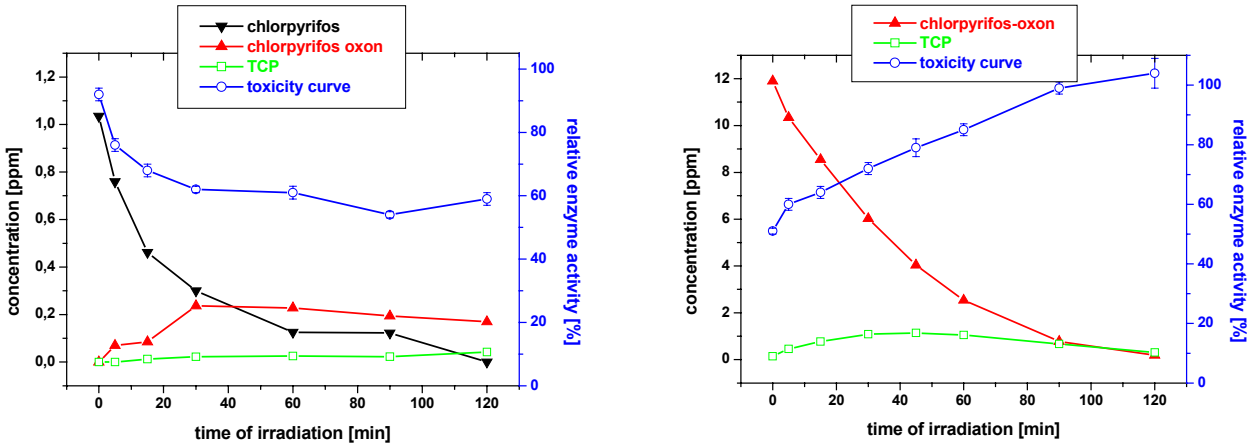

Figure 33: *The TiO_2 photocatalysis of pure analytical standard solution of chlorpyrifos (left) and chlorpyrifos-oxon (right). The disappearance curve of chlorpyrifos is black (▼), the curve of chlorpyrifos-oxon is red (▲), the formation curve of TCP is green (□), the toxicity curve is blue (○) and represented by the right scale.*

Beside the formation of chlorpyrifos-oxon (24% of initial chlorpyrifos concentration) in chlorpyrifos photocatalysis, the hydrolytic pathway was dominant in both cases. Two main products observed in TiO_2 photocatalysis were well known (Waila et al., 1988; Barcelo et al., 1993; Penuela and Barcelo, 1997) TCP and *O,O*-diethylphosphorothioate in case of chlorpyrifos and *O,O*-diethylphosphate chlorpyrifos-oxon. The two products were expected, since continuous hydroxyl attack should result in bond cleavage. By analyzing mass spectra (LC-MS) another by –product was identified at RT 24.8 min in negative mode with m/z 304, 306, 308 (M-H), and 196, 198, 200 (M-(OEt(PO)OH)). It was identified as *O*-ethyl-*O*-(3,5,6-trichloro-2-pyridyl) phosphate.

4.5.4 CONCLUSIONS

Chlorination represents a serious threat if chlorpyrifos is present in waters, since it is transformed into chlorpyrifos-oxon under drinking water treatment conditions (Wu and Laird, 2003; Duirk and Collette, 2006). But as a summary based on the presented behaviour of chlorpyrifos and its 1000-times more toxic by-product chlorpyrifos-oxon, neither ozone nor TiO_2 are good choice for safe degradation of OPs. In OPs degradation one should take all due precautions, since oxidation of OPs generally leads to more powerful toxicants. The efficiency of ozonation as also photocatalysis depends upon variety of parameters, but the resistance of the formed oxon toward photocatalysis (more than 2-times slower kinetics) and ozonation (only 21.5 % degraded chlorpyrifos-oxon during 2 h of ozonation) raises concerns. Changing pH, oxygen and ozone flow-rates, as also the amount of photocatalysts on the glass slides would result in different kinetics. The by-products, however would scarcely changed, except the hydrolysis would occur faster, and the mineralisation would be better. The implication of ozonated water in “safe” removal of OP polluted vegetables (Wu et al., 2007) is not only missing the right way but a very dangerous action. Since the end product in any chlorpyrifos or chlorpyrifos-oxon degradation process is toxic TCP degradation (Shemer et al., 2005, Barcelo et al., 1993), than also the use of chlorpyrifos till 2016 (2005/72/EC amending 91/414/EEC) should be revised.

5 DISCUSSION – GENERAL

OP compounds have found their use in agricultural practice for more than 4 decades. Nowadays, they are slowly replaced by other biocides, mostly from the group of neonicotinoides. Chlorpyrifos and chlorpyrifos-methyl, however, are the only representatives from OP group, which will be used till the year 2016 (2005/72/EC amending 91/414/EEC). On the other hand, the use of OP in general, is not diminished in non-European countries, where they are commonly used, i.e. China (Wu et al., 2007), or USA (Agricultural Chemical Usage 2005 Field Crops Summary, May 2006).

Because of their continuous impact on the environment, it is worth monitoring their presence in foodstuffs. The FIA-AChE-TLS, which was developed in our laboratory, offers a satisfactory answer to this issue. It is a rapid, reliable and sensitive method for detection of OPs in real samples. It was improved by introducing a direct oxidation procedure, which did not prolong the analysis time (extraction or/and preconcentration) (Mionetto et al., 1994; Fennouh et al., 1997; Wilkins et al., 2000; Montesinos et al., 2001; Andreescu et al., 2002). The oxidation procedure enables determination of thio-OPs in less than 15 minutes. In this way, the analysis of real samples containing OPs was shortened for 8 - times (Schultze et al., 2002, 2003, 2004). The LODs of specified OP compounds determined by improved FIA-AChE-TLS method are in all cases well below the maximal residue limits for OPs in foodstuffs according to Slovenian legislation (MRL = 500 ppb; Official Gazette of RS, 13 and 54,1999).

The dissipation of OPs in the environment, on the other hand, represents a serious threat to wildlife as well as to public health. In fact, a recent publication (Coupe and Blomquist, 2004) reports, that at least three of OPs, i.e. chlorpyrifos, malathion and diazinon, are frequently present in spring water to indicate their fate in the environment. For this reason, there is a growing interest in research and treatments development (advanced oxidation methods) for purification of polluted waters containing OP and their degradation products oxons, as well as commercial coproducts.

Malathion and its two commonly present transformation products, malaoxon and isomalathion were chosen for photodegradation studies. Experimental results of these studies were compared to the existing literature data on degradation and transformation of primary compounds (i.e. malathion) and their metabolites (malaoxon, isomalathion). Several irradiation methods were employed. The identification of formed product was based on mass spectra and identification of some compounds was only tentative, according to RT and characteristic ions. The degradation was directed always towards “safe” release of compounds into the environmental. Thus, after each irradiation experiment, toxicity tests using FIA-AChE-TLS bioassay were performed. The first experiment was done using 125 W Cermax Xenon parabolic lamp. The light source was unfiltered (λ = 200 nm – Vis). Analyses of samples containing malathion showed only slight decrease in AChE activity. The GC-MS analyses of irradiated samples containing malathion, on the other hand, revealed the presence of different substituted buta(e)nedioic acids diethyl esters. A model compound from this group, diethyl maleate, was chosen for the experiments and tested in FIA-AChE-TLS system. The activity of the enzyme remained intact, suggesting the whole group of substituted buta(e)nedioic acids diethyl esters were non-inhibiting AChE compounds. Similar degradation products were also identified in the case of radiolysis and TiO_2 photocatalysis of malathion. The difference between these classes of degradation compounds was in strength of observed AChE inhibition. The hydroxyl radical (oxidative) attack resulted, in addition to the formation of substituted buta(e)nedioic acids diethyl esters, also in the formation of 1000-times more toxic malaoxon. The formation of malaoxon correlated well with the strength of inhibition of the enzyme activity. When small trimethyl esters were formed ([OOS(O)], [OOS(S)]), the decrease in activity was even higher, indicating synergistic effects of these compounds. The degradation of malaoxon and malathion was followed under the same experimental conditions. Unfortunately, the degradation rate of the former was slower regardless of the irradiation treatment employed. Additionally, its degradation was always followed by the formation of toxic [OOS(O)]. The same characteristic was observed in isomalathion degradation with [OSS(O)] formation. The degradation rate constant of isomalathion, however, was smaller than that of malathion and larger than that of malaoxon. The lack of formation of ([OOS(O)], [OOS(S)], [OSS(O)]) in photolysis (λ = 254 nm) experiments of all three compounds (malathion, malaoxon and isomalathion) and lack of formation of malaoxon in photolysis of malathion resulted in no decrease in AChE activity.

Chlorpyrifos and its oxon analog – chlorpyrifos-oxon, were exposed, in addition to TiO_2 photocatalytic treatment and ozonation processes. Chlorpyrifos-oxon is a strong AChE inhibitor (Kousba et al., 2004) formed during photodegradation of chlorpyrifos using Xenon lamp and TiO_2 photocatalysis. The toxicity of chlorpyrifos irradiated solutions correlated negatively with the formation of chlorpyrifos-oxon. In ozone treatment, cycloaddition of ozone on the double bond P=S was expected from the literature (Laplanche et al., 1984), before the breakdown of the molecule - since chlorpyrifos is a member of phosphorothioates (as parathion and diazinon are). To the best of our knowledge, there were no data regarding the kinetics of transformation to chlorpyrifos-oxon, nor its susceptibility to further ozone attacks. It was noticed, that in pure analytical standard solution of chlorpyrifos the conversion into chlorpyrifos-oxon was rapid (15 min). Formed chlorpyrifos-oxon was found resistant toward further ozonation process. Even with higher concentrations of ozone only around 20% of the primary compound (after 2 h of ozonation) was degraded.

Since the oxidation of OPs in general leads to stronger toxins in comparison to primary compounds, the advanced oxidation processes (photocatalysis and ozonation) are promising technique for organophosphorus pesticide removal only coupled with toxicity tests.

6 CONCLUSIONS

1. FIA-AChE-TLS, developed in our laboratory is a rapid, reliable and sensitive method for detection of OPs. It was improved by introducing a direct oxidation procedure in the analysis of real samples (juices, water) with no additional analytical step that would prolong the analysis time (extraction or/and preconcentration). The AChE bioassay based on the investigated oxidation procedure enables determination of thio-OPs in the ppb concentration range in less than 15 minutes. In this way, the proposed analysis (Schultze et al., 2002, 2003, 2004) of real OPs polluted samples was shorten for 8 – times (Bavcon Kralj et al., 2006).

2. The application of the AChE bioassay has revealed that the anti-AChE toxicity of pesticide solutions subjected to photodegradation does not follow the degradation curves obtained by monitoring the dissaperance of parent compounds. The obtained toxicity curve indicate the formation of more toxic compound during irradiation. Two AChE inhibiting toxic photo-products, i.e., phosphorodithioic *O,O,S*-trimethyl ester and phosphorothioic *O,O,S*-trimethyl ester, were identified as a result of P—S—C bond cleavage in the case of azinphos-methyl, malathion and malaoxon degradation. In addition, formation of AChE inhibiting oxidation products identified as diethyl (dimethoxyphosphinyl)oxo - butanedioic acid diethyl ester was observed in the case of malathion and malaoxon degradation, while chlorpyrifos-oxon was detected as the only photoinduced compound in chlorpyrifos photodegradation under given experimental conditions (Xenon lght source) (Bavcon Kralj et al., 2007).

3. Radiolytic studies of malathion, isomalathion and malaoxon showed a pronounced toxicity of all irradiated samples. Small trimethyl phosphate esters were identified in all cases. Their formation and relative stability (none of them was totally degraded at the end of the experiment) towards γ-irradiation should cause a concern since they exhibit aging of AChE resulting in the delayed toxic effects. The formation of malaoxon in the case of malathion radiolysis coincided perfectly with induced AChE toxicity.

4. The malathion degradation and the degradation of its related compounds (Radotion. malaoxon, and isomalathion) were followed under photolytic and photocatalytic experiments. In degradation product study, several transformation products were identified based on mass spectra. They were divided in two groups; in AChE inhibiting and AChE non-inhibiting compounds. The main reactions producing AChE non-inhibiting compounds were isomerisation and oxidation. The presence of AChE inhibiting compounds was directly correlated with the reduced relative activity of the enzyme. The toxicity curves obtained from photocatalytic degradation of malathion and Radotion showed a strong inhibition of AChE enzyme. In both cases, the formation of malaoxon correlated well with the decreased relative enzyme activity. The observed toxicity of malaoxon and isomalathion was inversely proportional to the degradation curves. From the obtained data, it may be concluded, that the application of TiO_2 as a catalyst resulted in the formation of toxic compounds. In this regard photolysis was found safer.

5. The efficiency of removal of chlorpyrifos and its 1000-times more toxic by-product chlorpyrifos-oxon employing ozonation and photocatalysis is unappropriate. During these processes chlorpyrifos is transformed into chlorpyrifos-oxon, which is resistant toward further degradation. Changing the experimental parameters (pH, oxygen and ozone flow-rates, the amount of photocatalysts on the glass slides) would resulted in different kinetics, but the end product in any chlorpyrifos or chlorpyrifos-oxon degradation process is toxic TCP (Shemer et al., 2005, Barcelo et al., 1993). The use of chlorpyrifos till the year 2016 (2005/72/EC amending 91/414/EEC) should therefore be revised.

A general conclusion could be made at this point. Several degradation techniques were found to be efficient in removal of parent OP compounds. In this regard, it should be emphasized that there is a need for on line monitoring of OP's degradation products by an apropriate sensitive and fast response toxicity tests to ensure the complete degradation and removal of any toxic compounds. The FIA-AChE-TLS assay proved promising in that respect.

7 REFERENCES

Abdel Aal S.E., Dessouki A.M., Sokker H.H., 2001. Degradation of some pesticides in aqueous solutions by electron beam and gamma radiation. J. Radioanal. Nucl. Chem., 250: 329-334

Agricultural Chemical Usage 2005 Field Crops Summary Agricultural Statistics Board, May 2006, NASS, USDA

Ahmed F.E., 2001. Analyses of pesticides and their metabolites in foods and drinks. TrAC, 20: 649-661

Albareda-Sirvent M., Merkoçi A., Alegret S., 2001. Pesticide determination in tap water and juice samples using disposable amperometric biosensors made using thick-film technology. Anal. chim. acta, 442: 35-44

Aldridge W.N., Miles J.W., Mount D.L., Verschoyle R.D., 1978. The toxicological properties of impurities in malathion. Arch. Toxicol., 42: 95-106

Ali F.A.F. and Fukuto T.R., 1982. Toxicity of O,O,S-trialkyl phosphorothioates to the rat. J. Agric. Food Chem., 30: 126-130

Allmaier G.M., Schmid E.R., 1985. Effects of Light on the Organophosphorus Pesticides Bromophos and Iodofenphos and Their Main Degradation Products Examined in Rainwater and on Soil Surface in a Long-Term Study. J. Agric. Food Chem., 33: 90-92

Andreescu S., Noguer T., Magearu V., Marty J.L., 2002. Screen-printed electrode based on AChE for the detection of pesticides in presence of organic solvents. Talanta, 57: 169-176

Arnone A., Novo B., Pregnolato M., Resnati G., Terreni M., 1997. Conversion of Thio- and Selenophosphoryl into phosphoryl Group by Perfluro cis-2,3-Dialkyloxaziridines. J. Org. Chem., 62: 6401-6403

Arufe M.I, Romero J.L., Gamero J.J., Moreno M.J., 2000. Oxidation of cholinesterase-inhibiting pesticides: A simple experiment to illustrate the role of bioactivation in the toxicity of chemicals. Biochem. educ., 28: 174-177

D. Barcelo, G. Durand, N. De Bertrand, 1993. Photodegradation of the organophosphorus pesticides chlorpyrifos, fenamiphos and vamidon in water. Toxicol. environ. chem, 38: 183-199

Barcelo D., Lacorte S., Marty J.L., 1995. Validation of an ezymatic biosensor with liquid chromatography for pesticide monitoring. TrAC, 14: 7

Bavcon M., Trebše P., Zupančič-Kralj L., 2003. Investigations of the determination and transformations of diazinon and malathion under environmental conditions using gas chromatography coupled with a flame ionization detector. Chemosphere, 50: 595-601

Bavcon M., Trebše P., Franko M., 2006. Oxidation as a pre-step in determination of organophosphorus compounds by the AChe-TLS bioassay. Acta chim. slov., Vol. 53, No.1, 43-51

Bavcon Kralj M., Franko M., Trebše P., 2007. Photodegradation of organophosphorus insecticides - Investigations of products and their toxicity using gas chromatography-mass spectrometry and AChE-thermal lens spectrometric bioassay. Chemosphere, 67:99-107

Bellet E.M. and J.E. Casida, 1974. Products of Peracid Oxidation of Organophosphorus Compounds. J.Agr.Food Chem., Vol. 22, No.2, 207-211

Bello-Ramirez A.M., Carreon-Garabito B.Y., Nava-Ocampo A.A., 2000. A theoretical approach to the mechanism of biological oxidation of organophosphorus pesticides. Toxicology, 149: 63–68

Bruzik K.S. and Stec W.J., 1990. Reversible Oxidation of Phosphylthionates and Phosphylselenonates with Trifluoroacetic Anhydride. J. Org. Chem., 55: 6131-6135

Burrows H.D., Canle M., Santaballa J.A., Steenken S., 2002. Invited Review, Reaction pathways and mechanisms of photodegradation of pesticides. J. photochem. photobiol., B Biol., 67:71–108

Buxton G.V., Greenstock C.L., Hellman W.P., Ross A.B., 1988. Critical Review of Rate Constants for Reactions of Hydrated Electrons, Hydrogen Atoms and Hydroxyl Radicals (·OH/·O-) in Aqueous Solution. J.Phys.Chem.Ref. Data, 17: 533-538

Campos S.X., Vieira E.M., Cordeiro P.J.M., Rodrigues-Fo E., Murgu M., 2003. Degradation of the herbicide 2,4-dichlorophenoxyacetic acid (2,4)-dimethylamine salt by gamma radiation from cobalt-60 in aqueous solution containing humic acid. Radiat. Phys. Chem., 68: 781-786

Chambers, J.E., Levi P.E. (Eds.), Organophosphates, Chemistry, Fate, and Effects. Academic Press, San Diego, 1992

Chen Z.M., Zabik M.J., Leavltt R.A., 1984. Comparative Study of Thin Film Photodegradative Rates for 36 Pesticides. Ind. Eng. Chem. Prod, Res. Dev.: 23, 5-11

Chiron S., Fernandez-Alba A., Rodriguez A., 1997. Pesticide chemical oxidation processes: an analytical approach. TrAC: 16, no. 9

Chiron S., Rodriguez A., Fernandez-Alba A., 1998. Application of gas and liquid chromatography-mass spectrometry to the evaluation of pirimiphos methyl degradation products in industrial water under ozone treatment. J. Chromatogr. A, 823: 97-107

Chiron S., Fernandez-Alba A., Rodriguez A., Garcia-Calvo E., 2000. Review Paper, Pesticide Chemical Oxidation: State-Of-The-Art. Wat. Res., 34: 366-377

Cho Y.A., Lee H.S., Cha G.S., Lee Y.T., 1999. Fabrication of butyrylcholinesterase sensor using polyurethane-based ion-selective membranes. Biosens. bioelectron., 30: 435-438

Choi J.W., Kim Y.K., Oh B.K., Song S.Y., Lee W.H., 2003. Optical biosensor for simultaneous detection of captan and organophosphorus compounds. Biosens. bioelectron., 18: 591-597

Chukwudebe A., March R.B., Othman M., Fukuto T.R., 1989. Formation of Trialkyl Phosphorothioate Esters from Organophosphorus Insecticides after Exposure to Either Ultraviolet Light or Sunlight. J. Agric. Food Chem., 37: 539-545

Clothier B., Johnson M.K., Reiner E., 1981. Interactioon of some trialkyl phosphorothiolates with acetylcholinesterase characterisation of inhibition, aging and reactivation. Biochem. Biophys. Acta, 660: 306-316

Coupe R. H., Blomquist J. D., 2004. Water-soluble pesticides in finished water of community water supplies. Jour. AWWA 96 (10), 56-68

COMMISSION DIRECTIVE 2005/72/EC of 21 October 2005 amending Council Directive 91/414/EEC to include chlorpyrifos, chlorpyrifos-methyl, mancozeb,maneb, and metiram as active substances

Cremisini C., Di Sario S., Mela J., Pilloton R., Palleschi G., 1995. Evaluation of the use of free and immobilised acetylcholinesterase for paraoxon detection with an amperometric choline oxidase based biosensor. Anal. chim. acta, 311: 273-280

Černigoj U., Lavrenčič Štangar U., Trebše P., Opara Krašovec U., Gross S., 2006. Photocatalytically active TiO_2 thin films produced by surfactant-assisted sol-gel processing. Thin Solid Films 495: 327–332

Černigoj U., Lavrenčič Štangar U., Trebše P., 2007. Evaluation of a novel Carberry type photoreactor for the degradation of organic pollutants in water. J. photochem. photobiol.,A Chem., article in press.

Dannenberg A., Pehkonen S.O., 1998. Investigation of the Heterogeneously Catalyzed Hydrolysis of Organophosphorus Pesticides. J. Agric. Food Chem., 46: 325-334

Derbalah A.S., Nakatani N., Sakugawa H., 2004. Photocatalytic removal of fenitrothion in pure and natural waters by photo-Fenton reaction. Chemosphere, 57: 635–644

Dilling W.L., Lickly L.C., Lickly T.D., Murphy P.G., McKellar R.L.; 1984. Organic Photochemistry. 19. Quantum Yields for O,O-diethyl O-(3,5,6-trichloro-2-pyridinyl)phosphorothioate (chlorpyrifos) and 3,5,6-trichloro-2-pyridinol in dilute aqueous solutions and their environmental phototransformation rates. Environ.Sci.Technol.,18: 540-543

Dominguez C., Garcia J., Pedraz M.A., Torres A., Galan M.A., 1998. Photocatalytic oxidation of organic pollutants in water. Catal. today, 40: 85-101

Doong R.A., Chang W.H., 1997. Photoassisted titanium dioxide mediated degradation of organophosphorus pesticides by hydrogen peroxide. J. photochem. photobiol.,A Chem., 107: 239-244

Doong R.A., Chang W.H., 1998. Photoassisted iron compound catalytic degradation of organophosphorous pesticides with hydrogen peroxide. Chemosphere, 37: 2563 – 2572

Drzewicz P., Nalecz-Jawecki G., Gryz M., Sawicki J., Bojanowska-Czajka A., Gluszewski W., Kulisa K., Wolkowicz S., Trojanowicz M., 2004. Monitoring of toxicity during degradation of selected pesticides using ionizing radiation. Chemosphere, 57: 135-145

Duirk S.E., and Collette T.W., 2006. Degradation of chlorpyrifos in aqueous chlorine solutions: pathways, kinetics, and modeling. Environ.Sci.Technol., 40: 546-551

Durand G., Abad J.L., Sanchez-Baeza F., Messeguer A., Barcelo D., 1994. Unequivocal Identification of Compounds Formed in the Photodegradation of Fenitrothion in Water/Methanol and Proposal of Selected Transformation Pathways. J. Agric. Food Chem., 42: 814-821

Dzyadevych S.V., Chovelon J.M., 2002. A comparative photodegradation studies of methyl parathion by using Lumistox test and conductometric biosensor technique. Mater. sci. eng., C, 21: 55–60

Dzyadevych S.V., Soldatkin A.P., Chovelon J.M., 2002. Assessment of the toxicity of methyl parathion and its photodegradation products in water samples using conductometric enzyme biosensors. Anal. chim. acta, 459: 33-41

Dzyadevych S.V., Soldatkin A.P., Arkhypova V.N., El'skaya A.V., Chovelon J.M., Georgiou C.A., Martelet C., Jaffrezic-Renault N., 2005. Early-warning electrochemical biosensor system for environmental monitoring based on enzyme inhibition. Sens. actuators, B, 105: 81–87

Ellman G.L., Courtney K.D., Andres V., Jr., Featherstone R.M., 1961. A new and rapid colorimetric determination of acetylcholinesterase activity. Biochem. pharmacol., 7: 88-95

Farre M., Brix R., Barcelo D., 2005. Screening water for pollutants using biological techniques under European Union funding during the last 10 years. TrAC, 24: 532 – 545

Fennouh S., Casimiri V., Burstein C, 1997. Increased paraoxon detection with solvents using acetylcholinesterase inactivation measured with a choline oxidase biosensor. Biosens. bioelectron., 12: 97-104

Fernandez-Alba A.R., Hernando D., Aguera A., Caceres J., Malato S., 2002. Toxicity assays: a way for evaluating AOPs efficiency. Wat. Res., 36: 4255 – 4262

Flounders A.W., Singh A.K., Volponi J.V., Carichner S.C., Wally K., Simonian A.S., Wild J.R., Schoeniger J.S., 1999. Development of sensors for direct detection of organophosphates. Part II: sol–gel modified field effect transistor with immobilized organophosphate hydrolase. Biosens. bioelectron, 14: 715–722

Franko M., 2001. Review: Recent applications of thermal lens spectrometry in food analysis and environmental research. Talanta, 54: 1-13

Franko M., Sarakha M., Čibej A., Boškin A., Bavcon M., 2005. Photodegradation of pesticides and application of bioanalytical methods for their detection. Pure appl. chem., Vol. 77, No. 10, 1727-1736

Helinski J., Skrzypczynski Z., Wasiak J., Michalski J., 1990. Efficient Oxygenation of Thiophosphoryl and Selenophosphoryl Groups using Trifluoroacetic anhydride. Tetrahedron lett., 31: 4081-4084

Hernandez J., Robledo N.R., Velasco L., Quintero R., Pickard M.A., Vazquez-Duhalt R., 1998. Chloroperoxidase-Mediated Oxidation of Organophosphorus Pesticides. Pestic. biochem. physiol., 61: 87-94

Herriot A.W., 1971. Peroxy Acid Oxidation of Phosphinothioates, a Reversal of Stereochemistry. J. Am. Chem. Soc., 93: 13 June 30

Herzsprung P., Weil L., Quentin K.E., Zombola I., 1990. Determination of Organophosphorus Compounds and Carbamates by their Inhibition of Cholinesterase, Part 2: Estimation of Detection limits for Insecticide-determination by Concentration, Oxidation and Inhibition Values, Vom Wasser, 74: 339-35

Hincapie M., Maldonado M.I., Oller I., Gernjak W., Sanchez-Perez J.A., Ballesteros M.M., Malato S., 2005. Solar photocatalytic degradation and detoxification of EU priority substances. Catal. today, 101: 203–210

Hirahara Y., Ueno H., Nakamuro K., 2003. Aqueous photodegradation of fenthion by ultraviolet B irradiation: contribution of singlet oxygen in photodegradation and photochemical hydrolysis. Water res., 37: 468-476

Hua Z., Manping Z., Zongfeng X., Low G.K.C., 1995. Titanium dioxide mediated photocatalytic degradation of monocrotophos. Wat. Res., 29: 2681-2688

Huang J., Mabury S.A., 2000. The role of carbonate radical in limiting the persistence of sulfur-containing chemicals in sunlit natural waters. Chemosphere, 41: 1775-1782

Huston P.L., Pignatello J.J., 1999. Degradation of selected pesticide active ingredients and commercial formulations in water by the photo-assisted Fenton reaction. Wat. Res., 33: 1238-1246.

Ishiwata S., Kamiya M., 1999. Cyclodextrin inclusion: catalytic effects on the degradation of organophosphorus pesticides in neutral aquous solution. Chemosphere, 39: 1595-1600 - a

Ishiwata S., Kamiya M., 1999. Effects of humic acids on the inclusion complexation of cyclodextrins with organophosphorus pesticides. Chemosphere, 38: 2219-2226 - b

Ishiwata S., Kamiya M., 2000. Structural study on inclusion complexes of cyclodextrins with organophosphorus pesticides by use of rotational strength analysis method. Chemosphere, 41: 701-704

Jackson J.A., Berkman C.E., Thomson C.M., 1992. Stereoselective and chemoselective oxidation of phosphorothionates using MMPP. Tetrahedron lett., 33: 6061-6064

Jeanty G., Ghommidh C.H., Marty J. L., 2001. Automated detection of chlorpyrifos and its metabolites by continuous flow system-based enzyme sensor. Anal. chim. acta, 436: 119-128

Jokanović M., 2001. Biotransformation of organophosphorus compounds. Toxicology, 166: 139-160

Kamiya M., Kameyama K., 1998. Photochemical effects of humic substances on the degradation of organophosphorus pesticides. Chemosphere, 36: 2337-2344

Kamiya M., Kameyama K., 2001. Effects of selected metal ions on photodegradation of organophosphorus pesticides sensitized by humic substances. Chemosphere, 45: 231-235

Kamiya M., Nakamura K., 1995. Cyclodextrin inclusion effects on photodegradation rates of organophosphorus pesticides. Environ. Internat., 21: 299-304.

Katagi T., 1993. Photochemistry of Organophosphorus Herbicide Butamifos. J. Agric. Food Chem, 41: 496-501

Kerzhentsev M., Guillard C., Herrmann J.M., Pichat P., 1996. Photocatalytic pollutant removal in water at room temperature: case study of the total degradation of the insecticide fenitrothion (phosphorothioic acid O,O-dimethyl-O-(3-methyl-4-nitro-phenyl) ester). Catal. today, 27: 215-220

Kim Y.A., Lee H.S., Park Y.C., Lee Y.T., 2000. Convenient Method for Oxidation of Organophosphorus Pesticides in Organic Solvents. Environ. res. sec. A, 84: 303-309

Konstantinou I.K., Albanis T.A., 2003. Review, Photocatalytic transformation of pesticides in aqueous titanium dioxide suspensions using artificial and solar light: intermediates and degradation pathways. Appl. catal., B Environ., 42: 319-335

Konstantinou I.K., Sakellarides T.M., Sakkas V.A., Albanis T.A., 2001. Photocatalytic degradation of selected s-triazine herbicides and organophosphorus insecticides over aqueous TiO2 suspensions. Environ. Sci. Technol., 35: 398-405

Kouloumbos V.N., Tsipi D.F., Hiskia A.E., Nikolic D., van Breemen R.B., 2003. Identification of Photocatalytic Degradation Products of Diazinon in TiO2 Aqueous Suspensions Using GC/MS/MS and LC/MS with Quadrupole Time-of-Flight Mass Spectrometry. J Am Mass Spectrom, 14: 803-817

Kousba A.A., Sultatos L.G., Poet T.S., Timchalk C., 2004. Comparison of chlorpyrifos-oxon and paraoxon Acetylcholinesterase inhibition dynamics: potential role of a peripheral binding site. Toxicol. sci., 80: 239-248

Ku Y., Chang J.-L., Shen Y.-S., Lin S.-Y, 1998. Decomposition of diazinon in aqueous solution by ozonation. Wat.Res. Vol. 32, No. 6, 1957-1963

Ku Y., Jung I.L., 1998. Decomposition of Monocrotophos in Aqueous Solution by UV Irradiation in the Presence of Titanium Dioxide. Chemosphere, 37: 2589-2597

Ku Y., Lin H.S., 2002. Research note, Decomposition of phorate in aqueous solution by photolytic ozonation. Water res., 36: 4155-4159

Kumaran S., Morita M., 1995. Application of a cholinesterase biosensor to screen for organophosphorus pesticides extracted from soil. Talanta, 42: 649-655-

Kumaran S., Tran-Minh C., 1992. Determination of Organophosphorus and Carbamate Insecticides by Flow Injection Analysis. Anal. Biochem., 200: 187-194

Laplanche A., Martin G., Tonnard F., 1984. Ozonation schemes of organo phosphorus pesticides application in drinking water treatment. Ozone: sci. eng., 6: 207-219

La Rosa C., Pariente F., Hernández L., Lorenzo E., 1995. Amperometric flow-through biosensor for the determination of pesticides. Anal. chim. acta, 308: 129-136

Lavrenčič Štangar U., Černigoj U., Trebše P., Maver K., Gross S., Monatsh. 2006. Chem. 137: 647–655

Magara, Y. et al., 1994. Degradation of Pesticides by Chlorination During Water Purification. Water Sci. & Technol., 30: 119

Lee H.S, Kim Y.A., Cho Y.A., Lee Y.T., 2002. Oxidation of organhophosphorus pesticides for the sensitive detection of cholinesterase-based biosensor. Chemosphere, 46: 571-576

Luckenbach R., 1973. Phosphin-bzw. Arsinoxide durch Einwirkung von Dimethylsulfoxid auf Phosphin-bzw. Arsin-sulfide in saurer Losung. Communications, 307

Luckenbach R., Kern M., 1975. Stereospecific Conversion of Chiral Acyclic Tertiary Phosphine Sulfides into the Corresponding Tertiary Phosphine Oxides by Means Of Dimethyl Sulfoxide (DMSO). Chem. Ber., 108: 3533-3537

Magara, Y. et al., 1994. Degradation of Pesticides by Chlorination During Water Purification. Water Sci. & Technol., 30: 119

Malato S., Blanco J., Richter C., Maldonado M.I., 2000. Optimization of pre-industrial solar photocatalytic mineralization of commercial pesticides Application to pesticide container recycling. Appl. catal., B Environ., 25: 31-38

Malato S., Blanco J., Vidal A., Alarcon D., Maldonado M. I., Caceres J., Gernjak W., 2003. Applied studies in solar photocatalytic detoxification: an overview. Sol. energy, 75: 329 – 336

Mansour M., Feicht E.A., Behechti A., Scheunert I., 1997. Experimental approaches to studying the photostability of selected pesticides in water and soil. Chemosphere, 35: 39-50

Mansour M., Feicht E.A., Behechti A., Schramm K.W., Kettrup A., 1999. Determination photostability of selected agrochemicals in water and soil. Chemosphere, 39: 575-585

Marty J.L., Garcia D., Rouillon R., 1995. Biosensors: potential in pesticide detection. TrAC, 14, no. 7, 1995

Marty J.L., Mionetto N., Lacorte S., Barcelo D., 1995. Validation of an enzymatic biosensor with various liquid chromatographic techniques for determining organophosphorus pesticides and carbaryl in freeze-dried waters. Anal. chim. acta, 311: 265-271

Meikle R.W., Kurihara N.H., De Vries D.H., 1983. Chlorpyrifos: The photodecomposition rates in dilute aqueous solution and on a surface, and the volatilizytion rate from a surface. Arch.Environ.Contam.Toxicol., 12: 189-193

Mello D.L., Kubota L.T., 2002. Review of the use of biosensors as analytical tools in the food and drink industries, Analytical, Nutritional and Clinical Methods. Food chem., 77: 237–256.

Mengyeu Z., Shifu C., Yaowu T., 1995. Photocatalytic Degradation of Organophosphorus Pesticides Using Thin Films of TiO2. J. Chem. Tech. Biotechnol., 64: 339-344

Michalski J., Okruszek A., Stec W.,1970. Stereochemistry of oxidation of organophosphorus Thiono-Compounds and P(III) Compounds by nitric acid and dinitrogen tetroxide. Chem. commun., 1495-1497

Mikolyjczyk M. and Luczak J., 1975. Dimethyl Sulphoxide Oxidations: An Iodine-catalysed Conversion of Thio- or Selenophosphoryl and Thio-carbonyl Compounds into their Oxygen Analogues, Communication, Synthesys, February

Mionetto N., Marty J.L., Karube I., 1994. Acetylholinesterase in organic solvents for the detection of pesticides: Biosensor application. Biosens. bioelectron., 9: 463-470

Montesinos T., Pérez-Munguia S., Valdez F., Marty J.L., 2001. Disposable cholinesterase biosensor for the detection of pesticides in water-miscible organic solvents. Anal. chim. acta, 431: 231-237

Mulchandani A., Chen W., Mulchandani P., Wang J., Rogers K.R., 2001. Biosensors for direct determination of organophosphate pesticides. Biosens. bioelectron., 16: 225-230

Muszkat L., Bir L., Feigelson L., 1995. Solar photocatalytic mineralization of pesticides in polluted waters. J. photochem. photobiol., A Chem., 87: 85-88

Murov S. L., Carmichael I., Hug G. L. 1993. Handbook of photochemistry, 2sd Edition. Marcel Dekker

Naman S.A., Khammas Z.A.-A., Hussein F.M., 2002. Photo-oxidative degradation of insecticide dichlorovos by a combined semiconductors and organic sensitizers in aqueous media. J. photochem. photobiol., A Chem., 153: 229-236

Noblet J.A., Smith L.A., Suffet I.H., 1996. Influence of natural dissolved organic matter, temperature, and mixing on the abiotic hydrolysis of triazine and organophosphate pesticides. J. Agric. Food Chem., 44: 3685-3693

Nunes G.S., Skladal P., Yamanaka H., Barcelo D., 1998. Determination of carbamate residues in crop samples by cholinesterase-based biosensors and chromatographic techniques. Anal. chim. acta, 362: 59-68

Nunes G.S., Toscano I.A, Barcelo D., 1998. Analysis of pesticides in food and environmental samples by enzyme-linked immunosorbent assays. TrAC: 17, no. 2

Official Gazette of the Republic of Slovenia, 13, 5.3.1999. Uredba o monitoringu pesticidov v živilih in kmetijskih proizvodih.

Official Gazette of the Republic of Slovenia, 54, 8.7.1999. Pravilnik o mejnih vrednostih pesticidov v oziroma na rastlinah oziroma živilih rastlinskega izvora.

O'Shea K.E., Beightol S., Garcia I., Aguilar M., Kalen D.V., Cooper W.J., 1997. Photocatalytic decomposition of organophosphonates in irradiated TiO2 suspensions. J. photochem. photobiol.,A Chem., 107: 221-226

Patel P.D., 2002. (Bio)sensors for measurement of analytes implicated in food safety: a review. TrAC: 21, no. 2

Pehkonen S. O., Zhang Q., 2002. The degradation of organophosphorus pesticides in natural waters: a critical review. Critical Review in Environmental Science and Technology, 32: 17-72

Penuela G.A., Barcelo D., 1998. Photosensitized degradation of organic pollutants in water: processes and analytical applications. TrAC: 17, no. 10

Penuela G.A., Barcelo D., 1997. Comparative degradation kinetics of chlorpyrifos in water by photocatalysis with FeCl3, TiO2 and photolysis using solid-phase disk extraction followed by gas chromatographic techniques. Toxicol. environ. chem, 62: 135-147

Pignatello J.J., Sun Y., 1995. Complete oxidation of metolachlor and methyl parathion in water by the photoassisted fenton reaction. Wat. Res., 29: 1837-1844

Pogačnik L., Franko M., 1999. Determination of organophosphate and carbamate pesticides in spiked samples of tap water and fruit juices by a biosensor with photothermal detection. Biosens. bioelectron., 14: 569-578

Pogačnik L., Franko M., 2001. Validation of different commercially available cholinesterases for pesticide toxicity test. Annali di Chimica, 90 - a

Pogačnik L., Franko M., 2001. Optimisation of FIA system for detection of organophosphorus and carbamate pesticides based on cholinesterase inhibition. Talanta, 54: 631-641 - b

Pogačnik L., Franko M., 2003. Detection of organophosphate and carbamate pesticides in vegetable samples by a photothermal biosensor. Biosens. bioelectron., 18: 1-9

Rice D.W., Wisniewski J.A., Jowa L., Howd R.A., DiBartolomeis M.J., 1997. Healt risk assessment of malathion coproducts in malathion-bait used for agricultural pest eradication in urban areas. Pesticide and Environmental Toxicological Section, Office of Environmental Health Hazard Assessment, California Environmental Protection Agency, 1997

Sakkas V.A., Lambropoulou D.A., Sakellarides T.M., Albanis T.A., 2002. Application of solid-phase microextraction for monitoring the photocatalytic decomposition of fenthion and parathion in aqueous TiO2 suspensions. Anal. chim. acta, 467: 233-243

Sanchez-Baeza F., Durand G., Barcelo D., Messeguer A., 1990. Dimethyldioxiran conversion of phosphine sulfides and phosphorothioates into their corresponding oxygen analogues. Tetrahedron lett., 31: 3359-3362

Shemer H., Sharpless C.M. and Linden K.G., 2005. Photodegradation of 3,5,6-trichloro-2-pyridinol in aqueous solution. Water air soil poll., 168:145-155

Schulze H, Scherbaum E., Anastassiades M., Vorlová S., Schmid R.D., Bachmann T.T., 2002. Development, validation, and application of an acetylcholinesterase-biosensor test for the direct detection of insecticide residues in infant food. Biosens. bioelectron., 17: 1095-1105

Schulze H., Schmid R.D., Bachmann T.T., 2002. Rapid detection of neurotoxic insecticides in food using disposable acetylcholinesterase-biosensors and simple solvent extraction. Anal. Bioanal. Chem., 372: 268-272

Schulze H., Schmid R.D., Bachmann T.T., 2004. Activation of Phosphorothionate Pesticides Based on a Cytochrome P450 BM-3 (CyP102 A1) Mutant for Expanded Neurotoxin Detection in Food Using Acetylcholinesterase Biosensors. Anal. Chem., 76: 1720-1725

Schulze H., Vorlova´ S., Villatte F., Bachmann T.T., Schmid R.D., 2003. Design of acetylcholinesterases for biosensor applications. Biosens. bioelectron., 18: 201-209

Segall Y., Casida J.,1982. Oxidative Conversion of Phosphorothiolates to Phosphinyloxysulfonates Probably via Phosphorothiolate-S-Oxides. Tetrahedron lett., 23: 139-142

Simonian A.L., Efremenko E.N., Wild J.R., 2001. Discriminative detection of neurotoxins in multi-component samples. Anal. chim. acta, 444: 179-186.

Singh A.K., Flounders A.W., Volponi J.V., Ashley C.S., Wally K., Schoeniger J.S., 1999. Development of sensors for direct detection of organophosphates. Part I: immobilization, characterization and stabilization of acetylcholinesterase and organophosphate hydrolase on silica supports. Biosens. bioelectron., 14: 703-713

Skowronska A., Krawczyk E., 1983. A General Method for the Conversion of Thiophosphoryl and Selenophosphoryl Groups into Phosphoryl Groups by Ozone Oxidation. Communications, Synthesis, June

Stec W.J., Okruszek A., Michalski J., 1971. Optisch aktive Selenoxp-methyl-phenyl-propyl-phosphorane und ihre Umwandlungen. Angew. Chem., 83. Nr. 13

Stec W.J., Okruszek A., Michalski J., 1976. Stereochemistry of Oxidation of Thiono- and Selenophosphoryl Compounds with Hydrogen Peroxide. J. Org. Chem.

Talcott R.E., Mallipudi N.M., Umetsu N., Fukuto T.R., 1979. Inactivation of esterases by impurities isolated from technical malathion. Toxicol. Appl. Pharmacol., 49: 107-112

Terreni M., Pregnolato M., Resnati G., Benfenati E., 1995. Selective Sulfur Oxygenation in Phosphoroamidate, Thionophosphate, and Thiophosphate Agrochemicals by Perfluoro-cis-2,3-dialkyloxaziridine. Tetrahedron, 51: 7981-7992

Trebše P. and Arčon I., 2003. Degradation of organophosphorus compounds by X-ray irradiation. Radiat. Phys. Chem., 67: 527-530

Trojanowicz M., Drzewicz P., Panta P., Gluszewski W., Nalecz-Jawecki G., Sawicki J., Sampa M.H.O., Oikawa H., Borrely S.I., Czaplicka M., Szewczynska M., 2002. Radiolytic degradation and toxicity changes in γ-irradiated solutions of 2,4-dichlorophenol. Radiat. Phys. Chem., 65: 357-366

Velasco-Garcia M.N., Mottram T., 2003. REVIEW PAPER, Biosensor Technology addressing Agricultural Problems. Biosyst. eng., 84: 1-12

Villatte F., Marcel V., Estrada-Mondaca S., Fournier D., 1998. Engineering sensitive acetylcholinesterase for detection of organophosphate and carbamate insecticides. Biosens. bioelectron., 13: 157-164

Wagner G.W., Bartram P.W., Brickhouse M.D., Connell T.R., Creasy W.R., Henderson V.D., Hovanec J.W., Morrissey K.M., Stuff J.R., Williams B.R., 2000. Reaction of VX and GD with gaseous ozone. J.Chem.Soc., Perkin Trans., 2: 1267-1272

Walia S., Dureja P., Mukerjee S.K., 1988. New photodegradation products of chlorpyrifos and their detection on glass, soil, and leaf surfaces. Arch.Environ.Conmta.Toxicol., 17: 183-188 (1988).

Wan H.B., Wong M.K., Mok C.Y., 1994. Comparative study on teh quantum yields of direct photolysis of organophosphorus pesticides in agueous solution. J. Agric. Food Chem., 42: 2625-2630

Wang J., Krause R., Block K., Musameh M., Mulchandani A., Schoening M.J., 2003. Flow injection amperometric detection of OP nerve agents based on an organophosphorus - hydrolase biosensor detector. Biosens. bioelectron., 18: 255-260

Wen C., Hasegawa K., Kanbara T., Kagaya S., Yamamoto T., 2000. Visible light-induced catalytic degradation of iprobenfos fungicide by poly(3-octylthiophene-2,5-diyl) film. J. photochem. photobiol.,A Chem., 133: 59-66

Wilkins E., Carter M., Voss J., Ivnitski D., 2000. A quantitative determination of organophosphate pesticides in organic solvents. Electrochem. commun., 2: 786-790

Wozniak L.A., Stec W.J., 1999. Oxidation in Organophosphorus Chemistry: Potassium Peroxymonosulphate. Tetrahedron lett., 40: 2637-2640

Wu J., Luan T., Lan C., Lo T.W.H., Chan G.Y.S., 2007. Removal of residual pesticides on vegetable using ozonated water. Food control, 18: 466-472 - a

Wu J.G., Luan T.G., Lan C.Y., Lo W.H., Chan G.Y.S., 2007. Efficacy evaluation of low-concentration of ozonated water in removal of residual diazinon, parathion, methyl-parathion and cypermethrin on vegetable. J. food eng., 79: 803-809 - b

Wu J. and Laird D.A., 2003. Abiotic transformation of chlorpyrifos to chlorpyrifos oxon in chlorinated water. Environ. toxicol. chem.:22, No. 2, 261-264

Zamy C., Mazellier P., Legube B., 2004. Phototransformation of selected organophosphorus pesticides in dilute aqueous solutions. Water res., 38: 2305–2314

Zhang Q., Pehkonen S.O., 1999. Oxidation of Diazinon by Aqueous Chlorine: Kinetics, Mechanism, and Product Studies. J. Agric. Food Chem., 47: 1760-1766

Zona R. and Solar S., 2003. Oxidation of 2,4-dichlorophenoxyacetic acid by ionizing radiation: degradation, detoxification and mineralization. Radiat. Phys. Chem., 66: 137-143

8 ANNEXES

Abbeviations

ACh – acetylcholin
AChE – acetyl cholinesterase
AOPs – advanced oxidation processes
ASChI – acetylthiocholine iodide
BchE – butyryl cholinesterase
CAN – cerium ammonium nitrate
CDD – conductive detector
ChE – cholinesterase
ChO – cholinoxidase
CPG 240 – controlled-pore glass with 80-120 meshes
DAD – diode array detector
DMSO – dimethyl sulfoxide
DTNB – 5,5'-dithio-bis(2-nitrobenzoic acid)
DP – declustering potential
e – electron
ECD – electron capture detector
EI – electron impact ionization
EP – entrance potential
FIA – flow injection analysis
FIA-AChE-TLS bioassay – acetyl cholinesterase bioassay based on flow injection analysis with thermal lens spectrometric detection
FID – flame ionization detector
FMO – flavin-containing monooxygenases
GC – gas chromatography
GD – pinacolyl methyl phosphonofluoridate
GST – glutathion S transferase
h – hole
HPLC – high performance liquid chromatograpy
HO· – hydroxyl radical
IC – ionic chromatography
IMP – 2-isopropyl-6-methyl-4-pyrimidinol
IS – ionization source
LLE – liquid-liquid extraction
LD_{50} – lethal dose, the dose required to kill half the members of a tested population
LOD – limit of detection
*m*CPBA – *m*-chloroperoxybenzoic acid
MMTP – 3-methyl-4-methylthiophenol
MMSP – .dimethyl phosphorothioate and 3-methyl-4-methylsulfinylphenol
MS – mass spectrometry / spectrometer
NBS – *N*-bromosuccinimide
OOO(S) – *O,O,O*-trimethylphosphorothionate
OOS(O) – *O,O,S*-trimethylphosphorothioate
OOS(S) – *O,O,S*-trimethyl phosphorodithionate
OSS(O) – *O,S,S*-trimethylphosphorodithioate
2-PAM – pyridine-2-aldoxime methiodide
PBS – phosphate buffer saline
ppb – part per billion
ppm – part per million
$^1O_2$ – singlet oxygen
OP – organophosphorus pesticides
Oxone - potassium hydrogen monopersulfate
REL – reference exposure level
RDH – Riedel De Haen

Sens – sensitizer
SPE – solid phase extraction
SPME – solid phase micro extraction
TCP – 3,5,6-trichloro-2-pyridinol
TLC – thin layer chromatography
TLS – thermal lens spectrometry / spectrometer
TOC – total organic carbon
UV – ultra violet
VX – {*O*-ethyl *S*-[2-(diisopropylamino) ethyl] methylphosphonothioate} Xe lamps – xenon lamps

oxo-OP –

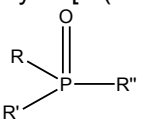

thio-OP –